nagra.

Arbeitsbericht NAB 22-04

TBO Bachs-1-1: Data Report

Dossier VII Hydraulic Packer Testing

August 2023

R. Schwarz, R. Beauheim, L. Schlickenrieder, E. Manukyan & A. Pechstein

National Cooperative for the Disposal of Radioactive Waste

Hardstrasse 73
P.O. Box
5430 Wettingen
Switzerland
Tel. +41 56 437 11 11

nagra.ch

nagra.

Arbeitsbericht NAB 22-04

TBO Bachs-1-1: Data Report

Dossier VII Hydraulic Packer Testing

August 2023

R. Schwarz[1], R. Beauheim[2], L. Schlickenrieder[1], E. Manukyan[3] & A. Pechstein[3]

[1] CSD Ingenieure AG
[2] INTERA Incorporated
[3] Nagra

Keywords:
BAC1-1, Nördlich Lägern, TBO, deep drilling campaign, hydrogeology, hydraulic packer tests, hydraulic conductivity, hydraulic head, fluid logging

National Cooperative for the Disposal of Radioactive Waste

Hardstrasse 73
P.O. Box
5430 Wettingen
Switzerland
Tel. +41 56 437 11 11

nagra.ch

Nagra Arbeitsberichte ("Working Reports") present the results of work in progress that have not necessarily been subject to a comprehensive review. They are intended to provide rapid dissemination of current information.

This NAB aims at reporting drilling results at an early stage. Additional borehole-specific data will be published elsewhere.

In the event of inconsistencies between dossiers of this NAB, the dossier addressing the specific topic takes priority. In the event of discrepancies between Nagra reports, the chronologically later report is generally considered to be correct. Data sets and interpretations laid out in this NAB may be revised in subsequent reports. The reasoning leading to these revisions will be detailed there.

This Dossier was prepared by a project team consisting of:
R. Schwarz (QC of test analyses, QC of test reports, writing)
R. Beauheim (performance and analysis of the hydraulic packer tests)
E. Manukyan (performance and analyis of the fluid logging measurements)
L. Schlickenrieder (writing)
A. Pechstein (project management, conceptualisation, review)

The present report is based on the mobilisation reports for the test equipment and on the reports for the performance and analysis of the hydraulic packer tests and fluid logging. These reports were written by the testing companies INTERA Inc. (R. Beauheim, R. Roberts (HydroResolutions LLC), T. Cavalera, J. Croisé, A. Dausse, M. Hayek, A. Färber, B. Paris, C. Yu and D. Zbinden), and Solexperts AG (U. Rösli, G. Mühlebach (Terratec Geophysical Services GmbH & Co. KG)).

Editorial work: P. Blaser and M. Unger

The Dossier has greatly benefitted from technical discussions with, and reviews by, external and internal experts. Their input and work are very much appreciated.

Table of Contents

List of Tables

List of Figures

1 Introduction

1.1 Context

To provide input for site selection and the safety case for deep geological repositories for radioactive waste, Nagra has drilled a series of deep boreholes ("Tiefbohrungen", TBO) in Northern Switzerland. The aim of the drilling campaign is to characterise the deep underground of the three remaining siting regions located at the edge of the Northern Alpine Molasse Basin (Fig. 1-1).

In this report, we present the results from the Bachs-1-1 borehole.

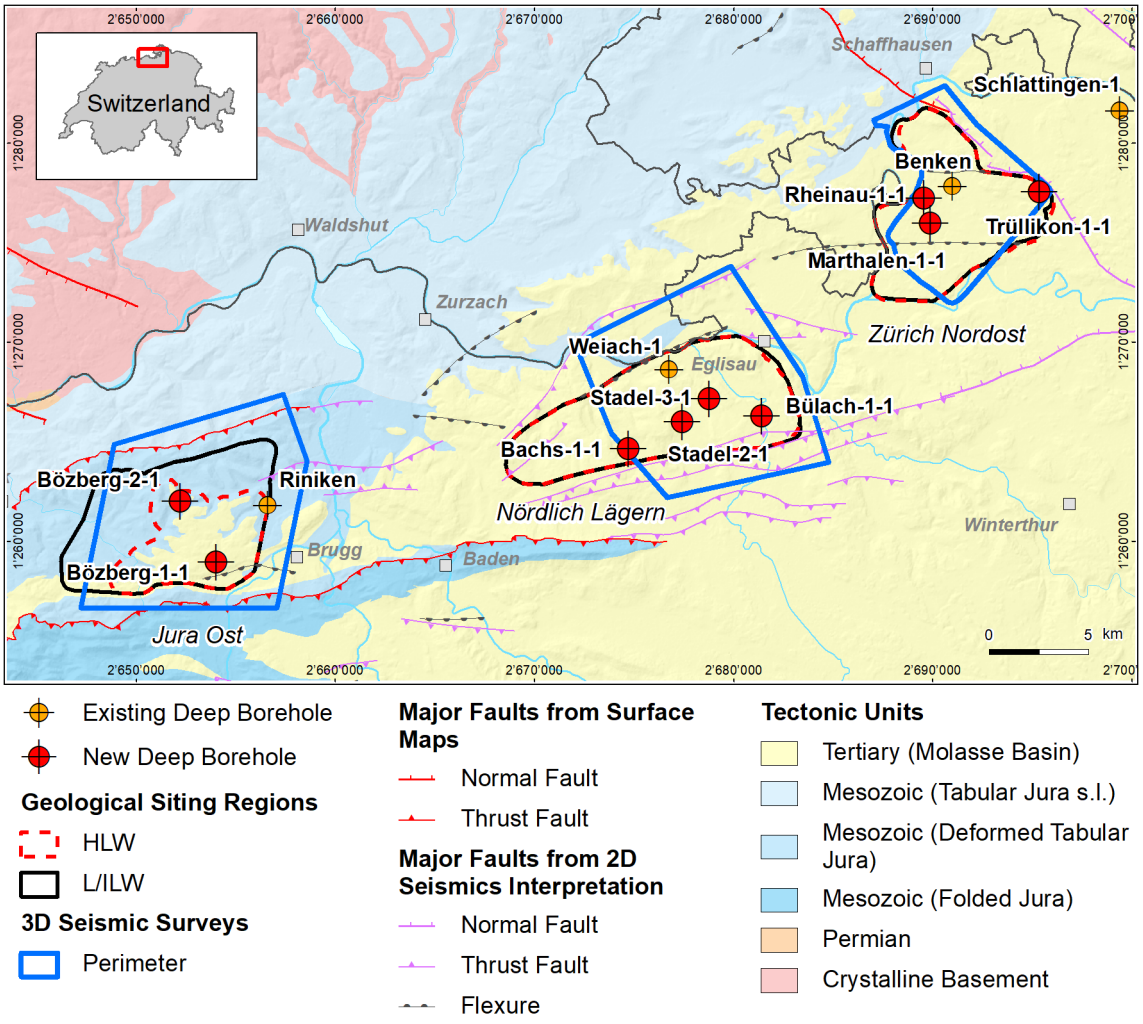

Fig. 1-1: Tectonic overview map with the three siting regions under investigation

1.2 Location and specifications of the borehole

The Bachs-1-1 (BAC1-1) exploratory borehole is the ninth (and last) borehole drilled within the framework of the TBO project. The drill site is located in the western part of the Nördlich Lägern siting region (Fig. 1-2). The vertical borehole reached a final depth of 1'306.26 m (MD)[1]. The borehole specifications are provided in Tab. 1-1.

Due to a loss of a measurement tool (dilatometer), the borehole was cemented up to 500 m MD and a sidetrack was initiated with a kickoff point (KOP) at about 600 m MD. This sidetrack was labelled Bachs-1-1B (BAC1-1B). BAC1-1B reached a final depth of 952 m MD but was abandoned during borehole reaming operations due to entering the original borehole BAC1-1. Therefore, the vertical borehole BAC1-1 was used again for the remaining investigations. For easier communication and labelling, the name BAC1-1 is generally used for this borehole, including the sidetrack, unless stated otherwise. A detailed description of all technical details about the drilling process can be found in Dossier I.

Tab. 1-1: General information about the BAC1-1 borehole

Siting region	Nördlich Lägern
Municipality	Bachs (Canton Zürich / ZH), Switzerland
Drill site	Bachs-1 (BAC1)
Borehole	Bachs-1-1 (BAC1-1) including sidetrack Bachs-1-1B (BAC1-1B)
Coordinates	LV95: 2'674'769.089 / 1'264'600.698
Elevation	Ground level = top of rig cellar: 450.35 m above sea level (asl)
Borehole depth	1'306.26 m measured depth (MD) below ground level (bgl)
Drilling period	10th September 2021 – 23rd April 2022 (spud date to end of rig release)
Drilling company	Daldrup & Söhne AG
Drilling rig	Wirth B 152t
Drilling fluid	Water-based mud with various amounts of different components such as[2]: 0 – 700 m: Bentonite & polymers 700 – 1'057 m: Potassium silicate & polymers[3] 1'057 – 1'129 m: Water & polymers 1'129 – 1'306.26 m: Sodium chloride brine & polymers

The lithostratigraphic profile and the casing scheme are shown in Fig. 1-3. The comparison of the core versus log depth[4] of the main lithostratigraphic boundaries in the BAC1-1 borehole is shown in Tab. 1-2.

---

[1] Measured depth (MD) refers to the position along the borehole trajectory, starting at ground level, which for this borehole is the top of the rig cellar. For a perfectly vertical borehole, MD below ground level (bgl) and true vertical depth (TVD) are the same. In all Dossiers depth refers to MD unless stated otherwise.

[2] For detailed information see Dossier I.

[3] Including sidetrack.

[4] Core depth refers to the depth marked on the drill cores. Log depth results from the depth observed during geophysical wireline logging. Note that the petrophysical logs have not been shifted to core depth, hence log depth differs from core depth.

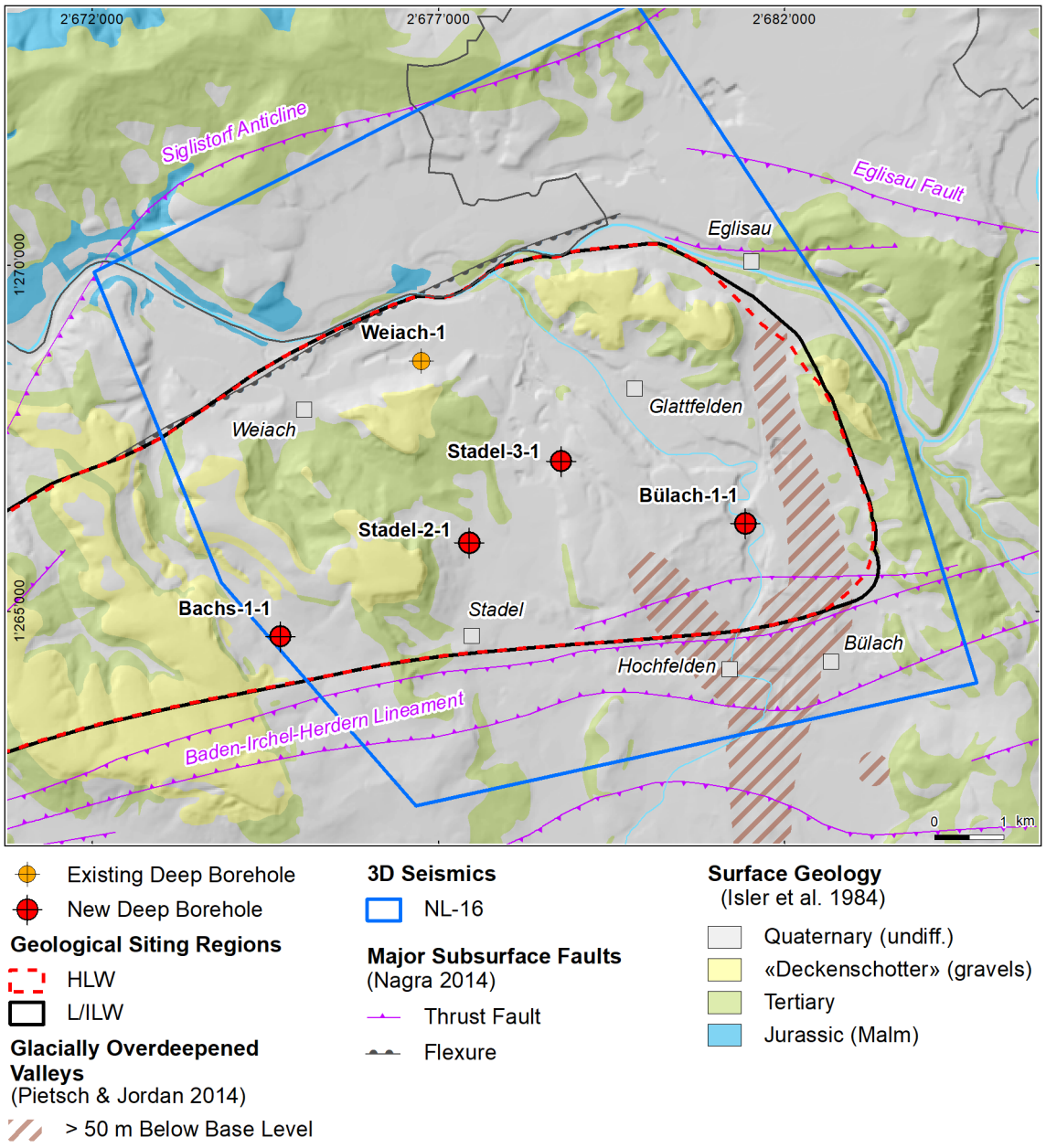

Fig. 1-2: Overview map of the investigation area in the Nördlich Lägern siting region with the location of the BAC1-1 borehole in relation to the boreholes Weiach-1, BUL1-1, STA3-1 and STA2-1

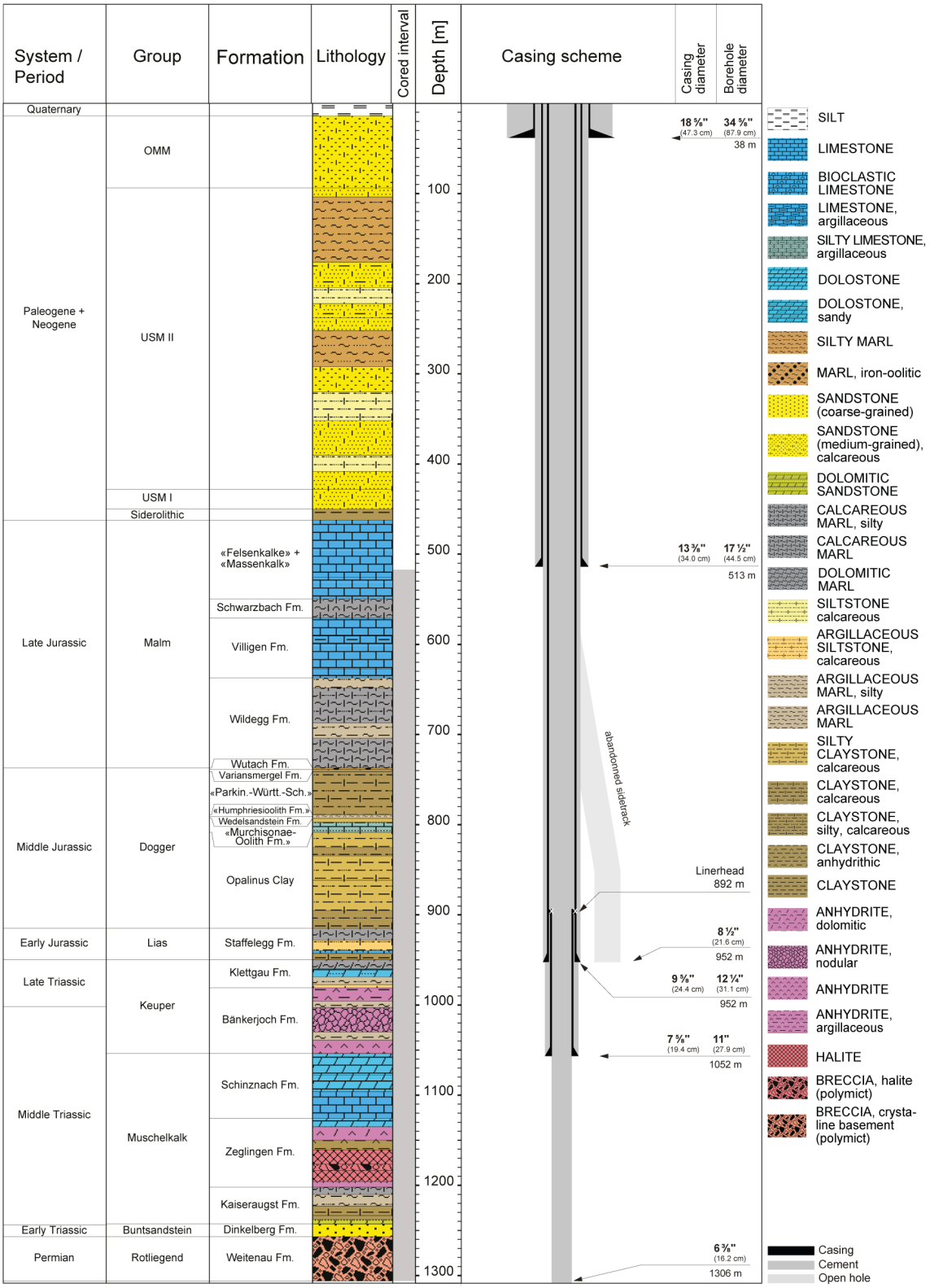

Fig. 1-3: Lithostratigraphic profile and casing scheme for the BAC1-1 borehole[5]

[5] For detailed information see Dossier I and III.

Tab. 1-2: Core and log depth for the main lithostratigraphic boundaries in the BAC1-1 borehole[6]

System / Period	Group	Formation		Core top depth in m (MD)	Log top depth in m (MD)	
Quaternary				**14**		—
Paleogene + Neogene	OMM			94		—
	USM			450		—
	Siderolithic			**462**		—
Jurassic	Malm	«Felsenkalke» + «Massenkalk»		549.69	550.03	—
		Schwarzbach Formation		570.98	571.29	—
		Villigen Formation		637.31	637.55	—
		Wildegg Formation		737.05	737.32	—
	Dogger	Wutach Formation		738.81	739.08	—
		Variansmergel Formation		741.22	741.47	—
		«Parkinsoni-Württembergica-Schichten»		788.92	789.12	—
		«Humphriesioolith Formation»		791.05	791.25	—
		Wedelsandstein Formation		793.11	793.31	—
		«Murchisonae-Oolith Formation»		808.34	808.57	—
		Opalinus Clay		914.91	915.30	—
	Lias	Staffelegg Formation		**949.73**	**950.07**	—
Triassic	Keuper	Klettgau Formation		980.93	981.27	—
		Bänkerjoch Formation		1053.90	1054.30	—
	Muschelkalk	Schinznach Formation		1125.75	1126.20	—
		Zeglingen Formation		1202.03	1202.43	—
		Kaiseraugst Formation		1242.82	1243.12	—
	Buntsandstein	Dinkelberg Formation		**1256.86**	**1257.26**	—
Permian	Rotliegend	Weitenau Formation	final depth	1306.26	1306.77	

[6] For details regarding lithostratigraphic boundaries see Dossier III and IV; for details about depth shifts (core goniometry) see Dossier V.

1.3 Documentation structure for the BAC1-1 borehole

NAB 22-04 documents the majority of the investigations carried out in the BAC1-1 borehole, including laboratory investigations on core material. The NAB comprises a series of stand-alone dossiers addressing individual topics and a final dossier with a summary composite plot (Tab. 1-3).

This documentation aims at early publication of the data collected in the BAC1-1 borehole. It includes most of the data available approximately one year after completion of the borehole. Some analyses are still ongoing (e.g. diffusion experiments, analysis of veins, hydrochemical interpretation of water samples) and results will be published in separate reports.

The current borehole report will provide an important basis for the integration of datasets from different boreholes. The integration and interpretation of the results in the wider geological context will be documented later in separate geoscientific reports.

Tab. 1-3: List of dossiers included in NAB 22-04

Black indicates the dossier at hand.

Dossier	Title	Authors
I	TBO Bachs-1-1: Drilling	P. Hinterholzer-Reisegger
II	TBO Bachs-1-1: Core Photography	D. Kaehr, M. Stockhecke & Hp. Weber
III	TBO Bachs-1-1: Lithostratigraphy	P. Jordan, P. Schürch, M. Schwarz, R. Felber, H. Naef, T. Ibele & F. Casanova
IV	TBO Bachs-1-1: Microfacies, Bio- and Chemostratigraphic Analyses	S. Wohlwend, H.R. Bläsi, S. Feist-Burkhardt, B. Hostettler, U. Menkveld-Gfeller, V. Dietze & G. Deplazes
V	TBO Bachs-1-1: Structural Geology	A. Ebert, E. Hägerstedt, S. Cioldi, L. Gregorczyk & F. Casanova
VI	TBO Bachs-1-1: Wireline Logging, Micro-hydraulic Fracturing and Pressure-meter Testing	J. Gonus, E. Bailey, J. Desroches & R. Garrard
VII	TBO Bachs-1-1: Hydraulic Packer Testing	R. Schwarz, R. Beauheim, L Schlicken-rieder, E. Manukyan & A. Pechstein
VIII	TBO Bachs-1-1: Rock Properties, Porewater Characterisation and Natural Tracer Profiles	E. Gaucher, L. Aschwanden, T. Gimmi, A. Jenni, M. Kiczka, M. Mazurek, P. Wersin, C. Zwahlen, U. Mäder & D. Traber
IX	*The geomechanical campaign in BAC-1-1 was limited to two oedometric tests. Hence, no dedicated Dossier IX was produced for NAB 22-04. The hydraulic conductivity values derived from the oedometric tests are documented in the Summary Plot.*	
X	TBO Bachs-1-1: Petrophysical Log Analysis	S. Marnat & J.K. Becker
	TBO Bachs-1-1: Summary Plot	Nagra

1.4 Scope and objectives of this dossier

The dossier at hand aims at providing a summary of the conducted hydrogeological investigations and acquired hydrogeological data, including assessments of tests and results, but without interpretation. A gas threshold pressure test (GTPT) was not conducted in this borehole.

This report focuses on fluid logging and hydraulic packer testing, and is organised as follows:

- Chapter 2 presents the general strategy for the hydrogeological investigations in the BAC1-1 borehole.
- Chapter 3 is dedicated to fluid logging which was performed in the drilled borehole Section II. It discusses all aspects including the test equipment used, general concerns for the analysis, fluid logging test activities, and fluid logging test results in borehole BAC1-1.
- Chapter 4 discusses all aspects of the hydraulic packer tests including planning of test strategies, test equipment used, general concerns for the analysis of tests, test activities and hydraulic packer test results in borehole BAC1-1. Selected tests and analyses are presented in detail. The results are summarised in tables and plots, and some assessments are made.
- Chapter 5 summarises and discusses the data and results, mainly for the hydraulic packer tests.

Finally, this report includes a set of appendices, which present relevant general project information and further investigation details.

2 Strategy for the hydrogeological investigations

2.1 Hydrogeological objectives of the TBO boreholes

The overall objectives of the hydrogeological investigations are the detailed determination of the hydraulic conductivity and hydraulic head in the aquifers, aquicludes and aquitards on the one hand, and the chemistry and isotopic composition of the deep groundwaters in the aquifers and the porewaters in the aquicludes and aquitards on the other. The results of the hydrogeological investigations in the TBO boreholes form an important dataset for site selection and the safety case. They are mainly needed for the characterisation of:

- Hydraulic and hydrochemical properties of the containment-providing rock zone, which consists of the host rock Opalinus Clay and the confining geological units above and below.
- Hydrogeological conditions in the aquifers providing the hydraulic and hydrochemical boundary conditions for the containment-providing rock zone and providing input for the identification of potential release paths as well as for the planning of future access structures.

2.2 Hydrogeological investigation concept for BAC1-1

The hydrogeological investigations for BAC1-1 comprised hydraulic packer testing and fluid logging. A fluid logging campaign was conducted in the Malm Group in Section II of the borehole. Because no sufficiently high transmissivities were detected to take a water sample, no hydraulic packer test was performed in this interval.

Hydraulic packer tests were used for the detailed hydraulic characterisation of selected borehole sections to determine transmissivity (T), hydraulic conductivity (K), hydraulic head (h) and to identify the appropriate flow model. Hydraulic packer tests were performed in scheduled testing phases between drilling phases, and also during drilling phases when potentially highly transmissive features or faults were encountered. Depending on the transmissivity of the test interval, different test methods were applied in BAC1-1 as follows:

- Pumping and constant flow rate injection tests
- Slug tests
- Pulse tests

These test methods were usually combined, i.e. executed one after the other as a test sequence in a test-specific order.

A gas threshold pressure test (GTPT) was not conducted in the BAC1-1 borehole.

In the siting region Nördlich Lägern a long-term monitoring system will be installed in nearby borehole STA3-1.

The detailed groundwater sampling, subsequent hydrochemical and isotope analyses (including results) are documented in Lorenz & Stopelli (*in prep.*). Further porewater investigations are the subject of Dossier VIII. The laboratory permeability measurements on drill-core sections are discussed in Dossier IX.

3 Flowmeter logging and fluid logging

3.1 Description of equipment

The fluid logging was performed with a selection of the equipment introduced below. For the pumping test phase the equipment of the field test contractor for hydraulic packer testing was used (*cf.* Section 4.2).

3.1.1 Borehole logging winch

The winch features a mechanical cable spooling device, an electronic and a mechanical depth measurement and a cable tension measurement. For specifications, see Tab. 3-1. The borehole logging winch is permanently mounted in the logging van and is powered by a motor. As soon as the motor is stopped, a brake is automatically engaged in the gearbox. Additionally, there is a manual brake and a clutch.

Tab. 3-1: Specifications for the borehole logging winch

Manufacturer	HEWA Feinwerktechnik Engineering GmbH, Marie-Curie-Str. 2, 79211 Denzlingen, Germany
Type	TT2000, Electrical, 220 V
Cable type	Rochester 3⁄16" 4-conductor cable Type 4-H-181A
Cable breaking strength	14.7 kN
Max. cable length	2'000 m
Logging speed range	0 – 30 m/min
Depth measurement	IVO BAUMER incremental encoder, 2'500 pulse / rotation; 500 mm circumference wheel mounted on the spooling device, mechanical depth counter
Cable tension gauge	External display or input for matrix logger
Safety joint	Cable head is set up to form a weak joint. In the case of a stuck probe, the cable is pulled from the cable head.

3.1.2 Matrix logger

The Matrix logger is a logging surface unit that interfaces the probe with the acquisition PC, using the Advanced Logic Technology (ALT) Matrix Logger software (for specifications, see Tab. 3-2). It records the data, depth and logging speed and has a digital interface. The unit supports several communication protocols and can therefore be used to run probes built by different manufacturers (among others electromind, Robertson Geologging, ALT). A browser module connects the acquisition software to an ALT WellCAD document and feeds the data directly into WellCAD. The data of several runs is displayed in one document.

The software used to control the unit and the probes is as follows:

- Heat Pulse: Matrix Heat: V3.3 build 2208 © Advanced Logic Technology, 2005 – 2012
- All other probes: Matrix Logger: V 13.2 build 2790 © Advanced Logic Technology, 1995 – 2021
- Processing: WellCAD 5.4 build 1001 © Advanced Logic Technology, 1993 – 2020

The winch features a mechanical cable spooling.

Tab. 3-2: Specifications for the matrix logger

Manufacturer	Advanced Logging Technology, 30H Rue de Niederpallen, Zoning de Solupla, L-8506 Redange, Luxembourg
Type	Matrix borehole logging system
Data transmission	The data is digitised in the probes and sent to the logging system with a resolution of 15 bit (0 – 32'768 cps resolution per channel) and 16 bit (0 – 65'536 cps resolution per channel), respectively, depending on the probe

3.1.3 FTC 60G flowmeter-temperature-conductivity-gamma probe

The probe is a combination of a LIM logging / electromind temperature-electrical-conductivity-gamma probe with an Intergeo impeller flowmeter head. For this reason, the actual dimensions of the probe as mentioned below differ from the dimensions on the manufacturer's data sheet. The probe was assembled on the field contractor's request by electromind. The Intergeo flowmeter head combines a larger diameter (88 mm) with jewelled bearings for the impeller instead of ball bearings which provides improved sensitivity compared to the standard electromind impeller head. For specifications, see Tab. 3-3.

This probe measures fluid temperature, electrical fluid conductivity, vertical fluid velocity and natural gamma rays. The electrical conductivity-temperature sensor is mounted on the side of the probe. Fluid can freely flow through it while going down and up. The flowmeter is an impeller type with a cage of 88 mm and is used if relatively higher fluid flow rates are expected. If lower flow rates are anticipated that might be below the detection limit, the performance of the impeller can be improved by using a diverter disc. The diverter disc seals the annulus between the impeller cage and the borehole wall and forces most of the fluid through the sensor. This increases the fluid velocity at the sensor. Different disks are available to adjust to the borehole diameter.

The diverter disc assembly is made from a base plate that is attached to the probe, and a flexible plastic disc that can be changed depending on the borehole diameter. The base plate for the FTC 60G probe is made of Nylon and its dimensions are 148 mm outer diameter, 140 mm inner diameter, 42 mm height.

Tab. 3-3: Specifications for the FTC 60G flowmeter-temperature-conductivity-gamma probe

Manufacturer	LIM logging / electromind s.a. 1 Rue de l'Industrie, 4801 Rodange, Grand Duche de Luxembourg + intergeo Haferland AG
Type	FTC 60G
Length	1'710 mm
Weight	5.5 kg
Cage diameter	88 mm
Operational temperature range	0 – 70 °C (up to 80 °C for a limited time)
Max. pressure	20 MPa
Borehole diameter range	> 96 mm
Temperature sensor range	0 – 70 °C (up to 80 °C for a limited time)
Temperature sensor accuracy	0.1 °C
Temperature sensor resolution	0.001 °C
Electrical conductivity sensor linear range	0 – 3'000 µS/cm (not on data sheet, information from manufacturer)
Electrical conductivity sensor accuracy	10 µS/cm
Electrical conductivity sensor resolution	1 µS/cm
Flowmeter threshold velocity (static)	1 m/min
Flowmeter impeller sensor resolution (theoretical)	0.003 m/min
Gamma detector	NaI 50 mm × 25 mm crystal

3.1.4 TCG temperature-conductivity-gamma probe

The probe measures fluid temperature, electrical fluid conductivity and natural gamma rays (for specifications, see Tab. 3-4). The electrical conductivity is referenced to 25 °C and the temperature-electrical conductivity sensor is mounted at the bottom. In the standard setup, the fluid enters the probe through openings at the bottom, flows through the sensor assembly and leaves the probe through openings at the side of the probe a bit further up. This geometry is optimised for logging going down.

Tab. 3-4: Specifications for the TCG temperature-conductivity-gamma probe

Manufacturer	Robertson Geologging Ltd., York Road, Deganwy, Conwy, LL31 9PX, UK
Type	TCG
Length	1'690 mm
Weight	4.5 kg
Tool diameter	38 mm
Operational temperature range	0 – 70 °C (up to 80 °C for a limited time)
Max. pressure	20 MPa
Borehole diameter range	> 50 mm
Temperature sensor range	0 – 70 °C (up to 80 °C for a limited time)
Temperature sensor accuracy	± 0.5 °C (not on data sheet, information from manufacturer)
Temperature sensor resolution	0.04 °C (not on data sheet, information from manufacturer)
Electrical conductivity sensor range	50 – 50'000 µS/cm
Electrical conductivity sensor accuracy	± 2.5% at 500 µS/cm (not on data sheet, information from manufacturer)
Electrical conductivity sensor resolution	4 µS/cm (not on data sheet, information from manufacturer)
Electrical conductivity temperature compensation	25 °C
Gamma detector	NaI 50 mm × 25 mm crystal

3.1.5 QL40 FTC temperature-conductivity-gamma probe

The probe measures fluid temperature, electrical fluid conductivity and natural gamma rays (for specifications, see Tab. 3-5). The electrical conductivity is referenced to 25 °C and the temperature-electrical conductivity sensor is mounted at the bottom. In the standard setup, the fluid enters the probe through openings at the bottom, flows through the sensor assembly and leaves the probe through openings at the side of the probe a bit further up. This geometry is optimised for logging going down.

Tab. 3-5: Specifications for the QL40 FTC temperature-conductivity-gamma probe

Manufacturer	Advanced Logging Technology, 30H Rue de Niederpallen, Zoning de Solupla, L-8506 Redange, Luxembourg
Type	QL40 FTC
Length	800 mm
Weight	3.3 kg
Tool diameter	40 mm
Operational temperature range	0 – 70 °C
Max. pressure	20 MPa
Borehole diameter range	> 76 mm
Temperature sensor range	- 20 – 80 °C
Temperature sensor accuracy	< 1%
Temperature sensor resolution	0.004 °C
Electrical conductivity sensor range	5 – 2.5 × 10^5 µS/cm
Electrical conductivity sensor accuracy	1% (500 – 2.5 × 10^5 µS/cm)
Electrical conductivity temperature compensation	25 °C
Gamma detector	NaI 50 mm × 25 mm crystal

3.1.6 Borehole geometry gamma probe

The four-arm caliper probe provides two continuous logs of borehole diameter (for specifications, see Tab. 3-6). They are recorded by two independent pairs of linked arms in contact with the borehole wall. The pairs are mounted on the probe with an angle of 90°. The probe is lowered into the borehole with the arms retracted. Once opened at the borehole bottom, the spring-loaded arms respond to borehole diameter variations as the probe is raised.

The X arms are aligned with the axis of the magnetometer package. The measured magnetic roll is the angle between magnetic North and the X caliper pair. It is measured in a clockwise direction from North to the caliper arm when viewed from above. This measurement is required to orientate any eccentricity of the borehole, thus allowing the stress direction to be determined.

The tool is used to identify the state of the boreholes:

- Fractures, cavities
- Diameter reduction/increase
- Possible ellipticity

Tab. 3-6: Specifications for the borehole geometry gamma probe

Manufacturer	Robertson Geologging Ltd., York Road, Deganwy, Conwy, LL31 9PX, UK
Type	BGGS
Length	3'540 mm
Weight	19.5 kg
Tool diameter	60 mm
Operational temperature range	0 – 70 °C (up to 80 °C for a limited time)
Max. pressure	20 MPa
Borehole diameter range	75 – 700 mm
Vertical sample rate	1 reading / cm
Caliper accuracy	± 5 mm (not on data sheet, information from manufacturer)
Caliper resolution	0.02 mm (not on data sheet, information from manufacturer)
Gamma detector	NaI 50 mm × 25 mm crystal

3.1.7 Gamma sensors

All probes described above are equipped with similar gamma-ray detectors. The detectors are of the scintillation type, set up for total count measurements. They consist of a NaI crystal (50 mm × 25 mm), a photomultiplier tube and a counting circuit. The output is counts per second (cps). No background radiation exists and has to be considered in a borehole.

The range of the sensors is 0 – 65'536 cps (16 bit). In a typical geological context of southern Germany and Switzerland the count rates normally do not exceed 300 – 400 cps with the given sensors.

Remarks on accuracy of a gamma measurement (Richards 1981): There is a statistical noise to the data, because it is possible to predict the rate of emission of gamma rays, but not which individual nuclei will disintegrate or not. It is possible to determine the true mean count rate (cps) for a given source of gamma-rays quite accurately by counting and averaging for a long time. The statistical noise produces a fluctuation of the readings around the true mean count rate. The expected standard deviation is the square root of the true mean count rate n.

The fractional standard deviation expresses the standard deviation as percentage of the true count rate:

fractional std. dev. = (std. dev.)/n*100

e.g. n = 10'000 cps → std. dev.: 100 cps, fractional std. dev.: 1%

n = 100 cps → std. dev.: 10 cps, fractional std. dev.: 10%

This means the precision of the measurement increases as the count rate increases.

3.1.8 Temperature-electrical conductivity meter

The WTW (Wissenschaftlich-technische Werkstätten GmbH) instrument pH/Cond 340i is a hand-held digital instrument to measure fluid pH, electrical conductivity and temperature (for specifications, see Tab. 3-7). This meter is used at the workshop to perform the electrical conductivity calibration of the logging tools, and on-site to check the calibration of electrical conductivity and temperature.

Tab. 3-7: Specifications for the temperature-electrical conductivity meter

Manufacturer	WTW (Wissenschaftlich-technische Werkstätten GmbH), Dr.-Karl-Slevogt-Straße 1, D-82362 Weilheim
Type	pH/Cond 340 i
Temperature sensor range	0 – 105 °C
Temperature sensor accuracy	± 0.1 °C
Electrical conductivity range	0 – 19.99 mS/cm (resolution 0.01), 0 – 199.9 mS/cm (resolution 0.1)
Electrical conductivity accuracy	± 0.5%
Reference temperature	25 °C

3.1.9 Centraliser

When the probes are run in the hole, they are equipped with a set of centraliser blades. The main purpose of the centralisers is to keep the probes off the borehole wall to prevent measurements being influenced by any debris that might be scraped off the borehole wall. For specifications, see Tab. 3-8.

The centralisers are made from brass rings with elastic copper – beryllium blades. The centraliser cage can be set up with different blades to cover different borehole diameter ranges. The blades are fixed to the probe by grub screws.

Tab. 3-8: Specifications for the centraliser

Manufacturer	LIM Logging / electromind s.a.
Type	Bow spring centraliser
Length	420 mm at 165 mm diameter, 530 mm at 215 mm diameter
Weight	Approx. 3 kg
Borehole diameter range	70 – 270 mm

3.1.10 Field analysis IT structure

Logging is performed directly into a WellCAD document to display previous and current measurements. For specifications of the IT structure, see Tab. 3-9.

Tab. 3-9: Specifications for the IT structure for field analysis

Processing software	WellCAD 5.2 build 1925 © Advanced Logic Technology, 1993 – 2018
Logging software	Matrix Logger: V 13.2 build 2790 © Advanced Logic Technology, 1995 – 2021
Logging software (heat pulse flowmeter only)	Matrix Heat: V3.3 build 2208 © Advanced Logic Technology, 2005 – 2012
Uninterrupted power supply	APC Back-UPS Pro 900 BR900-G, 900 VA / 540 Watt
Data back-up	External hard drive
Acquisition computer	Notebook, Windows 10 Pro

3.2 Performance and analysis

Fluid logging was conducted in borehole BAC1-1 from 04.10.2021 to 05.10.2021 in the cored borehole Section II after a fluid exchange of drilling fluid with freshwater was performed. The section was comprised of calcareous marlstone to limestone within the «Felsenkalke» +«Massenkalk», the Schwarzbach Formation, the Villigen Formation and the Wildegg Formation of the Malm Group.

The measurements were performed using the QL40 FTC temperature-conductivity-gamma probe described in Section 3.1.5. The objectives of the fluid logging analysis were detection of inflow zones and determination of their associated transmissivities. The transmissivity values of the inflow zones were derived from the total transmissivity determined by the analysis of the associated pumping test.

3.2.1 Description of measurements performed

For the execution of the test BAC1-1-FL1-MAL, drilling was carried out to a depth of 700 m MD, with the fluid logging being performed to a depth of approximately 690 m MD after the drilling fluid was exchanged with tap water. Tab. 3-10 provides the information on the open borehole section. An initial run with the temperature-conductivity-gamma probe (*cf.* Section 3.1.5) was performed before the pump was installed at a depth of 161.64 m MD. The pumping test included a rate withdrawal phase (RW) and subsequent recovery phase (RWR) (see Tab. 3-11 and Figs. 3-1 and 3-2). During the RW phase the pumping rate dropped to the limit of the flowmeter. For the RWR phase the downhole flow rate from the formation was calculated based on the pressure measurements and was nearly constant.

Within the RWR phase, the fluid logging Runs 3 to 8 were conducted. Tab. 3-12 and Fig. 3-3 present overviews of the fluid logging activities. Whereas for Runs 2 to 5 the logging was started around 7 m below the casing shoe, Runs 6 to 8 were conducted over the entire open borehole section length and some metres inside the casing, and as it became obvious during logging that

part of the inflow from the formation was taking place close to the casing shoe. Measuring within the casing would therefore capture the advective salinity front evolution due to the inflows below the casing shoe necessary to obtain a quantitative assessment of the inflow rates.

Tab. 3-10: Fluid logging BAC1-1-FL1-MAL: Information on the test interval

[1] Time between start of Run 1 and end of Run 8.

Test	**Depth**		**Length**	**Configuration**	**Hydraulic testing**		
	from [m MD]	to [m MD]	[m]		Start date	End date	Duration [1] [h]
BAC1-1-FL1-MAL	513.00	700.00	187.00	Open borehole	04.10.2021	05.10.2021	16.85

Tab. 3-11: Fluid logging BAC1-1-FL1-MAL: Pumping test phases

Phase	**RW**	**RWR**
Start date & time	04.10.2021 19:04	04.10.2021 20:56
End date & time	04.10.2021 20:56	05.10.2021 05:23
Duration [hh:mm]	01:52	08:27
Pressure (start / end) [kPa]	1'494.34 / 94.3	94.3 / 115.83

Tab. 3-12: Fluid logging BAC1-1-FL1-MAL: Runs with the temperature-conductivity-gamma probe

Logging Run	**Date**	**Start time**	**Start depth** [m MD]	**End time**	**End depth** [m MD]
1	04.10.2021	12:40	510.07	13:18	694.87
2	04.10.2021	20:25	521.07	20:56	690.07
3	04.10.2021	21:30	521.07	22:00	689.97
4	04.10.2021	22:30	521.07	22:59	689.97
5	05.10.2021	00:30	521.07	00:58	689.97
6	05.10.2021	02:00	499.97	02:31	689.87
7	05.10.2021	03:30	500.07	04:01	689.97
8	05.10.2021	05:00	500.07	05:31	689.97

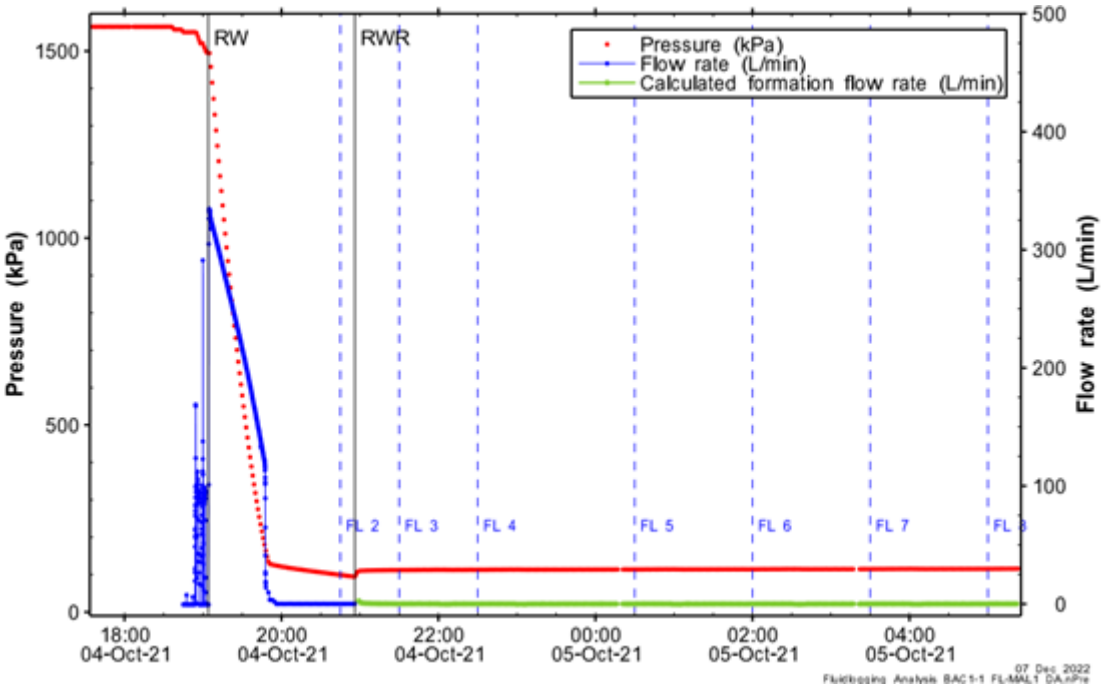

Fig. 3-1: Fluid logging BAC1-1-FL1-MAL: Flow rates and measured pressures during the RW and RWR phases, and the temporal position at which the fluid logging runs were performed

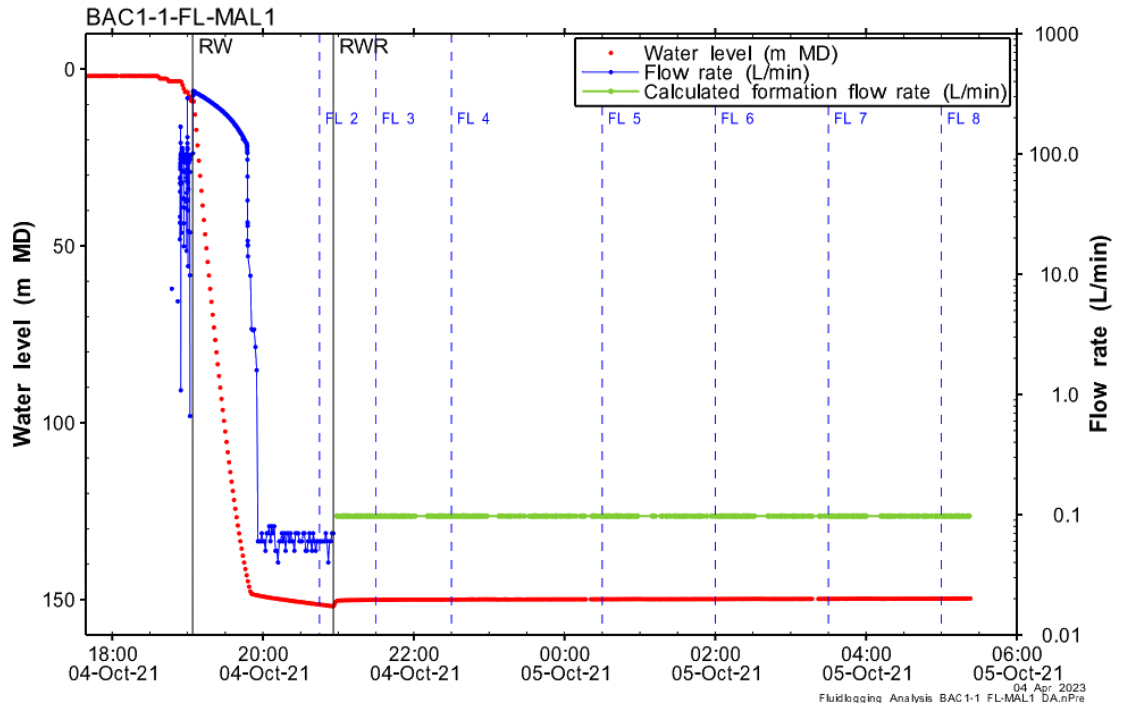

Fig. 3-2: Fluid logging BAC1-1-FL1-MAL: Calculated water level and measured surface flow rate during the RW phase and calculated formation flow rates based on water level variations in the casing during the RWR phase (rates as logarithmic scale), and the temporal position at which the fluid logging runs were performed

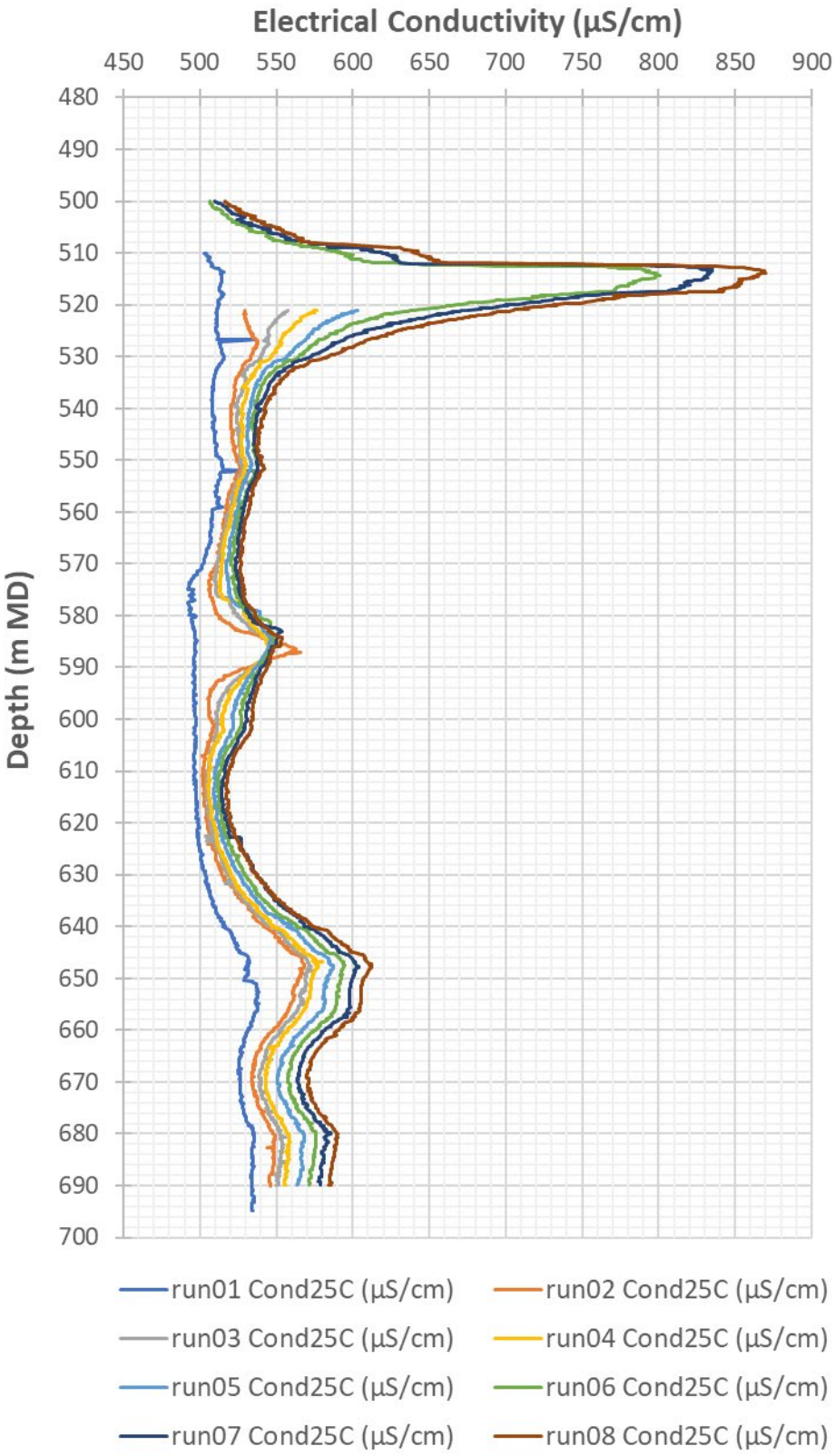

Fig. 3-3: Fluid logging BAC1-1-FL1-MAL: Measured electrical conductivity for Runs 1 to 8, calculated for a temperature of 25 °C

3.2.2 Analysis of pumping test data

The pumping test was analysed numerically using the software package nSIGHTS. The pre-test borehole history included the drilling phase and the fluid exchange. A radial composite flow model with a discrete skin zone was applied that was identified in the log-log diagnostic of the RWR phase. The perturbation analysis used optimised the simulated flow rate during the RW phase and the simulated pressure curve during the RWR phase to best represent the measured data. The optimised parameters were the hydraulic transmissivity T, the storage coefficient S and the static formation pressure P_f as well as the skin zone properties (skin hydraulic transmissivity, skin storage coefficient and skin thickness). The result of the perturbation analysis using 3'000 runs was an estimation of the best fit values and the confidence ranges (Tab. 3-13). The presented hydraulic conductivity along with the other formation parameters assumed a total contributing formation thickness of 187 m (513 – 700 m MD).

The analysis provided a best estimate for the transmissivity of the open borehole section (187 m) of 3.9×10^{-11} m^2 s^{-1} with 3.7×10^{-11} m^2 s^{-1} as a minimum and 1.3×10^{-10} m^2 s^{-1} as a maximum estimate.

Tab. 3-13: Fluid logging BAC1-1-FL1-MAL: Best estimates of the hydraulic parameters and their confidence ranges derived from the pumping test analysis in the framework of the fluid logging campaign

[1] Considering a contributing formation thickness of 187 m

[2] Pressure at the midpoint of the interval (606.5 m MD)

Parameter	**Minimum**	**Best estimate**	**Maximum**
Pumping test phases considered	RW + RWR		
Flow model	Radial composite flow model with a discrete skin zone		
Hydraulic conductivity (K) [1] [m s^{-1}]	2.0×10^{-13}	2.1×10^{-13}	6.9×10^{-13}
Total transmissivity (T) [1] [m^2 s^{-1}]	3.7×10^{-11}	3.9×10^{-11}	1.3×10^{-10}
Static formation pressure (P_S) [2] [kPa]	5'615	6'167	6'215

3.2.3 Fluid logging analysis

The fluid logging analysis was based on the implementation of a 1D advective-dispersive solute transport equation in a borehole with feed points along the borehole (Tsang & Hufschmied 1988 and Doughty & Tsang 2005).

Three complete runs of electrical conductivity (corrected to 25 °C equivalent conductivity) were considered for the analysis (Runs 6 to 8). The electrical conductivity of the runs that did not include the upper most part of the borehole was excluded from the analysis because an inflow zone could be clearly identified 5 – 6 m below the casing shoe, which could not be measured by these runs.

By visual inspection of the electrical conductivity for Runs 6, 7 and 8 (Fig. 3-3), five inflow zones were identified (Tab. 3-14).

Tab. 3-14: Fluid logging BAC1-1-FL1-MAL: Qualitatively detected inflow zones

Depth [m MD]	**Remark**
511.00 – 518.00	Indicated by electrical conductivity
582.00 – 586.00	Indicated by electrical conductivity
642.00 – 651.00	Indicated by electrical conductivity
653.00 – 660.00	Indicated by electrical conductivity
678.00 – 682.00	Indicated by electrical conductivity

The electrical conductivity logs obtained for Runs 7 and 8 were simulated and matched using the electrical conductivity distribution measured during Run 6 as the initial conditions in the borehole. Figs. 3-4 and 3-5 present the best matches between both measured and simulated profiles of electrical conductivity. In the quantitative analysis, the mapping of the five qualitatively determined inflows (Tab. 3-14) was simulated and refined.

The inflow zones finally identified by means of a quantitative analysis and their related inflow rate q_i, salinity C_i as well as the corresponding electrical conductivity EC_i are provided in Tab. 3-15.

The transmissivity values for the individual inflow zones (Tab. 3-15) were computed as the product of the total transmissivity of the logged borehole section obtained in the analysis of the pumping test data (Section 3.2.2) and the relative contribution of each of the individual flow rates to the total stabilised formation flow rate. Accordingly, the sum of the transmissivities of the inflows corresponds to the total transmissivity and it was assumed that the main source of uncertainty for the individual inflow zone transmissivity values was based on the total borehole section transmissivity derived by the corresponding pumping test analysis (Section 3.2.2). Hence, the confidence ranges for the transmissivity of the individual inflow zones were computed by propagating the uncertainty in each of the individual inflow zones of the total transmissivity of the whole borehole section provided in Section 3.2.2. Tab. 3-15 provides the results of the inflow zones.

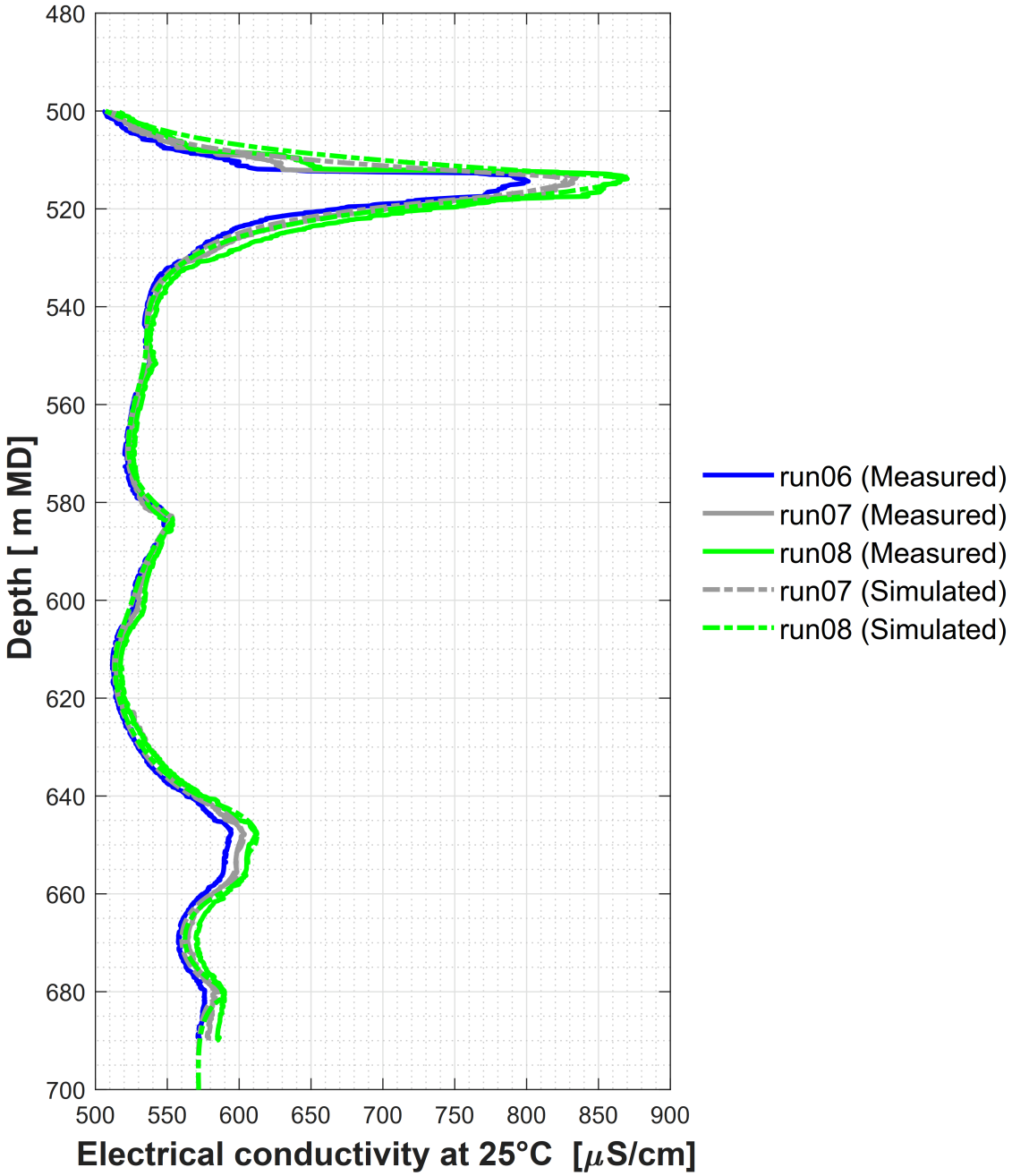

Fig. 3-4: Fluid logging BAC1-1-FL1-MAL: Measured and simulated Runs 7 and 8 using the measurement of Run 6 as the initial conditions

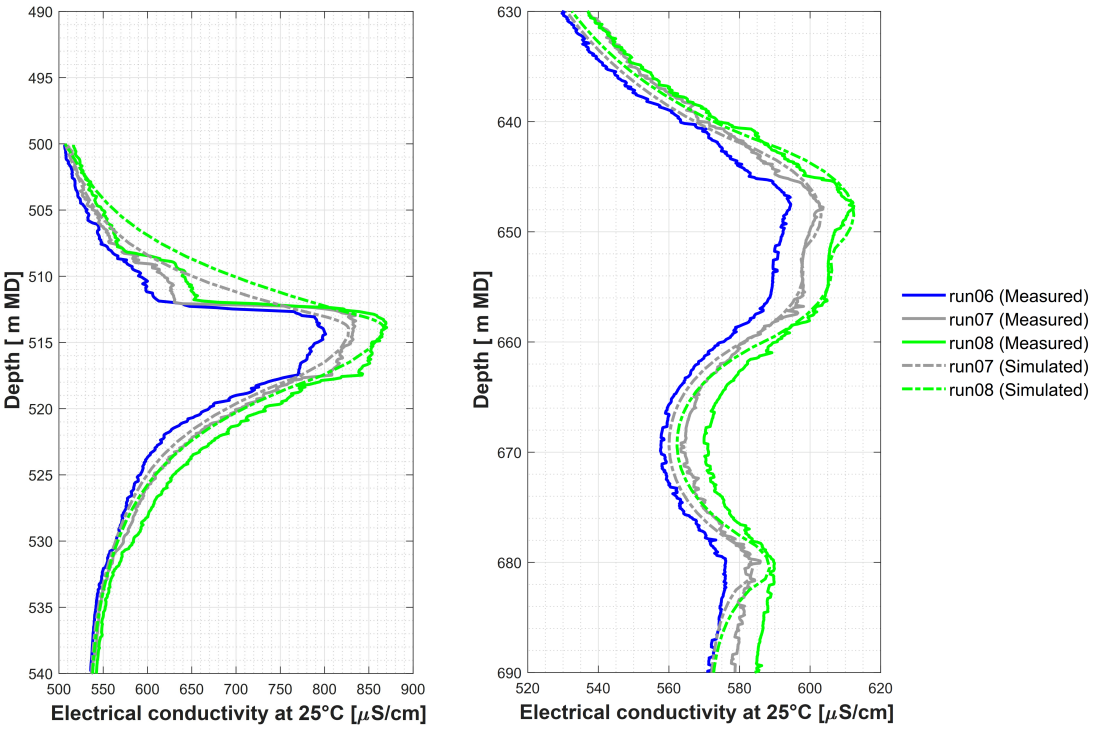

Fig. 3-5: Fluid logging BAC1-1-FL1-MAL: Measured and simulated Runs 7 and 8 using the measurement of Run 6 as the initial conditions (close-ups)

Tab. 3-15: Fluid logging BAC1-1-FL1-MAL: Depth and properties of the inflow zones (q_i, C_i, EC_i) and the best estimates and associated confidence ranges for transmissivity

[1] Based on the results presented by the field test contractor in the corresponding report.

[2] Inflow zone with two water conducting features.

Inflow zone	**Top** [m MD]	**Bottom** [m MD]	**q_i** [1] [l min^{-1}]	**C_i** [1] [g l^{-1}]	**EC_i** [1] [µS cm^{-1}]	**T_i min** [1] [m^2 s^{-1}]	**T_i best** [1] [m^2 s^{-1}]	**T_i max** [1] [m^2 s^{-1}]
1 [2]	511.00	515.00	0.035	8.0	13'720	1.3×10^{-11}	1.4×10^{-11}	1.5×10^{-11}
	516.00	518.00	0.023	6.5	11'586	8.5×10^{-12}	9.0×10^{-12}	9.5×10^{-12}
2 [2]	582.00	583.00	0.001	3.5	6'711	3.7×10^{-13}	3.9×10^{-13}	4.1×10^{-13}
	584.00	586.00	0.001	3.5	6'711	3.7×10^{-13}	3.9×10^{-13}	4.1×10^{-13}
3	642.00	651.00	0.01	2.0	3'970	3.7×10^{-12}	3.9×10^{-12}	4.1×10^{-12}
4	653.00	660.00	0.01	1.4	2'817	3.7×10^{-12}	3.9×10^{-12}	4.1×10^{-12}
5	678.00	682.00	0.02	0.7	1'430	7.4×10^{-12}	7.8×10^{-12}	8.2×10^{-12}

3.3 Summary and discussion of fluid logging results

A fluid logging campaign was performed in borehole Section II in order to hydraulically characterise the Malm Group between the depths of 511 and 700 m MD. Because no sufficiently high transmissivities were detected to take a water sample, no hydraulic packer test was conducted in this interval. The test interval of the hydraulic packer test BAC1-1-MAL1 (*cf.* Section 4) is below the fluid logging interval.

The analysis of the inflow zones was based on the evaluation of the electrical conductivity profiles from Runs 6, 7 and 8, performed during the pressure recovery phase RWR following a short pumping period. A visual inspection qualitatively indicated five separate inflow zones in the «Felsenkalke» + «Massenkalk» (511.00 – 549.69 m MD), Villigen Formation (570.98 – 637.31 m MD) and Wildegg Formation (637.31 – 700.00 m MD) of the Malm Group. The quantitative analysis resulted in a more refined definition with a total of seven water conducting features. The uppermost feature directly below the casing shoe presents the highest salinity and inflow rate. The total transmissivity of 3.9×10^{-11} m^2 s^{-1} calculated for the entire open borehole section by the analysis of the associated pumping test (Section 3.2.2) was attributed mainly to this uppermost feature (511 – 515 m MD) with a hydraulic transmissivity of 1.4×10^{-11} m^2 s^{-1} and the feature immediately below (516 – 518 m MD) with a hydraulic transmissivity of 9.0×10^{-12} m^2 s^{-1}.

The resulting hydraulic properties were based on a perturbation analysis of the corresponding pumping sequence RW-RWR using 3'000 runs. The confidence ranges of the total hydraulic transmissivity estimated by the associated pumping test (Section 3.2.2) ranged from 3.7×10^{-11} to 1.3×10^{-10} m^2 s^{-1}. This uncertainty range was used to characterise the uncertainty ranges of the hydraulic transmissivity of the separate water conducting features.

The main inflow was attributed to the «Felsenkalke» + «Massenkalk» (511 – 515 m MD and 516 – 518 m MD) with a transmissivity between 2.1×10^{-11} m^2 s^{-1} and 2.5×10^{-11} m^2 s^{-1}. No cores could be collected in this limestone section. The transmissivity of the other identified water conducting features ranges between 3.7×10^{-13} m^2 s^{-1} and 8.3×10^{-12} m^2 s^{-1}, generally more than one order of magnitude less than the uppermost feature.

4 Hydraulic packer tests

4.1 Test strategy

The geological formations examined within the TBO boreholes exhibit a wide range of transmissivities. The host rock, Opalinus Clay, and its confining units are expected to have very low transmissivities, whilst the regional aquifers like the Malm and the Muschelkalk formations are expected to have relatively high transmissivities.

Nagra has long established hydraulic testing strategies (e.g. Nagra 1997) to extract the maximum information in relation to the hydraulic characteristics of the various geological formations. Two testing strategies are preferred (Tabs. 4-1 and 4-2) depending on the transmissivity of the formation (low to very low or medium to high). A typical test sequence is divided into different test phases: test preparation, diagnostic and main phase. The test sequence may be concluded with a pulse test (PW/PI) to check if the total test interval compressibility changed during the test. Modifications to the strategies are made according to the preliminarily available information, the encountered specific test conditions and obtained results while testing. This may lead to the omission of certain test phases, e.g. the diagnostic phase.

The main difference in the two testing strategies is the selection of appropriate test types and phases as well as the duration of the test phases. In a formation with medium to high transmissivity, pressure disturbances due to drilling or temperature effects dissipate relatively quickly. Accordingly, the test preparation phase is short. The main phase delivers results of sufficient accuracy with respect to the hydraulic properties of the formation in a relatively short period.

In the case of formations with low to very low transmissivity, the test types and their duration are different. For the determination of hydraulic head, the borehole pressure history and test duration are important issues. Depending on the pressure difference between the static formation conditions and the pressure induced in the borehole during the pre-test pressure history, the estimates of hydraulic head can be strongly affected by non-static pressure conditions in the surrounding borehole area.

A further aspect of the testing strategy is the use of drilling fluid as a test fluid (see Tab. 1-1). The water-based drilling fluid used for drilling contained polymers as additives for interval BAC1-1-MUK1 and potassium silicate and polymers for all other intervals (*cf.* Dossier I). In contrast to previous exploration boreholes drilled by Nagra (e.g. Benken), no exchange of drilling fluid in the test intervals was performed in the BAC1-1 borehole prior to hydraulic testing. The main reason for this was the maintenance of borehole stability. An exception to this was the hydraulic test BAC1-1-BDO3 conducted with synthetic pore water as test interval fluid after a fluid exchange of the drilling fluid over the upper packer.

The hydraulic test BAC1-1-BDO3 was performed to determine the reopening pressure of a drilling-induced fracture and to understand the observed losses of about 15 m^3 of drilling fluid (*cf.* Dossier I). This artificially disturbed part of the formation was further investigated by hydraulic tests BAC1-1-OPA3. The hydraulic test BAC1-1B-BDO4, was performed in the sidetrack Bachs-1-1B (*cf.* Section 1.2) at about the same depth as tests BAC1-1-BDO3 and BAC1-1-OPA3. Because borehole stability risks prevented to run the micro-hydraulic fracturing (MHF) tool in the side track (BAC1-1B), the hydraulic packer test equipment was used to perform micro hydraulic fracturing, following test BAC1-1B-BDO4 in the sidetrack. The analysis of the MHF test performed in test interval BAC1-1B-BDO4 is documented Dossier VI.

Finally, the model implementation as a skin in the test analysis was assumed to adequately address any issues linked with drilling fluid properties at the borehole wall.

Tab. 4-1: Preferred test sequence for formations with medium to high transmissivity

[1] For explanation of abbreviations see Tab. A-3.

Test phase	**Phase**[1]	**Aims**
Test preparation phase	COM	Temperature and pressure equilibration in the test interval
	PSR	Pressure static recovery with closed shut-in tool; create pressure conditions for the initiation of the first test, first estimate of formation pressure; recognition of temperature and pressure trends
Diagnostic phase	PW	First estimates of hydraulic conductivity, which are used to plan the following test sequence
Diagnostic / main phase	SW	Estimation of hydraulic conductivity, which is used to plan the following test sequence, especially the pumping rate and drawdown of the RW phase
	SWS	Estimation of an accurate flow model and hydraulic parameters; hydrostatic pressure for subsequent pumping phase
Main phase	RW	Defined signal with a larger radius of influence; allows a representative groundwater sample of the formation to be taken as well as the detection of boundary conditions
	RWS	Estimation of an accurate flow model and hydraulic parameters as well as boundary conditions
Optional	PW/PI	Estimation of the total test interval compressibility at the end of the test

Tab. 4-2: Preferred test sequence for formations with low to very low transmissivity

[1] For an explanation of the abbreviations see Tab. A-3.

Test phase	**Phase**[1]	**Aims**
Test preparation phase	COM	Temperature and pressure equilibration in the test interval
	PSR	Pressure static recovery with closed shut-in tool; create pressure conditions for the initiation of the first test, first estimate of formation pressure; recognition of temperature and pressure trends
Diagnostic phase	PW	First estimates of hydraulic conductivity, which are used to plan the following test sequence
Main phase Version 1	SW	Estimation of hydraulic formation parameters during a flow phase
	SWS	Estimation of an accurate flow model and hydraulic parameters during shut-in conditions
	PW/PI (optional)	Estimation of the total test interval compressibility at the end of the test
Main phase Version 2	PW/PI	Estimation of hydraulic formation parameters (as an alternative to SW/SWS)

4.2 Test equipment

The most relevant components of the field test contractor's equipment have been drawn from the associated mobilisation report and are presented below.

4.2.1 Downhole equipment

The packer system referred to as the hydraulic test tool (HTT) was used for all hydraulic packer tests in open borehole sections. It consisted of a top and bottom inflatable packer (non-inflated outer diameter 114 mm for borehole BAC1-1, except for test BAC1-1-BDO3 where packers with an outer diameter of 146 mm were used) in order to confine a test interval of appropriate length for the intended test (Fig. 4-1). Inflow and outflow occurred through a perforated filter segment covered by a filter screen mounted on the 2⅞" tubing above the bottom packer.

Four pressure transducers, mounted in a probe carrier shell above the top packer and referred to as the quadruple sub-surface probe or quadruple probe (QSSP), measured the pressures below (P1), within (interval pressure P2) and above the test interval (annulus pressure P3) as well as in the test tubing above the downhole shut-in tool (P4). In addition, the pressure in the test interval was recorded with an autonomous memory gauge at the bottom of the filter screen (P2*).

Temperatures were measured at the level of the QSSP by the temperature sensors associated with each pressure transducer (referred to as T1, T2, T3, T4, respectively) and additionally by the sensor associated with the memory gauge mentioned above (named T2*).

A hydraulically controlled non-displacement downhole shut-in tool (SIT) placed above the probe carrier shell was used to isolate the test zone from the test tubing (2⅞" EUE API CT5 L80). A progressive cavity pump (PCP) or Moyno® type pump or a pump housing with a 4" submersible pump, integrated in the test tubing, was used for production pumping tests.

Additionally, a piston pulse generator (PPG) could be mounted in the test interval. The use of a PPG allowed for reduction of the uncertainty associated with determination of the test zone compressibility on conduction of pulse tests in formations with low transmissivity.

For testing in single packer configuration (Fig. 4-2), the system was set up without the bottom packer but with a prolongation of the interval string and the filter(s) at the bottom. Inflow and outflow occurred through one or two perforated filter segment(s) covered by a filter screen mounted on a 2⅞" tubing at the bottom of the prolongation.

The quadruple flat-pack consisted of three hydraulic steel tubes of ¼" outer diameter (OD) and one electrical conductor coated in a thermoplastic protective cover. Two steel tubes were used for packer inflation and one for control of the SIT and the pressure release valve (PRV), which was only used when the packers could not be sufficiently deflated by opening the packer lines at the surface.

Certain parts of the downhole equipment are described below in more detail.

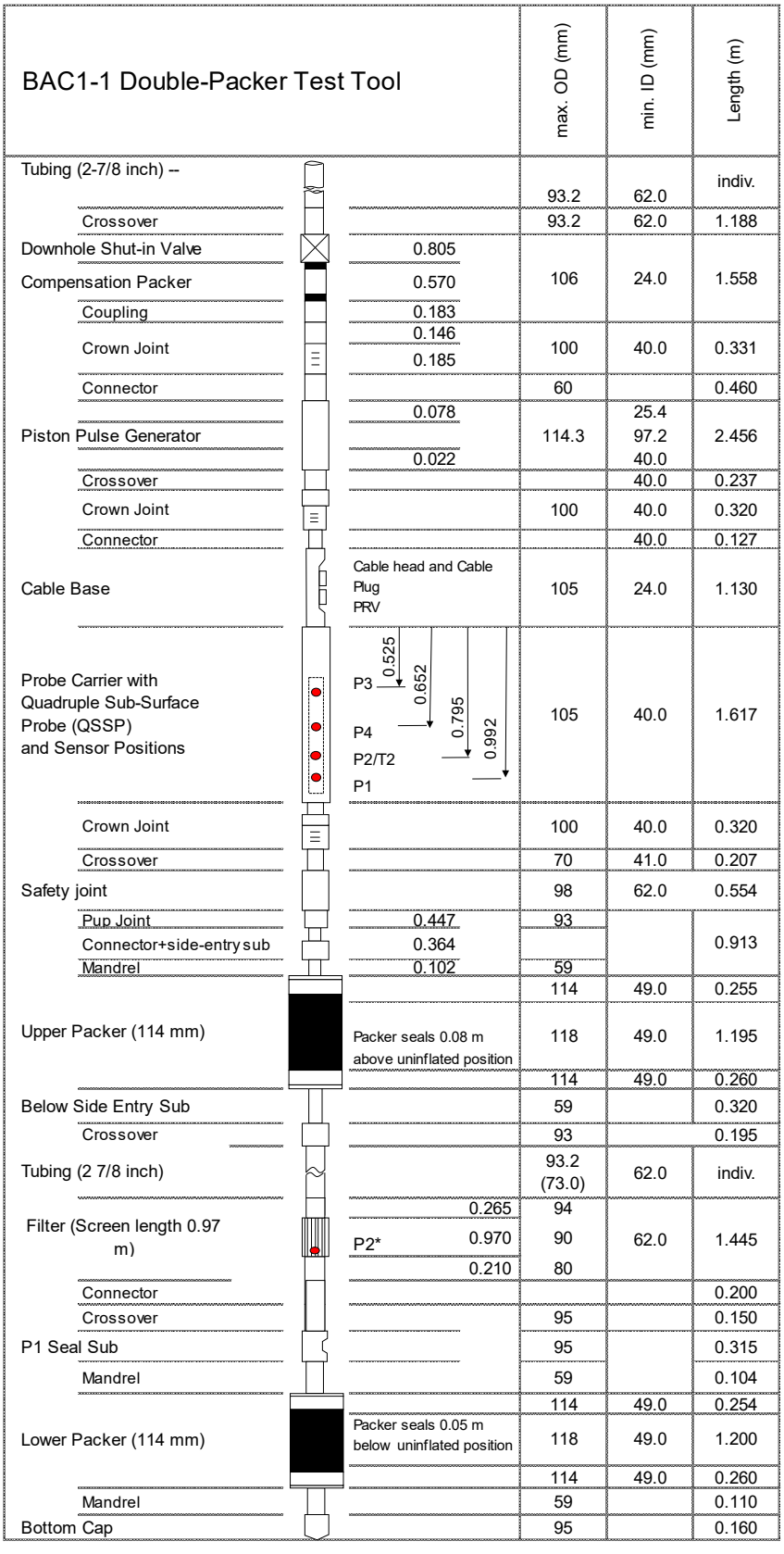

Fig. 4-1: General configuration and specifications of the HTT in double packer configuration

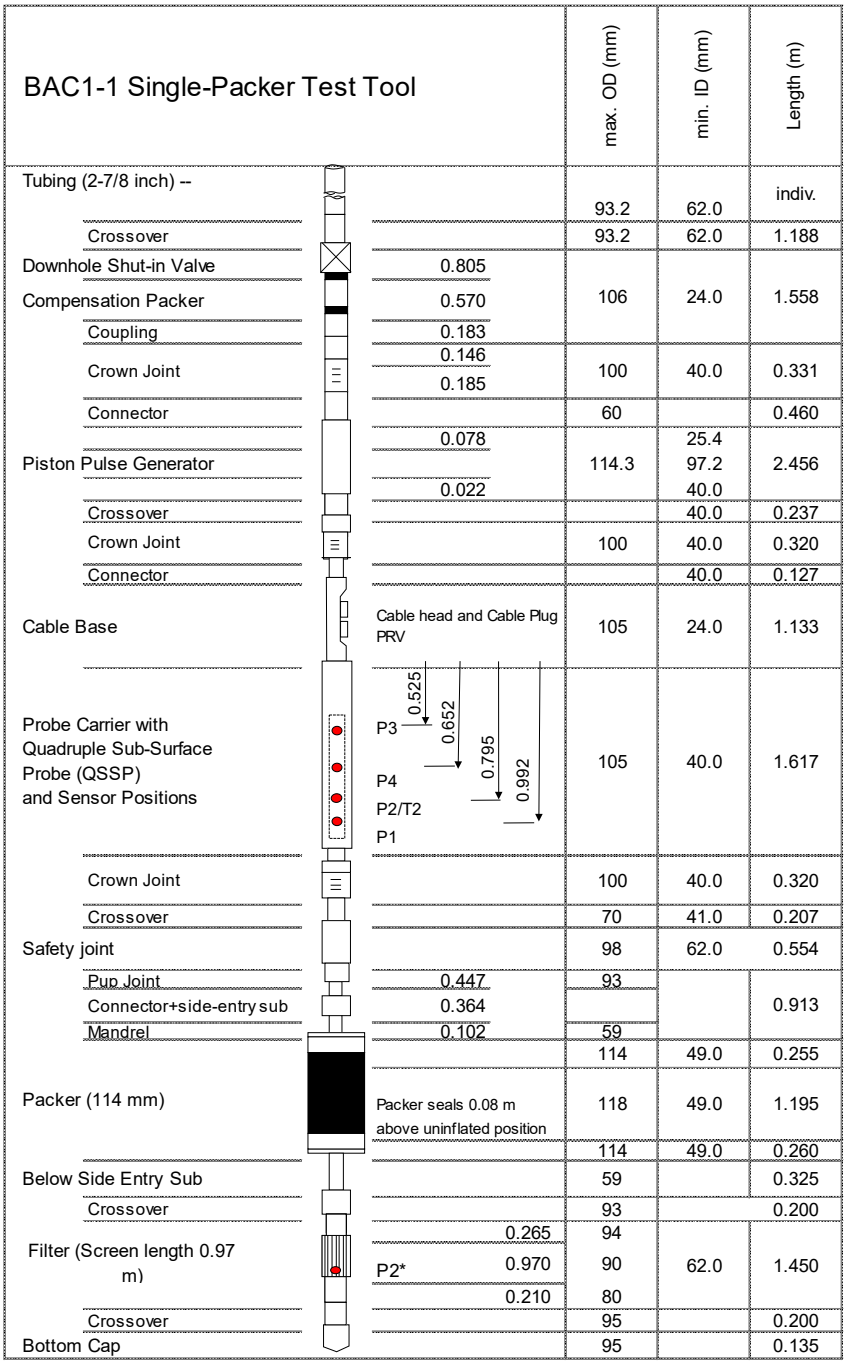

Fig. 4-2: General configuration and specifications of the HTT in single packer configuration

4.2.1.1 Heavy-duty double packer system

The technical data of the hydraulic test tool (HTT) are provided in Tab. 4-3. A summary of the downhole equipment with the most important specifications is given in Tab. 4-4.

Tab. 4-3: Specifications for the HTT

Tool Description	**HTT**
Packer configuration	Double packer or single packer
Maximum installation depth	1'400 m (vertical); 1'500 m (inclined) along borehole axis
Maximum fluid pressure	20'000 kPa
Maximum differential pressure	114 mm packer system for 162 mm borehole: ~ 12'200 kPa 146 mm packer system for 216 mm borehole: ~ 8'000 kPa
Maximum downhole temperature	80 °C
Range of interval length	3 – 100 m
Probe	QSSP
Shut-in tool (SIT)	Zero-displacement valve
Control lines	4 core encapsulated flat-pack • Hydraulic line – bottom packer (PA1) • Hydraulic line – top packer (PA2) • Hydraulic line – shut-in tool (SIT) and packer pressure release valve (PRV) • ⅛" (3.175 mm) OD tubing encased single conductor cable

Tab. 4-4: Specifications for the HTT components

Component	**Specifications**	**Minimum inner diameter ID** [mm]
Quadruple flat-pack	3 each ¼" OD × 0.035" WT 316L stainless steel welded and cold drawn annealed tubes 153'339 kPa nominal burst pressure 49'139 kPa maximum test pressure Incorporating 1 each ⅛" OD × 0.022" WT316L stainless steel 16 AWG solid CU conductor /P/N 024440) encapsulated to ¼" OD in TT200 thermoplastic Encapsulated as 33 mm × 11 mm in TT210 thermoplastic, suitable for maximum 98.9 °C brine service	
Tubing	2⅞" EUE API CT5 L80	62
Pup joints	2⅞" EUE API CT5 L80	62
Piston pulse generator (PPG) housing	4½" 4140 alloy steel pipe, WT 0.337", 15 lb/ft	97
Shut-in tool (SIT)	Duplex 1.4462	24
Pressure release valve (PRV)	Duplex 1.4462	24
Cable base	Duplex 1.4462	
Quadruple sub-surface probe (QSSP)	Duplex 1.4462 4 pressure sensors P1, P2, P3 and P4	3 × Ø19
Coarse thread safety joint	$3^{21}/_{32}$" OD, with $2^{7}/_{16}$" bore with 2⅞" EUE box × pin connections	64
Packers for large borehole diameter	IPI 5¾" (146 mm), steel wire reinforced, duplex, natural rubber Packer 1 Packer 2	 49 49
Packers for normal borehole diameter	IPI 4½" (114 mm), steel wire reinforced, duplex, natural or nitrile rubber Packer 1 Packer 2	 49 49
Filter	HP well screen: sand free filter screen mounted on 2⅞" tubing L 80 Length: 0.50 m Length: 1.00 m	 73 73

4.2.1.2 Packers

Two types of packers were available for use, a 114 mm packer for 162 mm diameter boreholes and a 146 mm packer for 216 mm diameter boreholes (Tab. 4-5). The packers were individually inflated with water through the packer inflation line. The inflation line was integrated in the quadruple flat-pack using a booster pump and anti-freeze was added to the water. Both packer pressure lines were connected to the packer control board at the winch and equipped with pressure sensors (pressure range 0 – 30'000 kPa) for packer pressure monitoring. The packer pressure sensors were connected to the data acquisition system (DAS) for continuous recording. To keep packer pressures constant, the packers were connected to a pressure-maintenance system (see Section 4.2.2.2).

Tab. 4-5: Specifications for the HTT packers

Manufacturer	Inflatable Packers International, Perth, Australia	
Packer types	IPI 4½" (114 mm)	IPI 5¾" (146 mm)
Material and type	Duplex, natural rubber or nitrile, sliding end	Duplex, natural rubber, sliding end
Reinforcement type	Steel wire reinforced	Steel wire reinforced
Borehole diameter	162 mm	216 mm
Packer diameters	125 – 230 mm (pressure dependent)	162 – 280 mm (pressure dependent)
Outer diameter, not inflated	114 mm max.	146 mm max.
Inner diameter	49 mm min.	49 mm min.
Overall length: Bottom packer Top packer	 1.93 m 2.08 m	 1.92 m 1.92 m
Rubber sleeve length	1.20 m	1.20 m
Thread connections	2⅞" EUE pin × 2⅞" EUE box	2⅞" EUE pin × 2⅞" EUE box
Max. working temperature for a period > 100 h	+80 °C	+80 °C
Packer inflation lines	Quadruple flat-pack, see Tab. 4-4	Quadruple flat-pack, see Tab. 4-4
Inflation method	Surface controlled	Surface controlled
Inflation fluid	Water and anti-freeze (if necessary)	Water and anti-freeze (if necessary)

4.2.1.3 Downhole sensors in the quadruple sub-surface probe

Four Keller PA-27XW transducers (for transducer types and specifications see Tab. 4-6) were used to monitor fluid pressures in the interval below the bottom packer (P1), within the testing interval (P2), in the annulus between the tubing and borehole wall above the top packer (P3) and in the test string (P4) above the downhole SIT. These four transducers were mounted in the QSSP probe, which was integrated in the probe carrier (see Fig. 4-1). The pressure sensors measured absolute pressure and corrected it to atmospheric pressure; the sensors showed a maximum of ± 8 kPa at atmospheric pressure conditions on-site.

Each pressure transducer had an associated temperature sensor (referred to as T1, T2, T3 and T4) for full thermal compensation of the pressure measurement (Tab. 4-6). The temperature sensor was mounted inside the pressure transducer housing. Because the temperature measurements were taken at the positions of the pressure transducers, they may not represent the effective temperature of the test interval fluid.

Tab. 4-6: Specifications for the pressure transmitters mounted in the QSSP

[1] FS = full scale

Pressure transducer type	Keller PA-27XW, custom-made
Manufacturer	Keller, Winterthur, Switzerland
Year of commissioning	2018
Pressure range (full scale)	0 – 20'000 kPa (absolute)
Accuracy	-0.004…0.005% FS[1]
Resolution	< 0.0007% FS
Minimum recording rate	1 Hz
Temperature range (FS)	-10 °C to 80 °C
Accuracy (temperature)	1 °C
Resolution (temperature)	0.01 °C
Output signal	RS485 (digital)

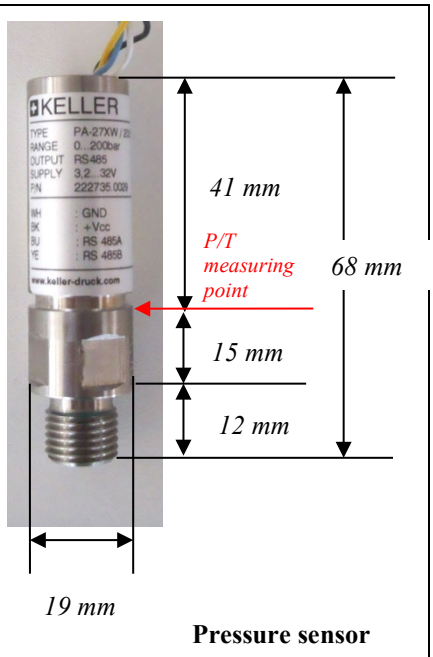

4.2.1.4 Autonomous data logger in test interval

Pressures and temperatures were recorded as redundant measurements in the interval at the lower end of the filter screen (referred to as P2* and T2*, respectively) with an autonomous data logger of the type DataCan Memory Pressure Gauges. The specifications are given in Tab. 4-7. The recorded pressure measurement is an absolute measurement.

Tab. 4-7: Specifications for the data logger

[1] FS = full scale

Data logger type	DataCan Memory Pressure Gauge 1.25" Welded Piezo III
Manufacturer	DataCan, Red Deer, Canada
Pressure range (FS[1])	0 – 20'684 kPa (absolute)
Pressure accuracy	0.0022% FS
Resolution	0.0003% FS
Temperature range	0 – 150 °C
Temperature accuracy	0.25 °C
Resolution	0.005 °C
Memory capacity	1'000'000 datasets
Minimum recording rate	1 Hz
Year of commissioning	2020

4.2.1.5 Zero-displacement shut-in tool

The downhole SIT controlled the fluid connection between the interior of the test tubing and the test interval. The SIT is a zero-displacement valve that is hydraulically operated via a hydraulic line integrated in the quadruple flat-pack using a booster pump. An axially moveable valve piston opens and closes the valve. The valve piston is moved via the hydraulic (closure) line by applying pressure to close the valve. Releasing the pressure with a pre-stressed spring resets the valve piston and opens the valve (pressure-free opening).

With a pressure compensation element, the pressure at interval depth (annulus pressure) is used to support the spring and to keep the opening/closing pressure constant for the entire borehole depth. The spring force is high enough to ensure a proper functioning of the valve even at low groundwater levels. The specifications are given in Tab. 4-8.

Tab. 4-8: Specifications for the zero-displacement shut-in tool

Zero displacement shut-in tool (SIT)	Manufactured by Solexperts
Maximum water flow rate	Below 40 l/min without friction loss, max. 350 l/min
Pressure loss caused by SIT at a flow rate of 1 l/min and 10 l/min	± 0 kPa
Closing pressure	9'000 – 10'500 kPa

4.2.1.6 Test tubing

The test rods were made of API 5CT-05 2⅞" tubing. The detailed specifications of the test tubing are summarised in Tab. 4-9.

Tab. 4-9: Specifications for the test tubing

Test tubing type	Seamless steel tubing and pup joints: 2⅞" 6.5 ppf L80 B*P EUE R2 API 5CT
Manufacturer	Normec, Celle, Germany
Steel grade	L80
Inner diameter	62.00 mm
Outer diameter	73.02 mm
Coupling outer diameter	93.20 mm
Thread	API 2⅞" EUE
Weight per meter	9.68 kg
Volume per meter	3.02 l
Individual tubing length	Range 2, ~ 9.5 m
Number of individual tubing lengths	154 (including 9 pup joints)
Total length of test tubing	Approx. 1'450 m
Lengths of pup joints	Length, quantity 0.38 m, 1 1.0 m, 1 2.0 m, 2 3.0 m, 2 4.5 m, 3

4.2.1.7 Slim tubing

The rate of pressure increase during the flow phase of a slug test depends on the formation transmissivity and the diameter of the test tubing, which mainly defines the wellbore storage of the test system during the slug. To improve the resolution of the pressure change, slim tubing was used to reduce the diameter of the test tubing for slug tests in formations with low transmissivity. However, the use of the slim tubing in formations with low transmissivity reduces the dominance of the wellbore storage term that is defined by the diameter. In this case, the wellbore storage term that is determined by the compressibility of the test fluid as well as the equipment (defined by determining the test zone compressibility during a shut-in phase) must be taken into account (Black et al. 1987).

The slim tubing consists of a stiff tube, which is installed into the test tubing. A packer at the bottom of the slim tubing with an outer diameter of 56 mm sealed the annulus between the 2⅞" tubing and the slim tubing. The water level in the slim tubing was measured with the P4 sensor from the QSSP. The technical specifications of the slim tubing are summarised in Tab. 4-10.

After lowering the water level in the 2⅞" test tubing for a slug withdrawal test to the specified depth, the slim packer and slim tubing were installed in the tubing below the water level. Afterwards, the slim tubing packer was inflated, and the test was started by opening the SIT valve. The water level only increased in the slim tubing. The use of a stiff tube ensured a constant inner diameter independent of the pressure (fluid level). It should be noted, however, that in the numerical analysis an effective diameter of the slim tubing must be used (Black et al. 1987).

Tab. 4-10: Specifications for the slim tubing

[1] FS = full scale

Types	Polyethylene tube	Stainless steel tube	Legris Polyamide Calibre tube
Inner diameter	12 mm	6 mm	4 mm
Outer diameter	16 mm	8 mm	6 mm
Length	300 m	300 m	700 m
Packer specifications	Diameter 56 mm, sealing length 1'000 mm, working pressure 1 – 13.5 MPa		
Packer pressure line	Polyamide OD: 6 mm; ID: 3 mm		
Packer pressure sensor	Keller PA-23SY, 0 – 5'000 kPa, accuracy 0.25% FS[1] Keller PA-27XW, 0 – 3'000 kPa, accuracy < 0.07% FS, linearity 0.2% FS		
Installation procedure	Slim packer installed on sucker rods		

4.2.1.8 Submersible pumps

Frequency driven 3" and 4" Grundfos submersible pumps can be used for pumping tests and during open-hole pumping, e.g. for fluid logging. The specifications are included in Tab. 4-11. The flow rate can be arbitrarily adjusted due to the frequency control of the pump.

Tab. 4-11: Specifications for the submersible pumps

Submersible pump types	4" down-hole pump	3" down-hole pump
Manufacturer	Grundfos, Fällanden, Switzerland	
Type	SP14-27E	SQE1-110
Regulation	Frequency-controlled	Frequency-controlled
Dimensions	101 × 3'040 mm	74 × 852 mm
Pumping rate at 150 m	100 l/min	10 l/min
Range of pumping rates	Max. 300 l/min	Max. 28 l/min
Maximum installation depth	160 m	160 m
Maximum temperature	40 °C	35 °C
Weight	57 kg (pump) 31 kg (motor)	6 kg
Pump housing	Yes	No
Specifications of pump housing	Length: 4.22 m OD max: 180 mm Weight: 130.3 kg	
Purpose	Pumping tests	Pumping tests, fluid logging

4.2.1.9 Progressive cavity pump

For constant rate or constant head withdrawal tests (pumping tests) a progressive cavity pump (PCP), a so-called Moyno® type pump, was used. The PCP consisted of a helical rotor and a twin helix in a rubber stator. The stator was integrated into the test tubing string and allowed for pumping, if necessary, but did not preclude any other test methods. For pumping, a suitable rotor had to be installed by means of the so-called sucker rods until the rotor had fully penetrated the stator. The pump specifications are listed in Tab. 4-12.

Tab. 4-12: Specifications for the PCP

Type	Progressive cavity pump (PCP)
Manufacturer	Netzsch
Dimensions	Drive head: L × W × H: 1'375 × 767 × 1'263 mm
Pumping rates	1.7 – 60 l/min Pumping rates of < 1.7 l/min can be reached by closing the valve installed in-line at the wellhead
Maximum installation depth	290 m
Temperature	10 °C to 70 °C
Sucker rods, type	¾" × 7.62 m
Sucker rods, quantity	38
Total length	Approx. 300 m
Available stators	1 for pump rates 10.4 – 60 l/min, Temp. 10 °C to 70 °C 1 for pump rates 1.7 – 5.5 l/min, Temp. 10 °C to 70 °C
Available rotors	3 for pump rates 10.4 – 60 l/min, Temp. 10 °C to 30 °C, 30 °C to 50 °C, 50 °C to 70 °C 3 for pump rates 1.7 – 5.5 l/min, Temp. 10 °C to 30 °C, 30 °C to 50 °C, 50 °C to 70 °C

4.2.1.10 Piston pulse generator

The piston pulse generator (PPG) is an optional downhole tool. It brings a unique and proven technology for conducting pulse tests to the more traditional low-permeability hydraulic testing realm. In an effort to reduce the uncertainty associated with determining the test zone compressibility, a hydraulic piston (i.e. the PPG) of known volume is incorporated into the HTT. This PPG resides within the test zone but not conventionally in between the packers. The PPG is contained within a housing that is located above the top packer and below the downhole SIT.

When deployed in a borehole, the piston is put into the appropriate position (fully extended or fully retracted), the packers are inflated, the SIT is closed, thereby isolating the test zone from the rest of the borehole, and the test zone is allowed to equilibrate for a period of time.

When it has been decided to initiate a pulse with the PPG, fluid from the pressurised fluid reservoir is routed to the appropriate hydraulic line (piston extend or piston retract) through the hydraulic control panel, thereby changing the position of the piston and changing the test zone volume by a known amount in less than two minutes. The resulting test zone pressure change is measured and can be used for the calculation of the interval storage / test zone compressibility. The specifications are listed in Tab. 4-13.

It should be noted that only one piston can be deployed at a time and the piston must be either fully extended or fully retracted. Therefore, only displacement volumes of 50 ml, 250 ml or 500 ml can be achieved once the HTT is deployed.

Tab. 4-13: Specifications for the piston pulse generator

PPG type	INTERA-PPG-1
Manufacturer	HydroResolutions
Dimensions of housing	OD: 0.1143 m Length: max. 2.455 m
Piston displacement	50, 250 or 500 ml
Weight	Max. 79 kg
Material	Steel

4.2.2 Surface equipment

The surface equipment consisted of the following equipment:

- Winch for quadruple flat-pack cable
- Flow control system
- Pressure-maintenance system
- PCP drive head and control unit
- Data acquisition system

Most of the surface equipment parts were installed in a mobile measuring trailer.

4.2.2.1 Flow board

For the control and measuring of pump (and injection) rates, a flow board with two flowmeters of type Yokogawa AXF were available. The flowmeters covered a flow rate range between 0.1 and 100 l/min (Tab. 4-14). The schematic layout of the flow control unit is displayed in Fig. 4-3.

Tab. 4-14: Specifications for the flowmeters

[1] FS = full scale

	Measuring range and accuracy			
	Lower limit		**Upper limit**	
	[l/min]	[% FS[1]]	[l/min]	[% FS]
AXF 010	0.1	1	11.78	0.35
AXF 025	1.0	1	100	0.35

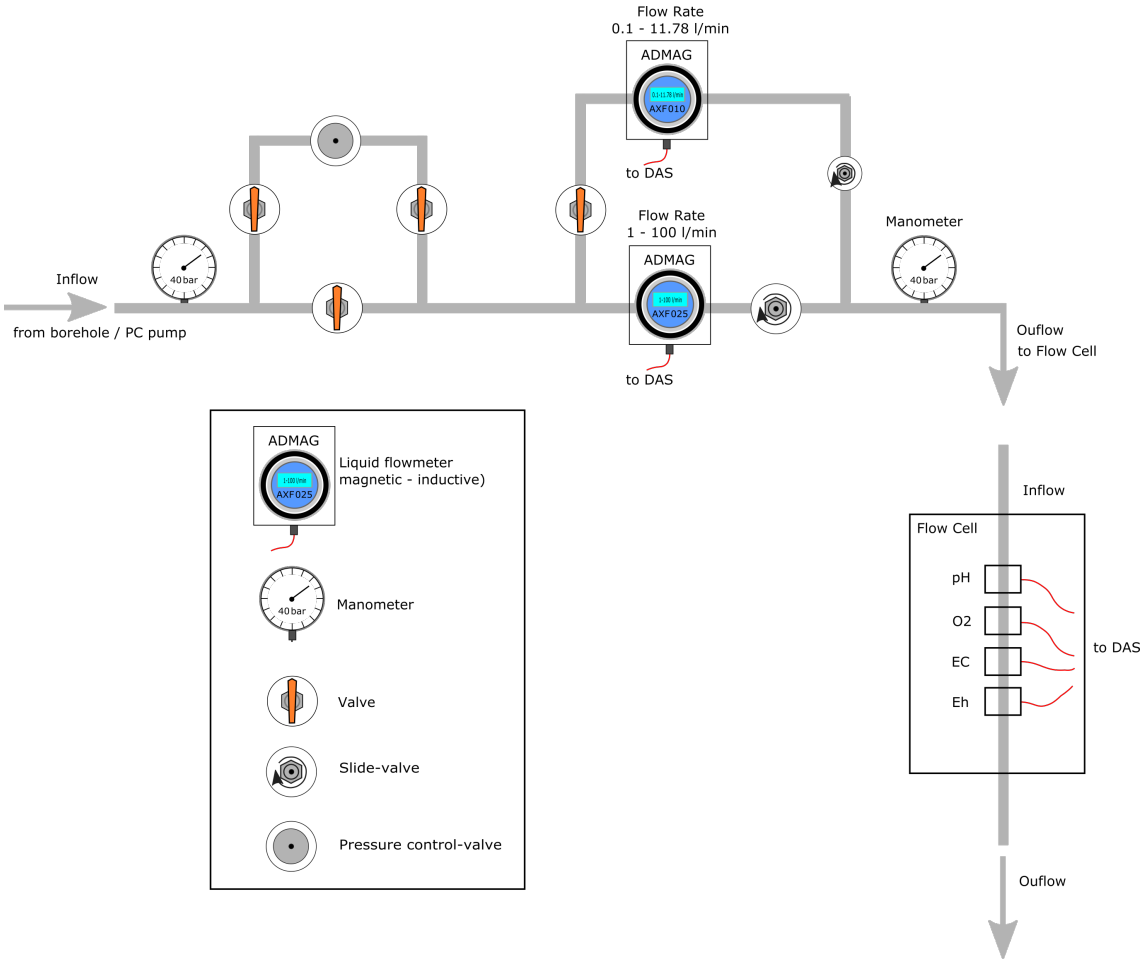

Fig. 4-3: Schematic layout of the flow control unit

4.2.2.2 Packer pressure-maintenance system

The packer pressure-maintenance system had four principal components: a pressurised nitrogen source (bottle) with pressure regulator, an Alicat pressure controller, a high-pressure hydraulic accumulator containing pressurised nitrogen over packer-inflation fluid, and a Mettler digital scale to monitor changes in the fluid volume in the reservoir. The Alicat flow controller was connected to the nitrogen bottle and to the reservoir. The desired packer-inflation pressure ("set" point) was entered into the controller, which had its own pressure sensor, and the controller then added nitrogen to the reservoir if the pressure dropped below the set point, or vented nitrogen from the reservoir if the pressure rose above the set point. The digital scale could be read manually in addition to being connected to the DAS. The packer pressure-maintenance system was installed in the mobile trailer. Fig. 4-4 illustrates a schematic layout of the packer pressure-maintenance system. Additionally, two transducers (type Keller PA-23SY, 30'000 kPa) mounted on the surface inflation control panel were used to monitor the packer inflation pressures.

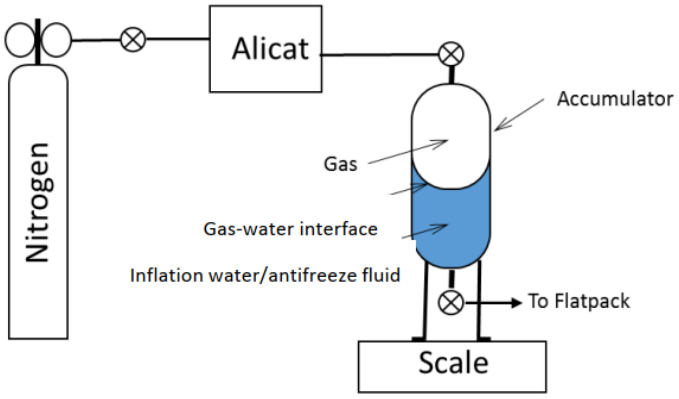

Fig. 4-4: Schematic layout of the packer pressure-maintenance system

4.2.2.3 Additionally recorded measurements at surface

A single pressure transducer (type Keller PAA-33X, 80 – 120 kPa absolute) was mounted outside the monitoring trailer and used to monitor barometric pressure and air temperature (Tab. 4-15).

During pumping tests, the physico-chemical parameters (e.g. pH, EC, Eh, temperature and oxygen concentration) of the extracted fluid were recorded. The specifications of the physico-chemical sensors are given in Tab. 4-16. The sensors were calibrated on-site before each use.

Tab. 4-15: Specifications for the atmospheric pressure sensor

[1] FS = full scale

Pressure sensor type	Keller PAA-33X
Manufacturer	Keller, Winterthur, Switzerland
Pressure range	80 – 120 kPa
Accuracy	0.02% FS[1]
Resolution	0.002% FS

Tab. 4-16: Specifications for the physico-chemical sensors

Sensor type	**EC**	**pH**	**Eh**	**O_2**	**Temp**
Manufacturer	Xylem analytics, Weilheim, Germany				JUMO
Model	WTW TetraCon 325	WTW SensoLyt DW	WTW SensoLyt PtA/Pt	WTW FDO 700 IQ	Pt 1000
Range	1 µS/cm – 2 S/cm	0 – 14	± 2'000 mV	0 – 20 mg/l	-50 °C – 150 °C
Accuracy	n/a	n/a	n/a	n/a	± 0.15 °C at 0 °C ± 0.35 °C at 100 °C
Resolution	n/a	n/a	n/a	0.01 mg/l (0.01 ppm)	0.0015 °C
Temperature range	0 °C – 100 °C	0 °C – 60 °C	0 °C – 60 °C	-5 °C – 50 °C	-50 °C – 150 °C

4.2.2.4 Data acquisition system

The data acquisition system (DAS) consisted of a Solexperts interface for digital and analogue sensors, an industrial PC, a screen and a keyboard. Data acquisition was performed through the Solexperts GeoMonitor II (GMII) software. The downhole pressures (P1, P2, P3, P4) and temperature measurements (T1, T2, T3, T4) were recorded in real time through the quadruple flat-pack cable assembly. Surface measurements like flowmeter rates, packer pressures, atmospheric pressure and temperature, and the physico-chemical parameters were recorded with the same scan rate as the downhole pressures from the QSSP.

The time intervals for scanning could be adjusted as required between 1 s (using a reduced number of sensors) and > 30 s.

The measurements were written to a data file on the PC hard drive in real-time with a continuous data collection and database model. From the PC hard drive, the data were transferred to another network PC continuously for 'online' analysis and data back-up. An uninterruptible power supply was utilised to protect the system from short power interruptions.

4.3 Test analyses

4.3.1 Workflow

For BAC1-1, the general on-site analysis approach involved mainly numerical techniques considering the entire borehole pressure history. Diagnostic plots were used mainly to present the results and to conduct more detailed consistency checks between measurements and simulations. This ensured a comprehensive evaluation of the recorded data. The numerical solutions were assessed further with a perturbation analysis. Prior to commencement of the hydraulic tests, the representation of the borehole history period and the starting input parameters were defined.

The on-site analysis workflow supported the test design to achieve the quality objectives defined by Nagra:

- Identification of the most appropriate flow model, e.g. by log-log diagnostic plots (Bourdet et al. 1989)
- Numerical simulation of individual test sequences in Cartesian coordinates
- Confirmation of the applied flow model suitability via diagnostic representations of the recorded and simulated pressure data
- Assessment of the suitability of the numerical solution and associated uncertainties through limited perturbation analyses
- Numerical simulation of the entire test sequence in Cartesian coordinates using the optimised parameter set obtained from individual phase analysis
- Confirmation of the consistency of the model applied to the entire dataset
- Consistency check of the test analysis and the estimated parameters by the technical supervisor

The results were used to continuously optimise the test design to achieve the quality objectives within the dedicated time of testing. A general flowchart of the analysis work is provided in Fig. 4-5.

The test data were analysed numerically using the nSIGHTS software (Geofirma Engineering Ltd. & INTERA 2011). For slug and pulse tests, the consistency checks typically involved one or more of the semi-log and log-log plots developed by Ramey et al. (1975). Production phases and recovery tests were presented by log-log diagnostic plots (Bourdet et al. 1989) or log-log derivative plots, if applicable also according to Horner (1951). A summary of the applied test analysis methods is presented in Tab. 4-17.

Tab. 4-17: Summary of analytical analysis methods

Test phase	**Analysis method**	**Reference**
Pulse test	Semi-log and log-log representations of the transient pressure change and derivative versus time	Ramey et al. (1975)
Slug test (flow phase SW)	Semi-log and log-log representations of the transient pressure change and derivative versus time	Ramey et al. (1975)
Slug test recovery (pressure recovery after slug flow phase, SWS)	Semi-log and log-log representations of the transient pressure change and derivative versus time	Bourdet et al. (1989)
Pressure recovery after constant rate tests	Log-log representations of the transient pressure change and derivative versus 'superposition time'	Bourdet et al. (1989)
	Diagnostics: Log-log stabilisation of the derivative	Horne (1995)
	Diagnostics: Semi-log representations of the transient pressure change	Horner (1951)

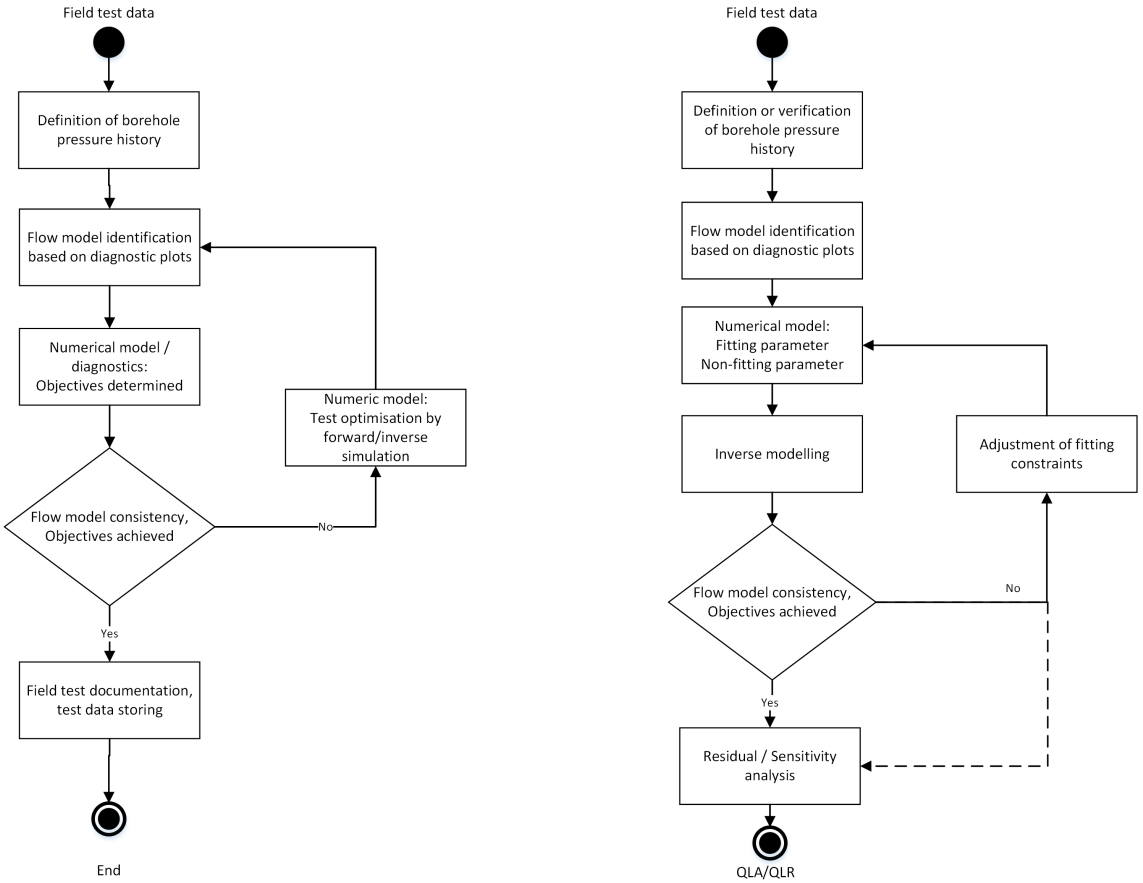

Fig. 4-5: Flowcharts for the on-site hydraulic packer test analysis (left) and Quick Look Analysis (QLA) (right)

The Detailed Analysis (DA) was performed off-site after the test was completed and was based on the Quick Look analysis (QLA) reported in the Quick Look Report (QLR). The QLR was reviewed as part of the Quality Control (QC) programme. During this task, open questions and potential ambiguities of the analysis were defined. Based on the outcome of the QC review, further specifications and, if necessary, further analyses were implemented. Fig. 4-6 provides the general flowchart of the DA, which includes perturbation and non-fitting parameter analyses, to obtain the most reasonable parameter results and ranges of uncertainty. The work is summarised in a Detailed Report (DR), with the QLR included as an Appendix.

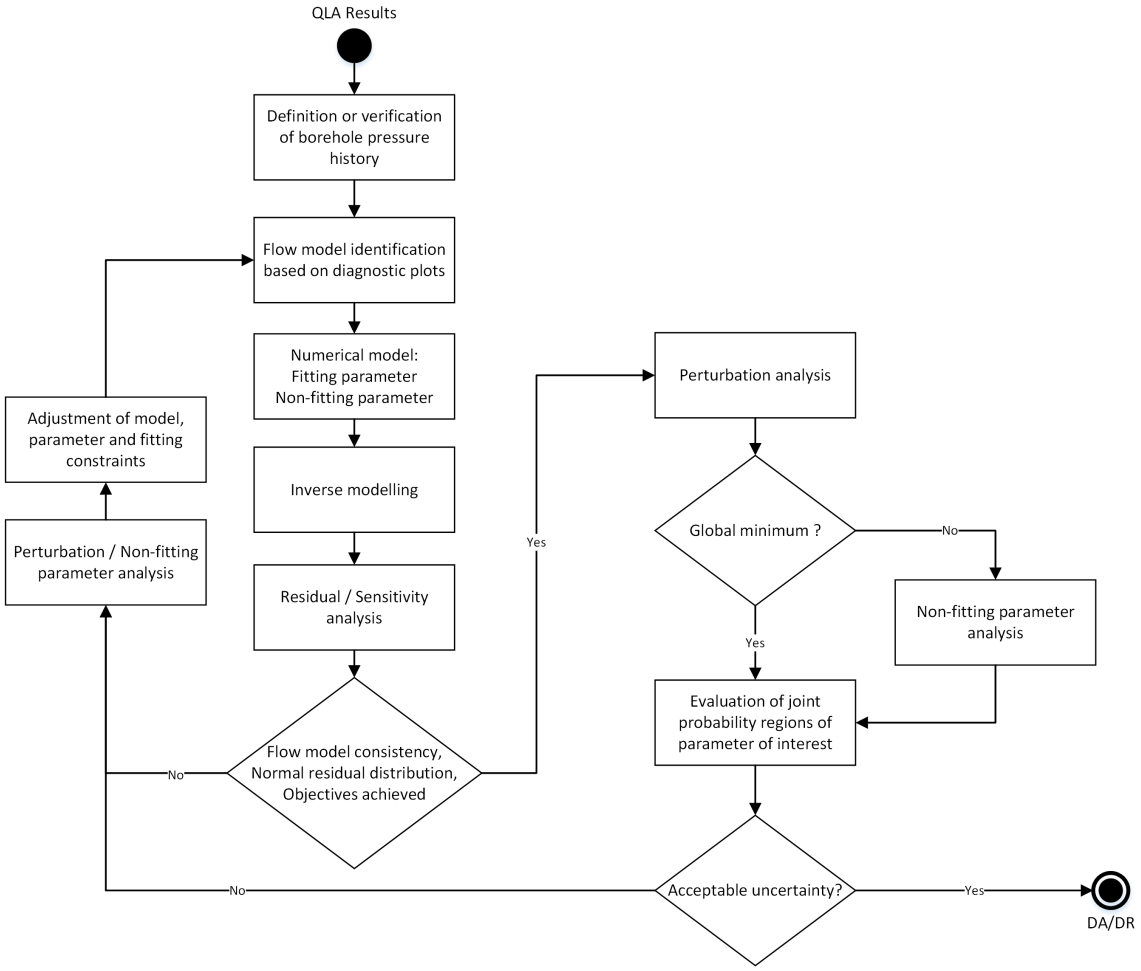

Fig. 4-6: Flowchart for the off-site Detailed Analysis (DA) of a hydraulic packer test

4.3.2 Special effects

The time series measured during hydraulic packer tests were the pressure and temperature inside the test interval. Their development over time was analysed to estimate the hydraulic properties of the formation surrounding the test interval. Various factors affected the recorded time series. All hydraulic tests are affected by factors beyond the test execution and the model used for their analysis (analytical solutions based on assumptions to derive them, numerical models based on the physical processes included in their base equation system). These are referred to as disturbances because they are not considered in the analysis. However, it is possible to describe the

development of temperature and pressure signals using the diffusion equation. Disturbances are of short duration in formations with medium to high transmissivity. In formations with low transmissivity, disturbances in the pressure or temperature field can have a significant influence on the pressure signal measured during the test in the test interval (e.g. Nagra 1997, Grauls 1999, Nagra 2001).

Any disturbances of the pressure field during the time before the hydraulic test is started, are summarised under the name 'borehole pressure history'. Disturbances in the pressure and temperature fields can be caused by drilling and other activities before testing. In addition, disturbances can occur even during testing, e.g. mechanical effects (including poroelastic effects) due to changes in the stress field surrounding the interval, or osmosis due to the chemical interaction of the formation with the drilling fluid. However, results from the experiment 'Deep Borehole Hydraulic Testing Experiment' in the Mont Terri Rock Laboratory showed that osmotic effects have no significant impact on the determination of transmissivity and hydraulic head (Marschall et al. 2003).

As the TBO boreholes are multi-purpose boreholes with many other objectives besides hydraulic packer testing, there is always a trade-off between disciplines regarding optimal test conditions. Most hydraulic packer tests were performed without exchange of drilling fluid with testing fluid in order to maintain borehole stability. In addition to this preventative measure, the numerical analysis tool can estimate the effect of these influences, so that plausibility ranges for the parameter estimations can be defined. In the following, possible individual special effects that have previously been identified, e.g. for the Benken borehole (Nagra 2001), are discussed in more detail.

4.3.2.1 Borehole history

All numerical analyses took into account the borehole pressure history. The borehole pressure history was constructed based on activities that took place prior to hydraulic testing. Drilling through the midpoint of the test interval was used as the starting point for the pressure history. The borehole pressure history data were incorporated into the numerical analyses. The following information was used:

- Date and time of drilling through the interval midpoint, from drilling logs
- Drilling fluid density
- Mud level in the borehole prior to testing
- Pressure records of preceding standpipe pressure and hydraulic testing

The drilling fluid densities were measured four times per day and documented in the drill mud report by the drill mud engineer from AKROS Oilfield Services GmbH. In addition, continuous recordings were available from the mud logging company GEODATA during periods of coring and mud circulation, and mud level measurements in the borehole were performed from time to time.

Most affected by the borehole pressure history is the determination of the static formation pressure or the hydraulic head / hydraulic potential (which are derived from the static formation pressure), which in turn depends on the transmissivity of the formation. In formations with low transmissivity, like the Opalinus Clay, determination of the static formation pressure can be impossible to carry out in a reasonable time due to the long duration of the pressure history. This was proven by measurements carried out using the Benken long-term monitoring system, which demonstrated that the static formation pressures of the Opalinus Clay determined by hydraulic tests were much higher than those subsequently determined by long-term measurements (e.g. Jäggi & Vogt 2020).

The specific periods of the borehole pressure history taken into account for the analysis of the hydraulic packer tests in borehole BAC1-1 are provided in Tab. 4-18.

Tab. 4-18: Specific periods of the borehole pressure history

History refers to the period prior to the separation of the test interval from the rest of the borehole through the inflation of the last packer.

Test name	**Drilling through midpoint:** date and time	**Start hydraulic testing:** date and time	**Borehole history duration** [h]
BAC1-1-LIA1	25.10.2021 22:59	01.11.2021 04:11	149.20
BAC1-1-LIA2	25.10.2021 00:27	05.11.2021 00:32	264.08
BAC1-1-OPA1	23.10.2021 15:10	08.11.2021 10:33	379.38
BAC1-1-OPA2	21.10.2021 12:09	10.11.2021 17:26	485.28
BAC1-1-BDO1	13.10.2021 16:29	15.11.2021 10:16	785.78
BAC1-1-OPA3	14.10.2021 16:32	18.11.2021 23:21	846.82
BAC1-1-BDO2	10.10.2021 15:04	20.11.2021 11:58	980.90
BAC1-1-MAL1	09.10.2021 16:07	23.11.2021 02:44	1'066.62
BAC1-1-BDO3	13.10.2021 21:23	28.11.2021 15:18	1'097.92
BAC1-1B-BDO4	11.01.2022 21:57	19.01.2022 01:45	171.80
BAC1-1-KEU1	07.02.2022 19:34	09.02.2022 09:06	37.53
BAC1-1-KEU2	07.02.2022 12:40	14.02.2022 18:54	174.23
BAC1-1-MUK1	26.03.2022 19:20	29.03.2022 01:00	53.67

4.3.2.2 Interval temperature changes during testing

All activities inside the open borehole also affect the temperature field in and around the borehole. In formations with low transmissivity, this temperature disturbance affects the pressure field surrounding the borehole due to coupled thermo-hydraulic processes. The analysis of hydraulic tests using the numerical software packages nSIGHTS (version 3.00), Multisim and WellSi can incorporate temperature changes during the hydraulic test that lead to a change in fluid volume and thus pressure within a closed test interval volume. The fluid volume change in the test interval was calculated using the volumetric thermal expansion coefficient of the fluid (water), which itself is temperature-dependent. The pressure change is linearly dependent on the interval fluid volume change using a proportionality factor, the compressibility of the interval.

4.3.2.3 Mechanical effects

The mechanical deformations caused by drilling- and testing-related stress redistribution in the formation can also influence the pressure response during a hydraulic test. Normally, the conceptual model for the description of the storage coefficient used in the underlying hydraulic models assumes a compressible pore volume and an incompressible grain structure. In this model, changes in pore pressure are considered as movement of the fluid into and out of the pore volume. The coupling between fluid volume change and mechanical deformations results in a time-dependent deformation for an elastic medium (Detournay & Cheng 1988). The Opalinus Clay has

shown a time-dependent deformation during tunnel excavation in Mont Terri (see Lisjak et al. 2015 for a summary of the observations and for a numerical interpretation of the data). Opalinus Clay time-dependent behaviour is most likely due to the undrained and drained excavation response, rather than mechanical creep phenomena. In formations with low transmissivity, time-dependent deformations can have an influence on the pressure signal observed in the test interval.

However, there are no data on mechanical deformations available for the tests in borehole BAC1-1 that would allow the characterisation of mechanical effects on the tests in formations with low transmissivity. Deformations of the borehole wall can be included in the analysis by all the numerical software packages used, by means of an appropriate parameterisation during the analysis in the same way as for temperature changes inside the interval. The resulting pressure change is caused by volume changes, which can be either linear or quadratic. The proportionality factor between the volume change and the pressure change is the interval compressibility.

4.4 Test activities

A total of thirteen test intervals were investigated in borehole BAC1-1 using the HTT in single and double packer configuration (including one test in the sidetrack BAC1-1B). The most important test specifications are summarised in Tab. 4-19. The hydraulic packer tests were performed in the following geological formations (*cf.* Dossier III):

- Malm Group with a focus on the lowermost part of the Effingen Member of the Wildegg Formation (BAC1-1-MAL1) after the fluid logging campaign (BAC1-1-FL1-MAL) performed over the «Felsenkalke» + «Massenkalk», the Schwarzbach Formation, the Villigen Formation and the Wildegg Formation including only the upper part of the Effingen Member (*cf.* Section 3)
- Dogger Group («Brauner Dogger») focusing on the Wutach Formation, Variansmergel Formation and «Parkinsoni-Württembergica-Schichten» (BAC1-1-BDO2) and on the «Parkinsoni-Württembergica-Schichten», «Humphriesioolith Formation», Wedelsandstein Formation and part of the «Murchisonae-Oolith Formation» (BAC1-1-BDO1). Two additional tests aimed at characterising a section containing a drilling-induced fracture at the bottom of the «Murchisonae-Oolith Formation» / top of the Opalinus Clay (BAC1-1B-BDO4 and BAC1-1-BDO3)
- Dogger Group with a focus on sub-units of the Opalinus Clay (BAC1-1-OPA1, BAC1-1-OPA2) and including the bottom of the «Murchisonae-Oolith Formation» containing a drilling-induced fracture (BAC1-1-OPA3)
- Staffelegg Formation of the Lias Group with the Gross Wolf, Rietheim, Grünschholz, Breitenmatt, Rickenbach and Frick Members (BAC1-1-LIA2) and an interval comprising the Frick, Beggingen and Schambelen Members of the Staffelegg Formation as well as the uppermost part of the Gruhalde Member of the Klettgau Formation of the Keuper Group (BAC1-1-LIA1)
- Klettgau Formation of the Keuper Group with the Gruhalde, Seebi, Gansingen and Ergolz Members (BAC1-1-KEU1) and excluding the Ergolz Member (BAC1-1-KEU2)
- Muschelkalk Group with mostly the Schinznach Formation including the Stamberg, Liederswil, Leutschenberg and Kienberg Members, and the top of the Zeglingen Formation (BAC1-1-MUK1)

All but one hydraulic test in the main borehole BAC1-1 were performed in the cored borehole section with a borehole diameter of 6⅜" with 114 mm (deflated diameter) packers and without any prior fluid exchange, i.e. with the drilling fluid being used as the interval test fluid. For the hydraulic test BAC1-1-BDO3, the larger diameter packers (146 mm) were used, and the drilling fluid was exchanged prior to testing. It was replaced first with NaOH and subsequently with synthetic pore water past the deflated upper packer. The sidetrack BAC1-1B was drilled destructively with a diameter of 8½" (*cf.* Dossier I) which required the 146 mm (deflated diameter) packers to be used for hydraulic test BAC1-1B-BDO4. Following test BAC1-1B-BDO4, several rate injection tests were performed to qualitatively supplement micro hydraulic fracturing at BAC1-1 (*cf.* Dossier VI).

The density and viscosity of the drilling fluid were recorded by the mud engineer in daily mud reports. Mud losses were reported in the main borehole BAC1-1 while drilling through the bottom part of the «Murchisonae-Oolith Formation» / the topmost part of the Opalinus Clay (total 15 m^3) and before testing of the Muschelkalk Group (about 5 m^3). No losses occurred in the section where the fluid logging (BAC1-1-FL1-MAL) was conducted.

Sodium-Fluorescein (uranine) at concentrations of approximately 1 ppm was used to trace the drilling fluid. The test tubing was typically filled with tap water traced with sodium-naphthionate or 1.5-naphthalene disulfonate acid (for the hydraulic tests in shales) at concentrations of approximately 10 ppm. The SIT was closed during the entire time the HTT was lowered to the test depth and also during installation. Therefore, in test intervals with low transmissivity, the interval fluid density was not affected by traced water in the test tubing as mainly withdrawal tests were performed and no or only very little fluid flow occurred. If a pressure increase of more than 100 kPa was observed in the test interval during inflation of the top packer, the SIT was opened and the COM phase started. Due to the higher density of the drilling fluid in the test interval, for formations with low transmissivity, it was assumed that no flow occurred from the test tubing into the test interval during the COM phase. Flow from the formation into the borehole by means of a longer test phase of pressure reduction in the interval (i.e. a slug or pumping test phase) was created during all tests, except for BAC1-1-BDO1 (a sequence of pulse tests).

A swabbing tool was used to create the pressure difference between the test tubing and the test interval. For each of the pumping tests, the PCP was used and the position of the stator of the PCP in the test string was optimised up to the limit of the allowable pumping head. If two tests were performed sequentially without pulling the HTT out of the borehole between tests, a stator was already installed for the first test (usually the deeper test).

For the hydraulic tests BAC1-1-KEU1 and BAC1-1-MUK1, drilling was stopped for hydraulic testing. Both tests were performed directly after pulling out of hole (POOH) the coring string. The tests BAC1-1-LIA1 and BAC1-1B-BDO4 followed petrophysical measurements and, in addition, a checktrip and a blow-out preventer (BOP) test were carried out before BAC1-1-LIA1. For the other tests, a longer section was drilled and then the hydraulic tests were performed, which resulted in a longer borehole pressure history. The measured pressures (measured by the downhole sensors in the QSSP) and pumping rates (measured by the flow board at the surface) for all tests conducted in borehole BAC1-1 are provided in Figs. 4-7 to 4-20. The figures are taken directly from the reports of the field test contractor.

The temperature increase in the test intervals was included in the analysis of the hydraulic packer tests for formations without a pumping period (low transmissivity). The temperature increase from the start of the initial pressure recovery after closing the shut-in valve (PSR) until the end of the test ranged from 0.33 K to 4.82 K for all tests, with the exception of BAC1-1-KEU1 and BAC1-1-MUK1, i.e. the two hydraulic tests including a production phase.

Tab. 4-19: Hydraulic packer testing in borehole BAC1-1: test interval and test specifications

[1] For an explanation of the test names and test phases see Tabs. A-2 and A-3, respectively.

[2] FM = flow model, T = transmissivity, h_s = static hydraulic head, WS = water sample.

Test name[1]	**Interval depth** [m MD]	**Interval midpoint** [m MD]	**Packer configuration**	**Test phases**[1]	**Testing period** (duration)	**Geological information** [depth and length values rounded; groups and formations usually named from top down; for details see Dossier III]	**Objectives**[2] [secondary aims in brackets ()]
BAC1-1-MAL1	712.56 – 735.00	723.78	Double	INF, COM, PSR, PW1, SW, SWS, PW2, DEF	23.11. – 26.11.2021 (77.0 h)	Malm Group: bottom part of the Effingen Member of the Wildegg Formation; calcareous marl, thin interbeds of argillaceous marl and limestone; abundant interbeds (up to 50 cm thick) of argillaceous limestone at 723 – 731 m MD. The test was designed to target the Effingen Member including a fault zone between 726.83 and 726.89 m MD.	T, (h_s), FM
BAC1-1-BDO2	736.00 – 758.44	747.22	Double	INF, COM, PSR, PW, SW, SWS, DEF	20.11. – 22.11.2021 (58.6 h)	Malm Group: bottom 1.05 m of the Wildegg Formation with calcareous marl, some glauconites and comprising oncoids and iron-ooids Dogger Group («Brauner Dogger»): fossiliferous iron-oolitic marl and limestone of the Wutach Formation (1.76 m); 2.41 m of the fossiliferous Variansmergel Formation comprised of a variation from claystone to argillaceous and calcareous marl with few iron-ooids; top 17.22 m of the «Parkinsoni-Württembergica-Schichten» with thin- to medium-bedded gradual alternation of silty marl and claystone with thin limestone or calcareous marl beds (strongly bioturbated, incl. burrows). The test was designed as an overview test to target the iron-oolith of the Wutach Formation as well as the bed alternations in the upper part of the «Parkinsoni-Württembergica-Schichten».	T, (h_s), FM
BAC1-1-BDO3	769.00 – 816.17	792.59	Double	INF, COM, PSR, SW, SWS, SI, RI, RIS, DEF	28.11. – 03.12.2021 (122.9 h)	Dogger Group («Brauner Dogger»): bottom 19.92 m of the «Parkinsoni-Württembergica-Schichten» with silty or calcarous claystone and bioclastic argillaceous marl; 2.13 m of «Humphriesioolith Formation» with claystone rich in burrows and bioclastic calcareous marl; 2.06 m of Wedelsandstein Formation bioclastic calcareous marl interbedded with fossiliferous limestone; 15.23 m of «Murchisonae-Oolith Formation» with three distinct sections of bioclastic argillaceous marl at the top, silty claystone to claystone in the middle and sandy limestone at the bottom; 7.83 m of the 'Sub-unit with silty calcareous beds' of the Opalinus Clay. The test targeted a large test interval including a drilling-induced fracture at approx. 795 m to 813 m MD (log depth) (*cf.* Doss. V) and aimed to determine its reopening pressure.	T, (h_s), FM

Tab. 4-19: continued

Test name[1]	**Interval depth** [m MD]	**Interval midpoint** [m MD]	**Packer configuration**	**Test phases**[1]	**Testing period** (duration)	**Geological information** [depth and length values rounded; groups and formations usually named from top down; for details see Dossier III]	**Objectives**[2] [secondary aims in brackets ()]
BAC1-1-BDO1	776.40 – 798.84	787.62	Double	INF, COM, PSR, PW1, PW2, DEF	15.11. – 18.11.2021 (80.6 h)	Dogger Group («Brauner Dogger»): bottom 12.52 m of the «Parkinsoni-Württembergica-Schichten» with silty claystone and bioclastic argillaceous marl; 2.13 m of «Humphriesioolith Formation» with claystone rich in burrows and bioclastic calcareous marl; 2.06 m of Wedelsandstein Formation bioclastic calcareous marl interbedded with fossiliferous limestone; 5.73 m of «Murchisonae-Oolith Formation» with a section of bioclastic argillaceous marl at the top, silty claystone to claystone below, and a thin layer of sandy limestone at the bottom. This test was designed as an overview test to target the above-mentioned formations. The purpose of the test was to hydraulically characterise these formations and to check whether any parts may have contributed to the mud losses that happened below. The test interval is entirely included within the BAC1-1-BDO3 interval.	T, (h_s), FM
BAC1-1B-BDO4 (sidetrack BAC1-1B)	797.00 – 812.72	804.86	Double	INF, COM, PSR, PW1, PW2, PW3, PI, SW, SWS, RI, DEF	19.01. – 22.01.2022 (71.2 h)	Dogger Group («Brauner Dogger»): the bottom 11.34 m of «Murchisonae-Oolith Formation» with some silty claystone with burrows at the top, bioclastic argillaceous marl to claystone below, followed by about 8 m of sandy to bioclastic limestone at the bottom; the top 4.38 m of the 'Sub-unit with silty calcareous beds' of Opalinus Clay. The aim of this test was to hydraulically investigate the sandy to bioclastic limestone of the «Murchisonae-Oolith Formation» and the top of the Opalinus Clay in the side track. It covers approximately the depth of the drilling-induced fracture in the main borehole.	T, (h_s), FM
BAC1-1-OPA3	800.00 – 822.44	811.22	Double	INF, PSR, PW, SW, SWS, DEF	18.11. – 20.11.2021 (33.5 h)	Dogger Group («Brauner Dogger»): the bottom 8.34 m of the «Murchisonae-Oolith Formation» with bioclastic argillaceous marl to claystone at the very top, followed by sandy to bioclastic limestone below; the top 14.10 m of the 'Sub-unit with silty calcareous beds' of Opalinus Clay. The test interval included a drilling-induced fracture at approx. 795 m to 813 m MD (log depth) (*cf.* Doss. V)	T, (h_s), FM

Tab. 4-19: continued

Test name[1]	**Interval depth** [m MD]	**Interval midpoint** [m MD]	**Packer configuration**	**Test phases**[1]	**Testing period** (duration)	**Geological information** [depth and length values rounded; groups and formations usually named from top down; for details see Dossier III]	**Objectives**[2] [secondary aims in brackets ()]
BAC1-1-OPA2	880.80 – 894.17	887.49	Double	INF, COM, PSR, PW1, SW, SWS, WBS, PW2, DEF	10.11. – 13.11.2021 (72.1 h)	Dogger Group («Brauner Dogger»): test interval entirely within the homogeneous 'Mixed clay-silt-carbonate sub-unit' of the Opalinus Clay; inclined bedding most prominent at approx. 884 – 886 m MD. The test aimed to target the clay rich lower section of the Opalinus Clay including a zone with inclined bedding.	T, (h_s), FM
BAC1-1-OPA1	901.70 – 915.07	908.39	Double	INF, COM, PSR, PW, SW, SWS, DEF	08.11. – 10.11.2021 (52.2 h)	Dogger Group («Brauner Dogger»): test interval mostly within the 'Clay-rich sub-unit' of the Opalinus Clay at the base of the formation with 13.07 m of bioturbated claystone and 0.14 m of argillaceous marl at the base. Lias Group: limestone bed forming the top 0.16 m of the Gross Wolf Member of the Staffelegg Formation The test targeted the clay rich lower section of the Opalinus Clay including a fault zone between appr. 911 and 913 m MD.	T, (h_s), FM
BAC1-1-LIA2	915.70 – 929.07	922.39	Double	INF, COM, PSR, PW, SW, SWS, DEF	05.11. – 08.11.2021 (79.0 h)	Lias Group, Staffelegg Formation: at the top 3.94 m of the Gross Wolf Member with argillaceous to calcareous marl; then 5.85 m of the Rietheim Member of argillaceous marl with calcareous marl and fossiliferous interlayers, and bituminous shale along the bottom; followed by 2.63 m of the Grünschholz, Breitenmatt and Rickenbach Members of glauconitic and very fossiliferous marl and bioclastic limestone; and 0.95 m of the Frick Member with argillaceous silt- to sandstone. The test was designed as an overview test and targeted the upper part of the Staffelegg Formation, the Gross Wolf to Grünschholz Members.	T, (h_s), FM
BAC1-1-LIA1	930.20 – 952.00	941.10	Single	INF, COM, PSR, PW1, SW1, SWS1, SW2, SWS2, PW2, DEF	01.11. – 03.11.2021 (61.6 h)	Lias Group, Staffelegg Formation: 9.32 m of the Frick Member of argillaceous silt- to sandstone followed by silty to sandy claystone; then 3.52 m of the Beggingen Member with bioclastic limestone, claystone, argillaceous marl, some iron-oolitic; then 6.69 m of the Schambelen Member of claystone with thin layers of siltstone Keuper Group, Klettgau Formation: 2.27 m of Gruhalde Member made of dolomitic marl. The test was designed as an overview test and targeted the lower part of the Staffelegg Formation including the Frick, Beggingen and Schambelen Members. The interval also includes a fracture zonel within the Beggingen Member as well as at the top of the Schambelen Member.	T, (h_s), FM

Tab. 4-19: continued

Test name[1]	**Interval depth** [m MD]	**Interval midpoint** [m MD]	**Packer configuration**	**Test phases**[1]	**Testing period** (duration)	**Geological information** [depth and length values rounded; groups and formations usually named from top down; for details see Dossier III]	**Objectives**[2] [secondary aims in brackets ()]
BAC1-1-KEU1	957.20 – 979.00	968.10	Single	INF, COM, PSR, SW, SWS, RW, RWS, PW, PI, DEF	09.02. – 13.02.2022 (101.2 h)	Keuper Group, Klettgau Formation: 2.55 m of dolomitic marl of the Gruhalde Member; then 6.28 m of the Seebi Member with dolostone (sandy) with dolomitic marl interlayers followed by dolomitic sandstone and argillaceous to dolomitic marl; followed by 2.72 m belonging to the Gansingen Member consisting of dolostone, in parts with microbial mats with vugs, some ooids; the remaining 10.25 m of the Ergolz Member composed of variegated argillaceous marl with nodular dolomitic horizons, medium-grained sandstone and fine-grained argillaceous and micaceous sandstone, and claystone. This overview test targeted the potential transmissive members of the Klettgau Formation, Seebi to Ergolz Members.	T, h_s, (FM), WS
BAC1-1-KEU2	957.20 – 968.21	962.71	Double	INF, COM, PSR, SW, SWS, DEF	14.02. – 16.02.2022 (46.6 h)	Keuper Group, Klettgau Formation: the test interval covered the test interval BAC1-1-KEU2 minus the bottom 0.54 m of the Gansingen Member, and the Ergolz Member. The objective of the test was to characterise the upper Klettgau Formation excluding the Ergolz Member.	T, hs, (FM)
BAC1-1-MUK1	1'080.90 – 1'129.00	1'104.95	Single	INF1, PSR1, SW, SWS, DEF1, INF2, PSR2, RW, RWS, PI, DEF2	29.03. – 01.04.2022 (72.4 h)	Muschelkalk Group, mostly Schninznach Formation: 15.05 m of the Stamberg Member, dolostone with interlayers of dolomitic to argillaceous marl, some bioturbation, locally porous, some open vugs; then 4.71 m of the Liedertswil Member of limestone, some dolomitic, some argillaceous or bioclastic; followed by 25.09 m of the Leutschenberg and Kienberg Members with alternations of limestones (mudstone, wackestone, bioclastic, biomicrite); at the bottom: 3.25 m of the «Dolomitzone» of the Zeglingen Formation consisting of dolomitic limestone, dolostone locally with chert nodules, and anhydrite veins and nodules Approximately 5 m^3 of drilling mud was lost to the formation during coring. This test was performed as overview of the Schinznach Formation, fracture zones in the Liedertswil / Leutschenberg+Kienberg Members including a zone with numerous fractures and macro-pores.	T, h_s, FM, WS

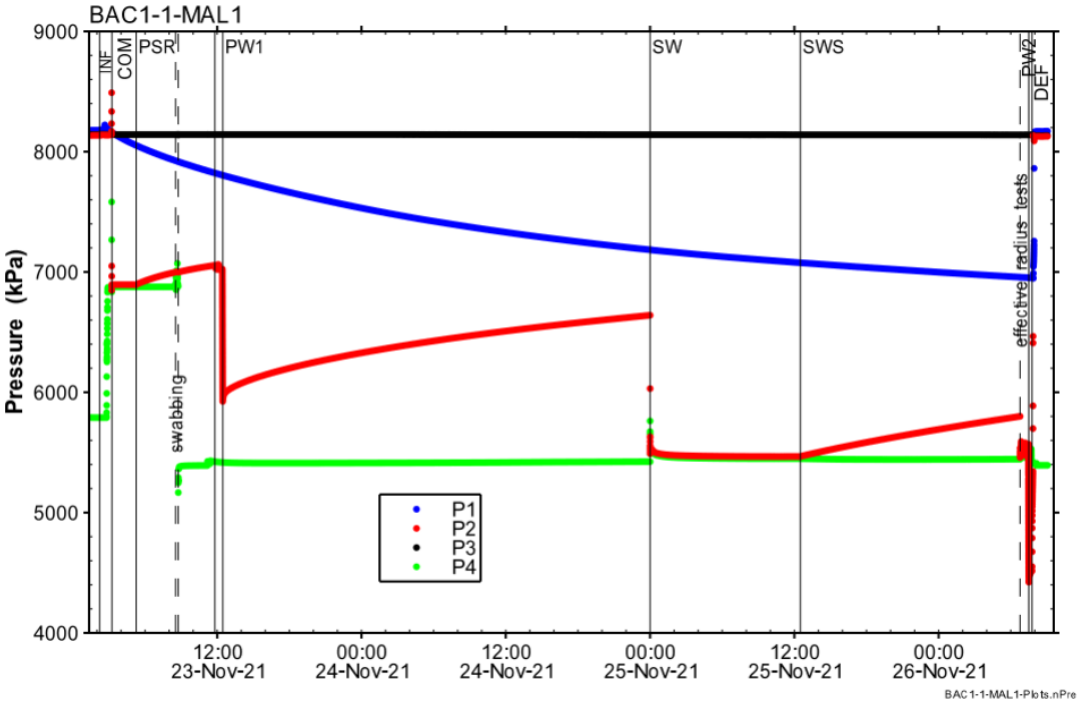

Fig. 4-7: Hydraulic packer test BAC1-1-MAL1: Overview plot of pressure vs. time and date

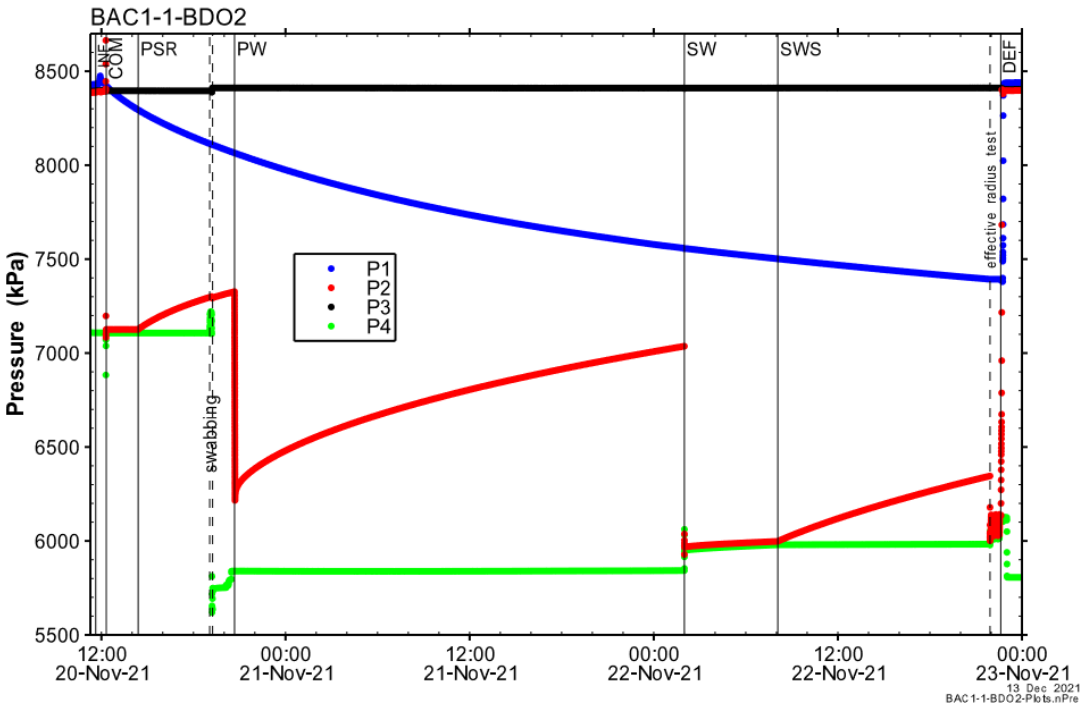

Fig. 4-8: Hydraulic packer test BAC1-1-BDO2: Overview plot of pressure vs. time and date

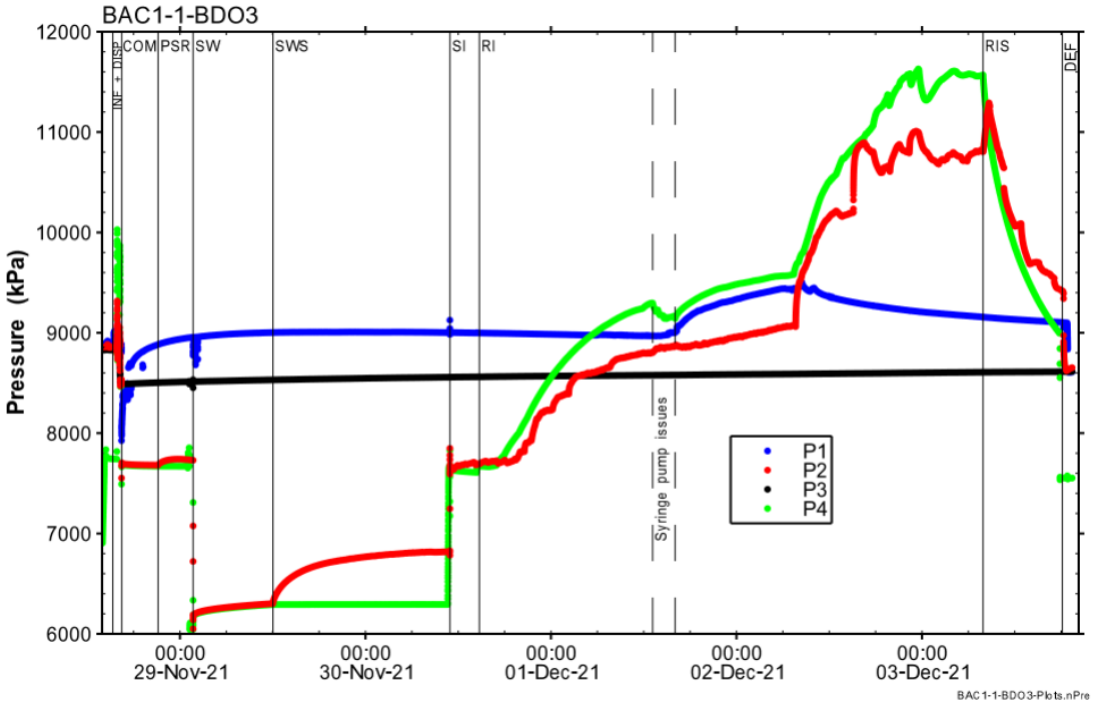

Fig. 4-9: Hydraulic packer test BAC1-1-BDO3: Overview plot of pressure vs. time and date

Note the erratic behaviour of the QSSP P2 gauge after the SI test indicating a malfunction. The QSSP P4 gauge shows correct pressure measurements during the RI events confirmed by the DataCan memory pressure gauge P2*. Injection rates during the RI test varied between 20 ml/min and 4.9 l/min with a total volume of approximately 4.25 m^3 injected over 65.2 hours.

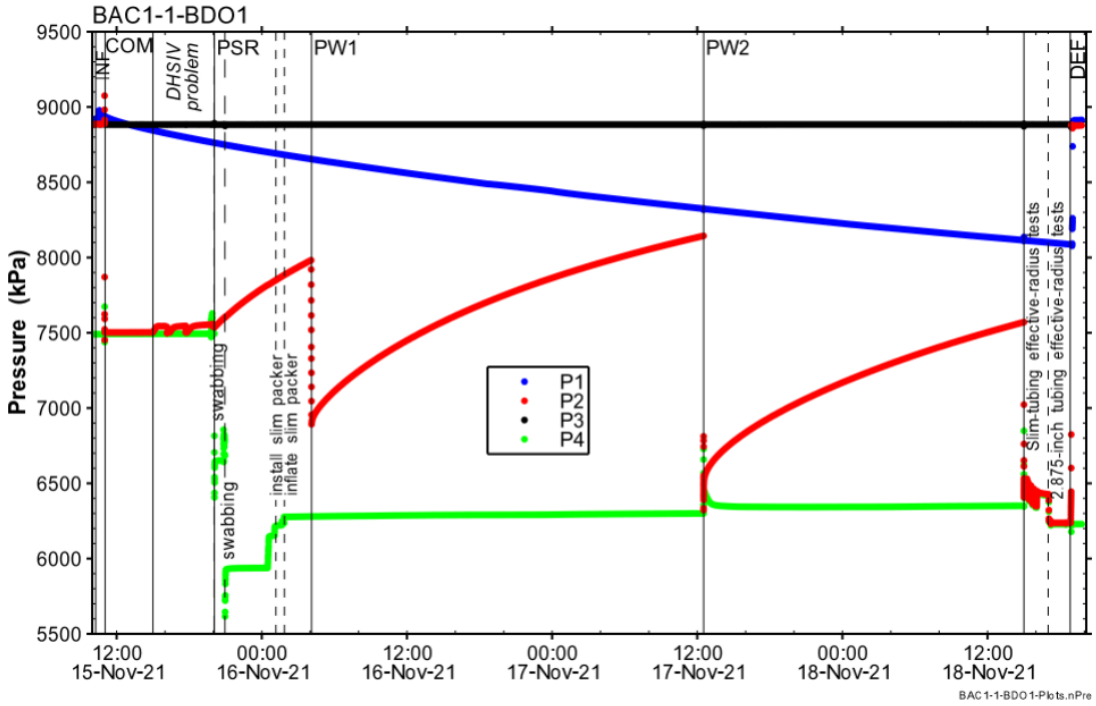

Fig. 4-10: Hydraulic packer test BAC1-1-BDO1: Overview plot of pressure vs. time and date

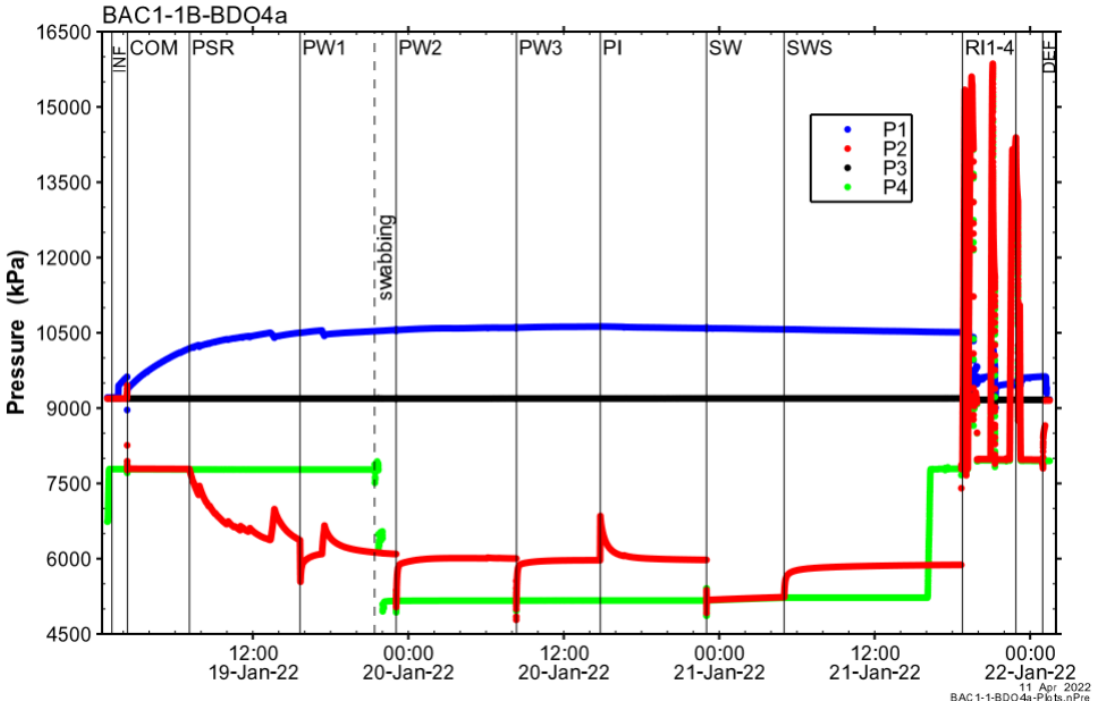

Fig. 4-11: Hydraulic packer test BAC1-1B-BDO4: Overview plot of pressure vs. time and date

Note the inflections between the test interval pressure (QSSP P2) and the bottom interval pressure (QSSP P1), particularly during PSR and PW1. The inflections persisted over the entire test sequence with decreasing magnitude. Tests RI1-4 were performed to gain qualitative information on the stress regime in the sidetrack BAC1-1B (*cf.* Dossier VI).

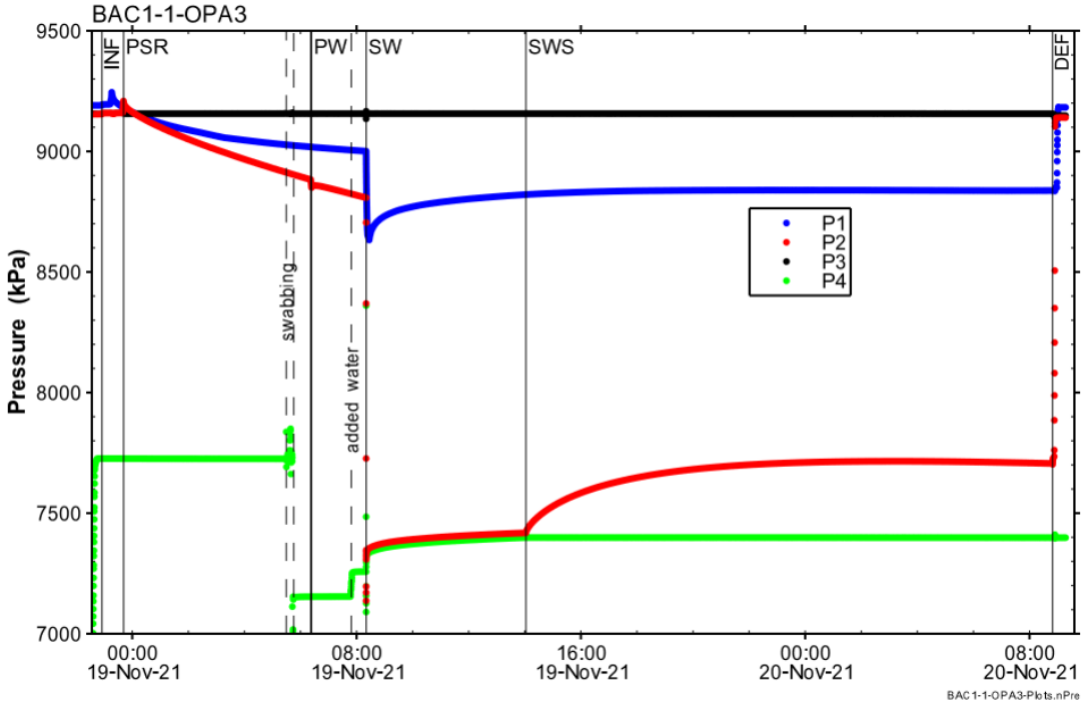

Fig. 4-12: Hydraulic packer test BAC1-1-OPA3: Overview plot of pressure vs. time and date

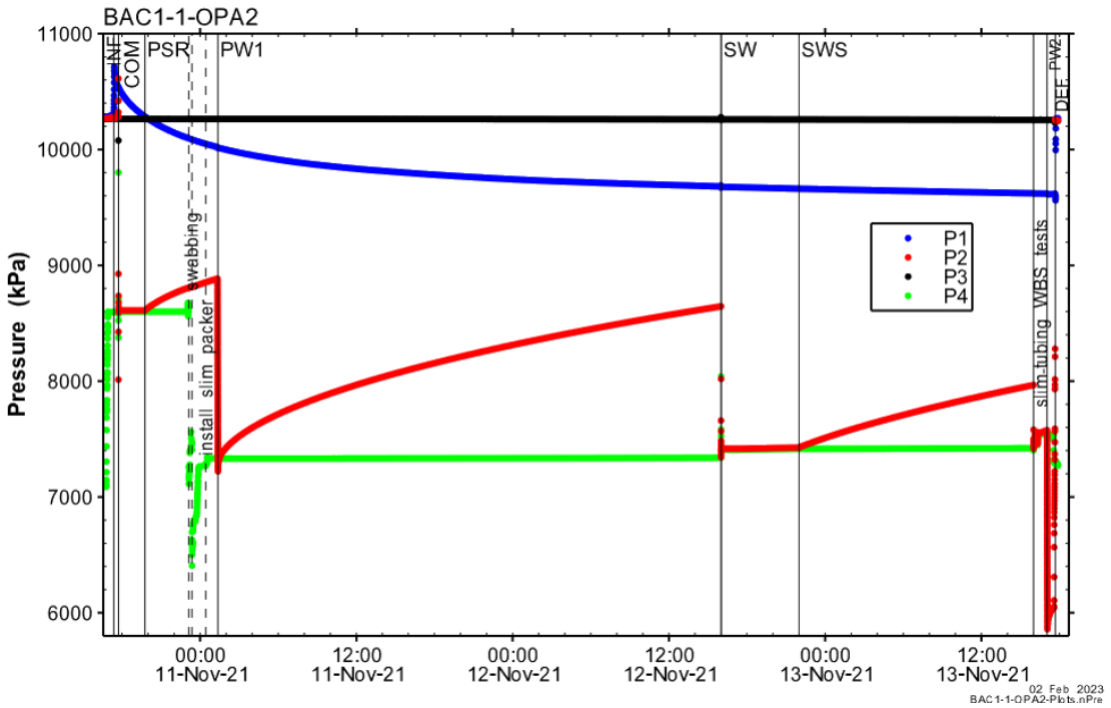

Fig. 4-13: Hydraulic packer test BAC1-1-OPA2: Overview plot of pressure vs. time and date

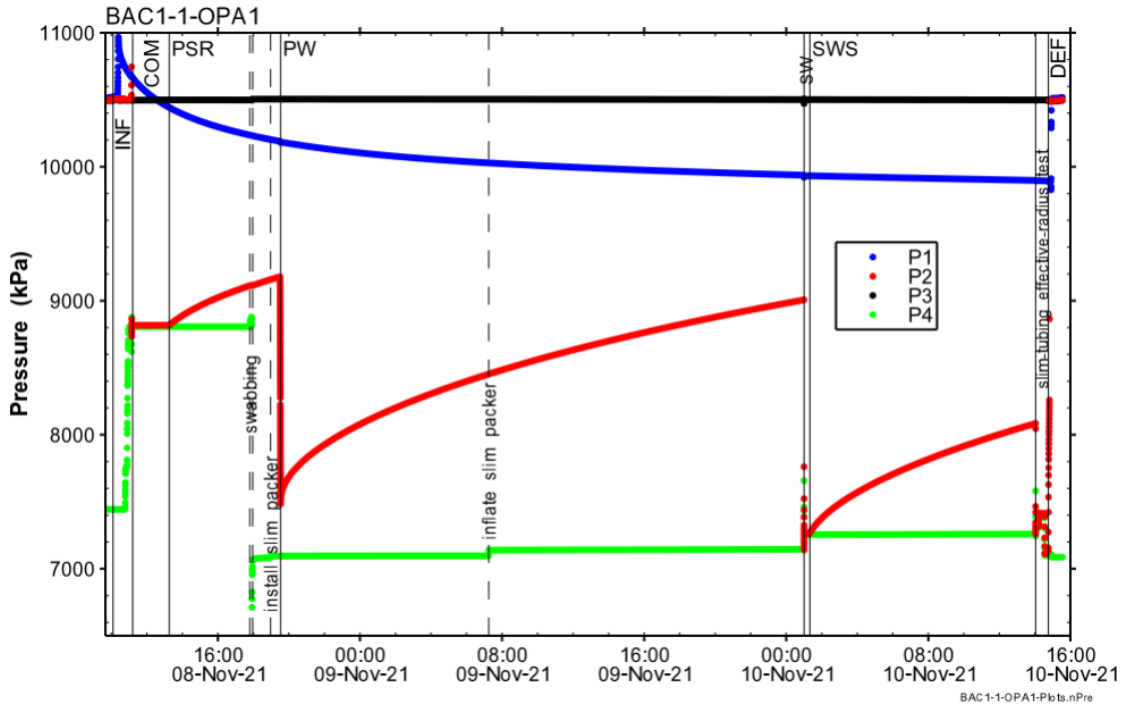

Fig. 4-14: Hydraulic packer test BAC1-1-OPA1: Overview plot of pressure vs. time and date

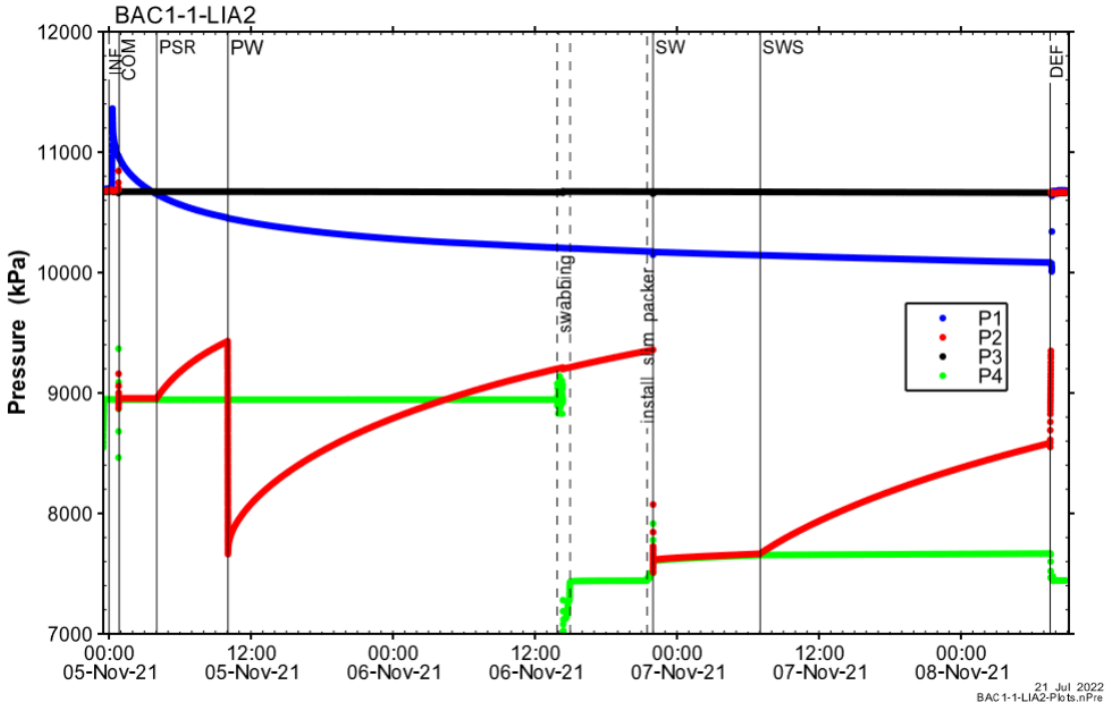

Fig. 4-15: Hydraulic packer test BAC1-1-LIA2: Overview plot of pressure vs. time and date

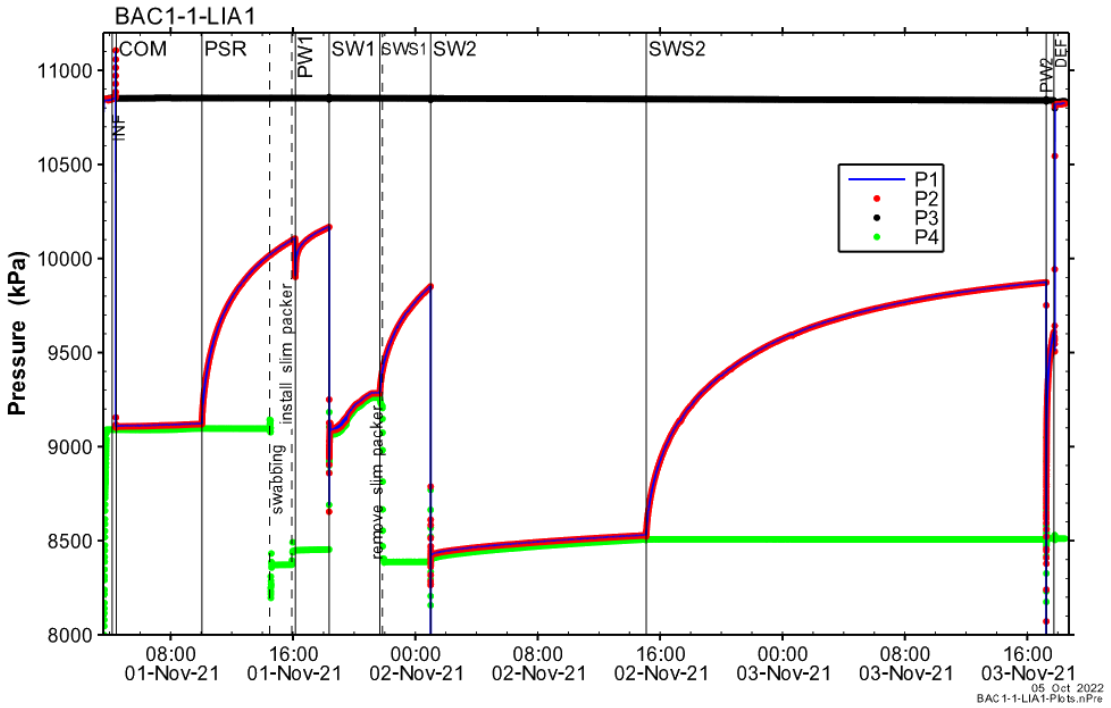

Fig. 4-16: Hydraulic packer test BAC1-1-LIA1: Overview plot of pressure vs. time and date

Note the malfuntion of the slim tubing during SW1. The SW2 was performed using the test tubing.

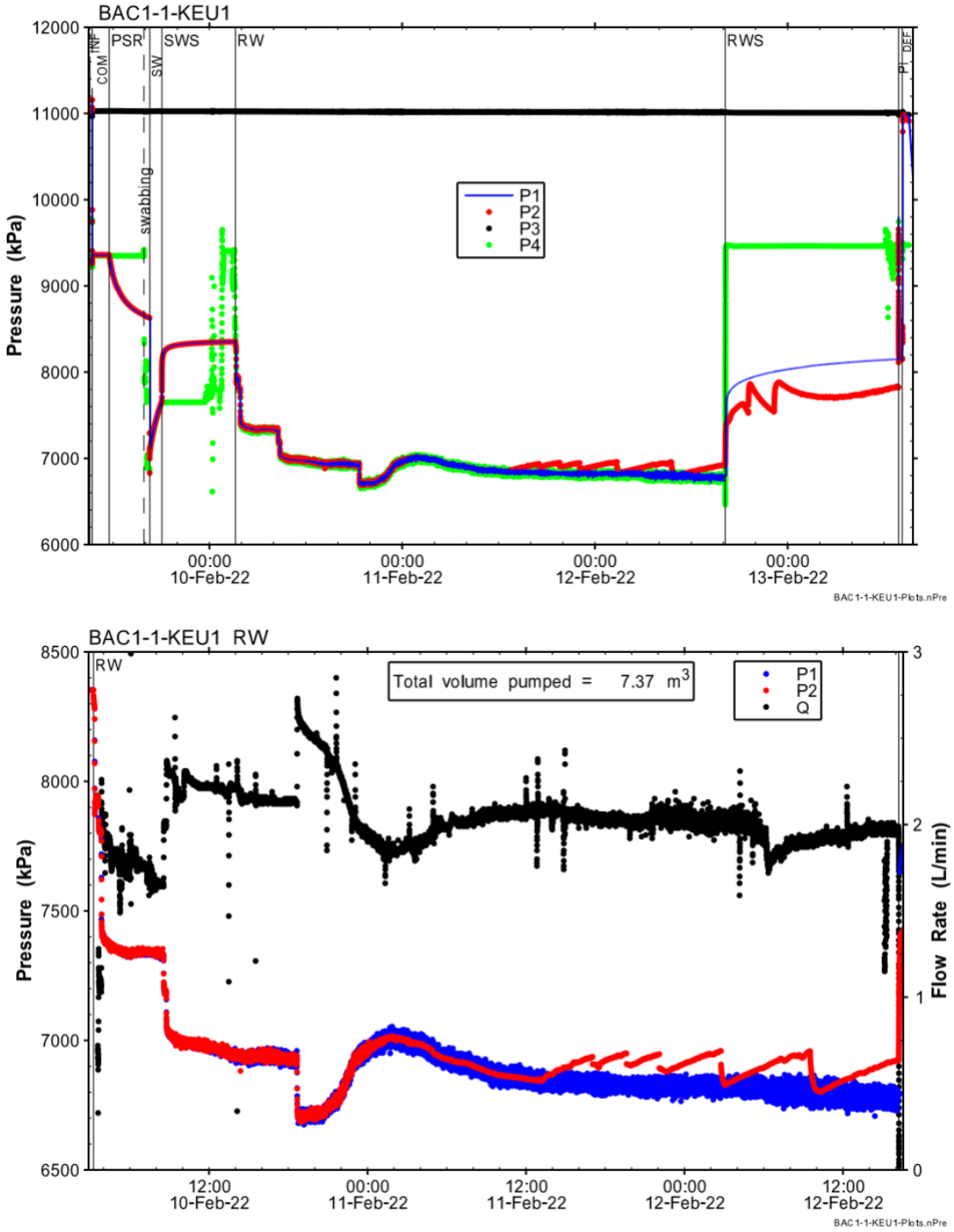

Fig. 4-17: Hydraulic packer test BAC1-1-KEU1: Overview plot of pressure (top) and interval pressure (P2) and rate (Q) during the RW (bottom) vs. time and date

Note that the analysis used the QSSP P1 measurements (bottom) due to erratic behaviour of the QSSP P2 gauge indicating a malfunction and the fact that BAC1-1-KEU1 was a single packer test.

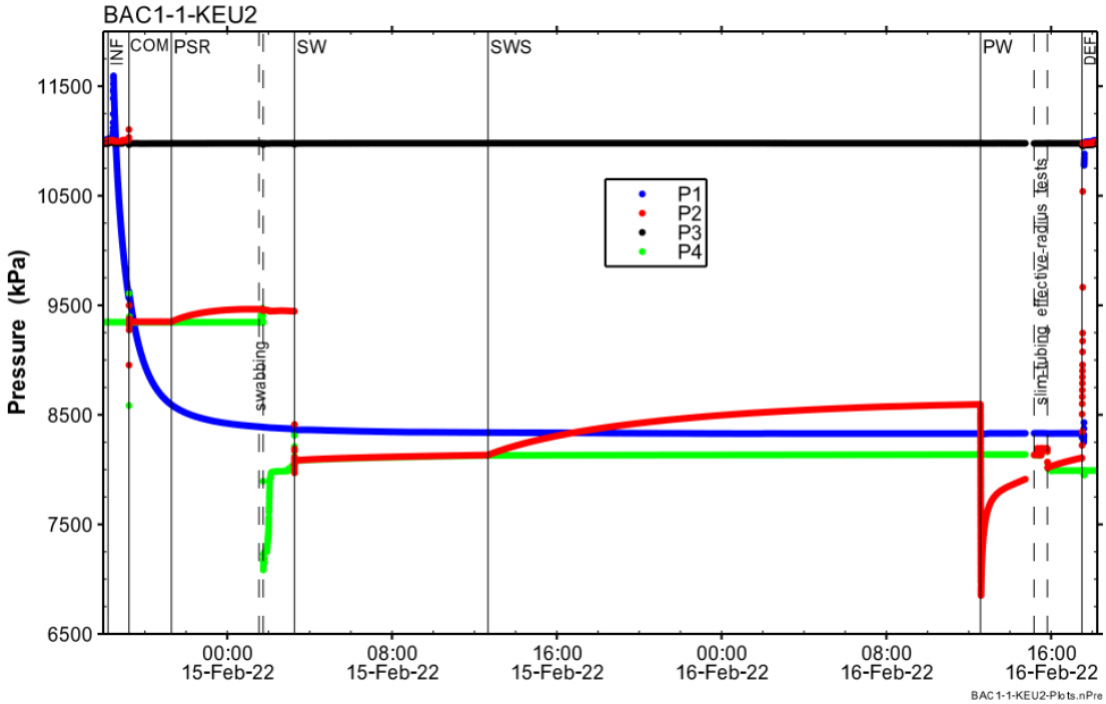

Fig. 4-18: Hydraulic packer test BAC1-1-KEU2: Overview plot of pressure vs. time and date

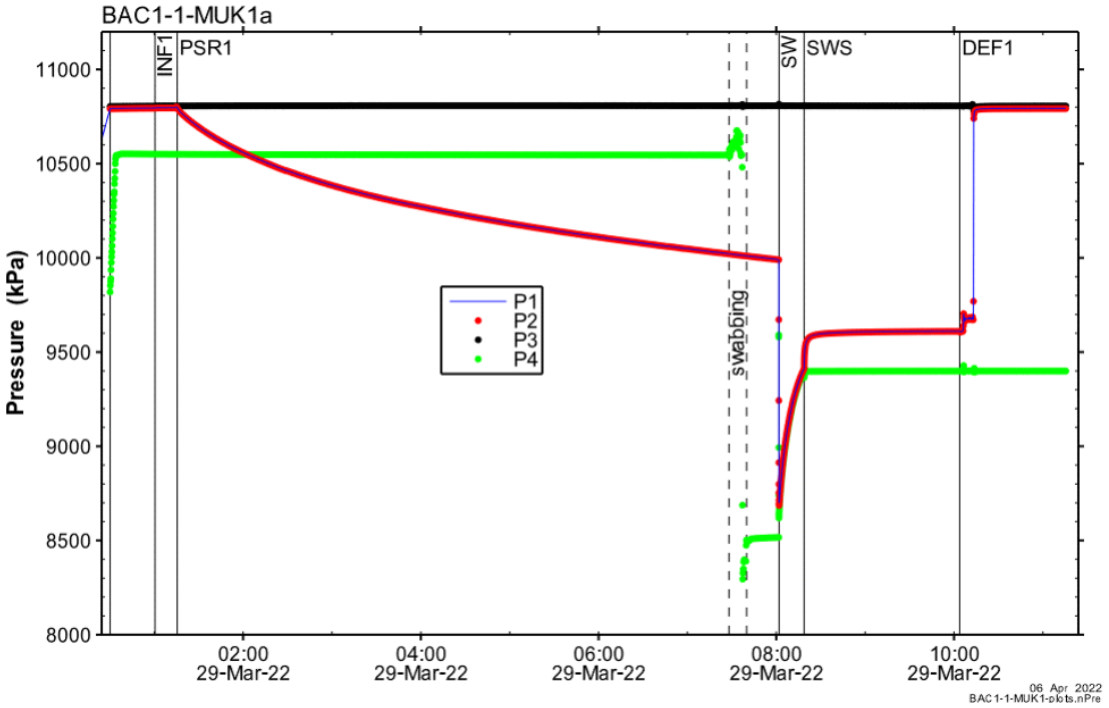

Fig. 4-19: Hydraulic packer test BAC1-1-MUK1: Overview plot of pressure before first deflation vs. time and date

Note the partial POOH of the system after the first test part (BAC1-1-MUK1a) for the installation of a different stator to optimize the pumping rate of the subsequent test part (BAC1-1-MUK1b).

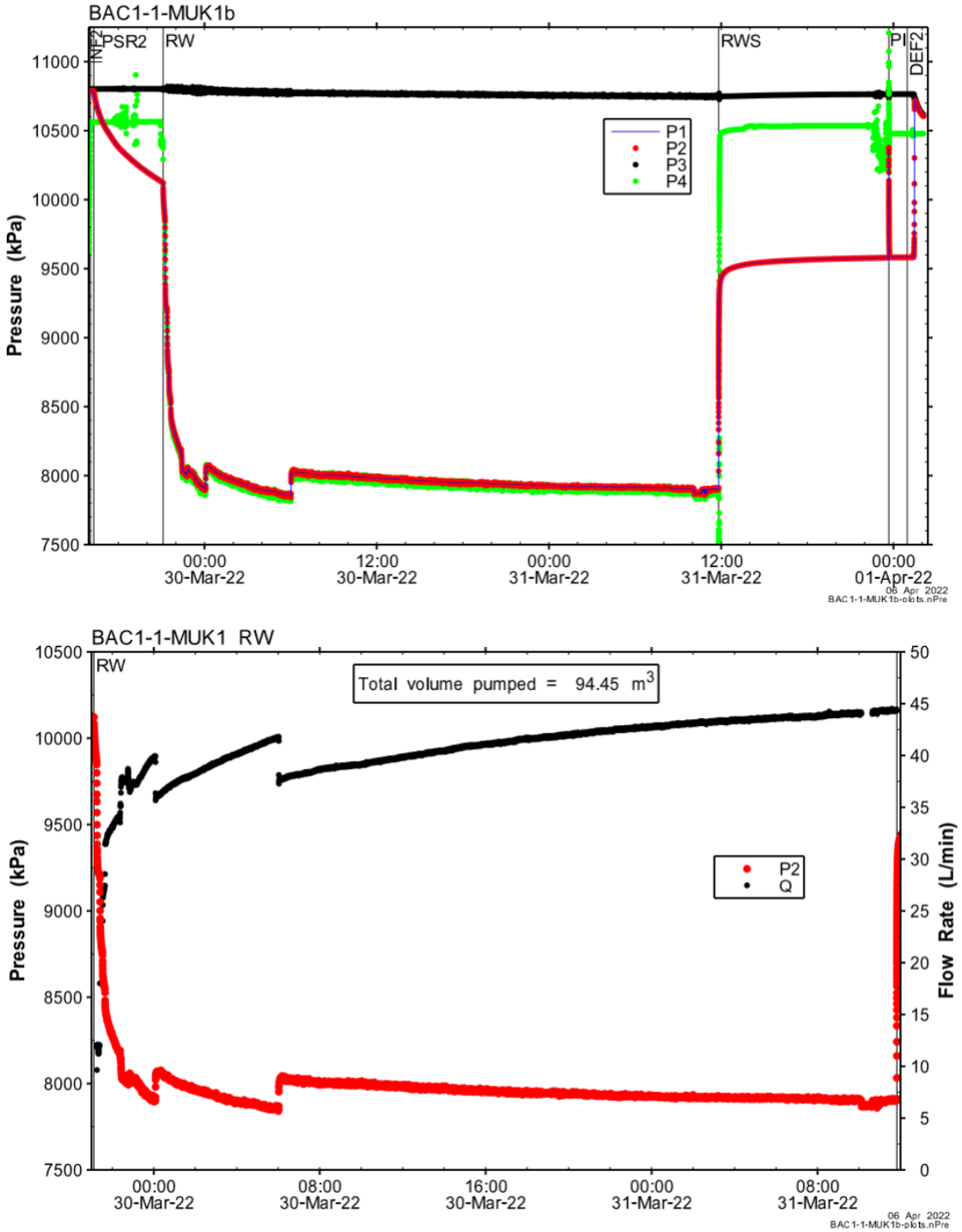

Fig. 4-20: Hydraulic packer test BAC1-1-MUK1: Overview plot of pressure since the second inflation (top) and interval pressure (P2) and rate (Q) during the RW (bottom) vs. time and date

4.5 Details of selected tests

Two of the hydraulic packer tests are presented below in more detail: BAC1-1-BDO2 and BAC1-1-LIA2. Both tests were performed in the combination of a pulse withdrawal test phase followed by a slug withdrawal and slug recovery test phase. Both tests illustrate an example of an analysis of the confining geological units above and below the host rock Opalinus Clay. These formations are characterised by low to medium transmissivity.

The two test analysis examples are presented in this section in more detail. The results of the test analyses are provided in Section 4.6 together with the results of all other tests performed.

4.5.1 Hydraulic packer test BAC1-1-BDO2

The hydraulic packer test BAC1-1-BDO2 is an example of testing formations with low to medium transmissivity using a short hydraulic test execution duration (58.6 h) after a long pressure history duration (980.9 h). For the analysis, the measurements of the QSSP P2 sensor were used at a depth of 731.81 m MD. Fig. 4-8 presents the P2 measurements.

4.5.1.1 Interval characterisation

The hydraulic test BAC1-1-BDO2 was performed in double packer configuration. The interval was located at the top of the Dogger Group («Brauner Dogger»), characterised by 1.76 m of fossiliferous iron-oolitic marl and limestone of the Wutach Formation, 2.41 m of the fossiliferous Variansmergel Formation composed of a variation from claystone to argillaceous and calcareous marl with few iron-ooids and 17.22 m of the top of the «Parkinsoni-Württembergica-Schichten» with a thin- to medium-bedded gradual alternation of silty marl and claystone with thin limestone or calcareous marl beds (strongly bioturbated, incl. burrows) (*cf.* Dossier III). The very top of the interval covered 1.05 m of the Wildegg Formation (i.e. the bottom of the Malm Group) with calcareous marl, some glauconites and comprising oncoids and iron-ooids.

The main focus of this hydraulic test was the characterisation of the hydraulic properties of the Wutach Formation, Variansmergel Formation and the upper part of the «Parkinsoni-Württembergica-Schichten». The primary test objective was to obtain a reliable estimate of T (and K) for the formation based on the determination of the flow model. A secondary objective was to obtain an estimate of the hydraulic head (h_s) / static formation pressure (P_s) of the tested interval. Details of the interval and test duration are provided in Tab. 4-20.

Tab. 4-20: Hydraulic test BAC1-1-BDO2: Information on the test interval

Test	**Depth**		**Length**	**Packer configuration**	**Hydraulic testing**		
	from [m MD]	to [m MD]	[m]		Start date	End date	Duration [h]
BAC1-1-BDO2	736.00	758.44	22.44	Double	20.11.2021	22.11.2021	58.6

4.5.1.2 Test execution

Fig. 4-21 shows the system installation record as provided by the field test contractor. The equipment components are described in Section 4.2.

The hydraulic test tool (HTT) was installed in borehole BAC1-1 on 15.11.2021 for the previous hydraulic testing in intervals BAC1-1-BDO1 (776.40 – 798.84 m MD) and BAC1-1-OPA3 (800.00 – 822.44 m MD). After these two hydraulic tests, the HTT was repositioned in the borehole for the hydraulic test BAC1-1-BDO2 on 20.11.2021. The packers were seated in competent rock of the lower Malm Group and the Dogger Group based on a study of cores, the fullbore formation microimage log and the caliper log. The entire borehole, including the test interval, was filled with potassium-silicate drilling fluid during the BAC1-1-BDO2 testing period. The test was started by inflating the bottom packer (INF1), followed by the inflation of the top packer (INF2) using a 2:1 mixture of anti-freeze:water. The SIT was opened when the top packer began to isolate the interval volume.

The COM phase lasted 2 hours and 5 minutes which allowed some of the pressure and temperature transients caused by tool installation and packer inflation to dissipate before the SIT was again closed to initiate the PSR phase. The PSR phase lasted 6 hours and 17 minutes in order to allow the test interval pressure to establish a recovery trend after being isolated. Late in the PSR phase, the test tubing was swabbed to lower the pressure in the tubing (P4) below the pressure in the test interval (P2) so that a slug withdrawal (SW) test could be initiated by opening the SIT. A slim packer was installed in the test tubing with a 4-mm inner diameter slim tubing to reduce the wellbore storage during the SW. Prior to this, and to allow more time for temperature equalisation in the test string, a pulse withdrawal (PW) was initiated by retraction of a 250 ml piston inside the PPG housing. The PW lasted for a period of 29 hours and 17 minutes. Then the SIT was opened to initiate the SW that was terminated after 6 hours and 5 minutes by closing the SIT to initiate a slug withdrawal shut-in phase (SWS). The SWS phase lasted 13 hours and 49 minutes. Before the deflation (DEF) of the packers, the SIT was opened again, and the pressure change in the test tubing was measured during repeated retracting and extending of the 250 ml piston inside the piston pulse generator housing. This well-defined volume change and the corresponding pressure change were used to evaluate the compressibility of the open system while the slim tubing was in place. The SIT was closed after testing had been finished and remained closed during deinstallation of the slim packer and relocation of the HTT to the subsequent test interval BAC1-1-MAL1.

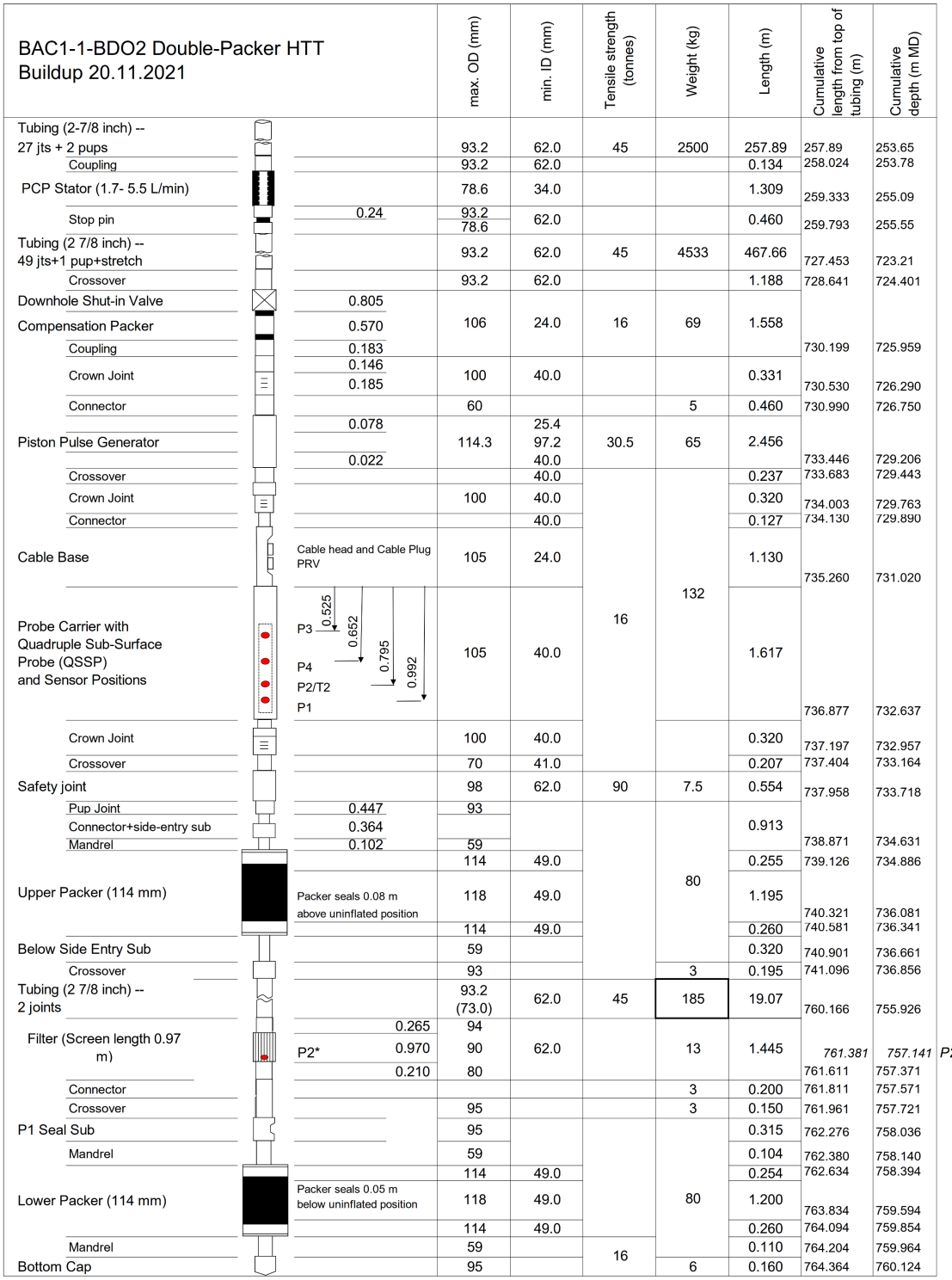

Fig. 4-21: Hydraulic test BAC1-1-BDO2: Downhole equipment installation record with system layout as used in the field test

4.5.1.3 Analysis

Borehole pressure history

The borehole pressure history used for the analysis of test BAC1-1-BDO2 is shown in Fig. B-1 (see Appendix B) and summarised in Tab. 4-21. The calculation of the mean fluid density using the measurements of the P2 pressure sensor (prior to packer inflation) gave a density of 1'168 kg m^{-3}. This value corresponds to the documented density of the drilling fluid during drilling (1'200 kg m^{-3}). For periods without a level measurement (e.g. during petrophysical logging), the drilling fluid level was assumed to be at the level of the drain pipe. During periods with no active drilling fluid circulation, the drillers generally kept the borehole full to this level and this corresponds to the situation where the HTT had reached the test depth. Therefore, the pressure measured by the P2 pressure sensor at the time the test depth had been reached was used for those periods (8'386 kPa). During coring, checktrips and circulation, Geodata monitored the drilling fluid circulation pressures using a pressure gauge mounted above the rig floor. These pressures were extrapolated to the depth of the P2 transducer (731.81 m MD) by adding the measured pressure at the P2 gauge when the HTT was first emplaced, and the borehole filled with drilling fluid (8'386 kPa). During the previous hydraulic tests (BAC1-1-LIA1, BAC1-1-LIA2, BAC1-1-OPA1, BAC1-1-OPA2, BAC1-1-BDO1 and BAC1-1-OPA3), the BAC1-1-BDO2 test interval was in the annulus above the HTT and was nearly unaffected by the pressure changes occurring during the tests. Therefore, the pressure over this period was simply approximated as full borehole conditions, i.e. 8'386 kPa. Hence, it was assumed that the drilling fluid level was at the level of the drain pipe. Once the HTT was at test depth and data acquisition began, the P2 pressure sensor measured pressure directly.

Tab. 4-21: Hydraulic test BAC1-1-BDO2: Borehole pressure history

[1] Pressure at the P2 sensor level (731.81 m MD) was calculated from the history information, i.e. fluid level and density.

[2] Drilling through interval midpoint (747.22 m MD).

[3] Pressure measured when the borehole was filled with drilling fluid (i.e. when the P2 sensor arrived at test depth and before packer inflation).

Description	**Start date and time**	**Duration** [h]	**Pressure** [1] [kPa]	
		Total: 980.90	**Start**	**End**
Drilling [2]	10.10.2021 15:04	390.93	11'741	8'386 [3]
Pull out of hole (POOH) of coring string	26.10.2021 22:00	19.75	8'386 [3]	8'386 [3]
Checktrip	27.10.2021 17:45	14.25	8'386 [3]	8'386 [3]
Petrophysical logging	28.10.2021 08:00	68.00	8'386 [3]	8'386 [3]
BOP test	31.10.2021 04:00	24.18	8'386 [3]	8'386 [3]
BAC1-1-LIA1	01.11.2021 04:11	92.35	8'386 [3]	8'386 [3]
BAC1-1-LIA2	05.11.2021 00:32	82.02	8'386 [3]	8'386 [3]
BAC1-1-OPA1	08.11.2021 10:33	54.88	8'386 [3]	8'386 [3]
BAC1-1-OPA2	10.11.2021 17:26	83.07	8'386 [3]	8'386 [3]
Checktrip	14.11.2021 04:30	29.77	8'386 [3]	8'386 [3]
BAC1-1-BDO1	15.11.2021 10:16	85.08	8'386 [3]	8'386 [3]
BAC1-1-OPA3	18.11.2021 23:21	36.62	8'386 [3]	8'386 [3]
Start testing BAC1-1-BDO2 (inflation of the second packer)	20.11.2021 11:58	-	8'386 [3]	-

Flow model evaluation

The hydraulic test sequence was analysed using a radial homogeneous flow model with a time-varying step-changing skin considering the analyses of the Ramey B diagnostic plots for the PW and SW phases and a log-log diagnostic plot for the SWS phase. Figs. B-2 and B-3 show the diagnostic plots of the PW and the SW phases, respectively, with pressures normalised to an assumed static formation pressure of 8'600 kPa. Fig. B-4 provides the log-log diagnostic plot of the SWS with a simple derivative. Only the derivative of the PW phase indicates the existence of a negative skin by a pronounced inflection of the derivative (Fig. B-2). The derivatives of other phases do not provide indication of the presence of a negative skin, but the existence of a skin cannot be generally ruled out. Therefore, a traditional skin model was applied with a step change in the hydraulic conductivity per test phase in a small near-borehole area (K_s). This was supported by early simulations (e.g. during the quick-look analysis), which had shown an improved fit of the simulation to the early measurements using a homogeneous flow model for the formation (K) with a discrete skin on the borehole wall. The SWS phase pressure derivative shows that the response during this phase was dominated by the wellbore storage (unit slope) up to the end of the test (where the derivative (blue line) begins to deviate slightly from the unit slope in Fig. B-4).

Analysis of the test sequence (PW-SW-SWS)

In the analysis, the temperature changes inside the test interval were considered during all test phases. The measurements of the memory gauge (T2*) provided the temperature in the test interval. The parameter optimisation focused on the formation parameters static pressure (P_f), hydraulic conductivity (K) and specific storage (S_s), as well as on the skin zone parameters thickness (t_s), hydraulic conductivity (K_s) and specific storage (S_{ss}) whereby the latter two are time-dependent with one parameter set per test phase. After some initial fitting, a perturbation analysis was performed using 1'000 optimisations. A fit discriminant of 1.35 was used to eliminate outliers and to build the base of the uncertainty range estimation. 454 perturbation optimisations were accepted as providing reasonable fits to the data. Figs. B-5, B-6 and B-7 present the distribution of the normalised objective function value over the matched formation parameters. Tab. 4-22 shows the best estimates and the resulting uncertainty ranges.

Tab. 4-22: Hydraulic test BAC1-1-BDO2: Formation parameter estimation based on the perturbation analysis of the sequence PW-SW-SWS using a radial homogeneous flow model with a time-varying step-changing skin considering the borehole pressure history and temperature changes inside the test interval

[1] Static formation pressure at the depth of the P2 sensor (731.81 m MD).

PW-SW-SWS results	**K** [m s^{-1}]	**S_S** [m^{-1}]	**P_f** [1] [kPa]
Best estimate	7.6×10^{-14}	6.3×10^{-7}	8'434
Uncertainty range	5.5×10^{-14} – 1.1×10^{-13}	1.6×10^{-7} – 9.2×10^{-7}	8'090 – 8'830

All selected simulations provided lower normalised objective function values than the fit discriminant. Figs. B-8 and B-9 show the Cartesian and Ramey B horsetail plots, respectively, of the PW phase for these 454 simulations. Figs. B-10 and B-11 show the Cartesian and Ramey B horsetail plots, respectively, of the SW phase. Figs. B-12 and B-13 present the Cartesian and log-log horsetail plots, respectively, of the SWS phase for these 454 simulations.

Formation parameter estimates and associated uncertainty ranges

The best estimates and uncertainty ranges for both the static formation pressure and the hydraulic conductivity were derived from the analysis of the test sequence PW-SW-SWS. Further analyses to assess the effect of the borehole pressure history on the uncertainty of the results were not considered due to prior analysis results from other TBO boreholes. The influence of the borehole pressure history is always included in the analysis as described above (see Tab. 4-21) using pressure records from measurements taken during coring and hydraulic testing. Previous analysis results (from the BUL1-1 and MAR1-1 boreholes) showed no significant influence of small changes in drilling fluid density. The test zone compressibility was determined from the pressure change measured with the QSSP P2 sensor at the pulse initiation (Fig. B-14) and the associated volume change, whereby the volume change was clearly defined by the piston volume of the PPG. Inaccuracies in the determination of the wellbore storage and the associated volume change are thereby reduced to a minimum.

The Jacobian plots (Fig. B-15 presents these for the longest test phase PW) show that the sensitivities to K, S_S and P_f were still rising at the end of the test phase, indicating that the maximum sensitivity of these parameters was not reached. By contrast, the sensitivities of the skin zone properties (K_S, S_{SS} and t_S) reached their maximum early in the test phase. However, the

quantile-normal plot of the residuals for the PW phase (Fig. B-16) displays a generally normal distribution of residuals, indicating an appropriate model selection. Fig. B-17 presents the distribution of the residuals over time that indicates a good agreement between simulation and measurements, especially for the late times of the PW phase where the formation parameter sensitivities increase. The highest residuals are observed at the beginning of the pulse withdrawal test phase (PW), when pressure was changing most rapidly. At late time of the PW, the residuals are less than ± 0.7 kPa, during the SW less than ± 0.5 kPa and during the SWS less than ± 1 kPa. The scatter plots of Fig. B-18 show the well-defined correlations among the formation fitting parameters K, P_f, and S_S. All of this information provides good evidence for a well constrained estimate of the formation properties, especially the hydraulic conductivity and static formation pressure.

For the BAC1-1-BDO2 slug test which was performed with a slim tubing while thermal equilibration in the test tubing was still ongoing, thermal expansion of the fluid in the test tubing below the slim packer needs to be considered for estimating the uncertainty ranges. This process was observed before and after the slug phase and, therefore, must also have been occurring during the SW phase, contributing to an unknown portion of the observed slug recovery which cannot be handled by the numerical model used. By attributing too much slug recovery to formation flow, the simulations presumably overestimate the hydraulic conductivity (K). This additional flow only exists during the slug phase. It does not affect the simulation in phases where the SIT is closed (PW, SWS). However, the pressure recovery of 32 kPa during the SW was well matched by the simulation (Fig. B-10). Furthermore, the shut-in test phases (PW, SWS) could be simulated with equal quality (Figs. B-8 and B-12) relative to the slug phase (SW). Therefore, an additional consideration of this source of uncertainty is not necessary. The best estimate and the bandwidth of the hydraulic conductivity are directly taken from the results of the PW-SW-SWS analysis. Tab. 4-23 presents the results of the analysis of the formation parameters for BAC1-1-BDO2. The hydraulic conductivity appears to be robustly defined with little uncertainty.

Tab. 4-23: Hydraulic test BAC1-1-BDO2: Best estimates for the formation parameters and associated uncertainty ranges

[1] Static formation pressure at midpoint of test interval (747.22 m MD).

Results	**K** [m s^{-1}]	**P_S** [1] [kPa]
Best estimate	7.6×10^{-14}	8'615
Uncertainty range	5.5×10^{-14} – 1.1×10^{-13}	8'271 – 9'011

4.5.2 Hydraulic packer test BAC1-1-LIA2

The hydraulic packer test BAC1-1-LIA2 is an example of a testing formation with low to medium transmissivity using a medium hydraulic test execution duration (79.0 h) after a medium pressure history duration (264.1 h). The analysis is based on the measurements of the QSSP P2 sensor at a depth of 911.51 m MD, as presented in Fig. 4-15.

4.5.2.1 Interval characterisation

The hydraulic test BAC1-1-LIA2 was performed in double packer configuration. The interval was located in the Staffelegg Formation of the Lias Group. It covers from top to bottom: 3.94 m of the Gross Wolf Member with argillaceous to calcareous marl; then 5.85 m of the Rietheim

Member of argillaceous marl with calcareous marl and fossiliferous interlayers, and bituminous shale along the bottom; followed by 2.63 m of the Grünschholz, Breitenmatt and Rickenbach Members of glauconitic and very fossiliferous marl and bioclastic limestone; and 0.95 m of the Frick Member with argillaceous silt- to sandstone (*cf.* Dossier III).

The main motivation for this hydraulic test was the characterisation of the hydraulic properties of the Staffelegg Formation from the Gross Wolf to the Grünschholz, Breitenmatt and Rickenbach Members. The primary test objective was to obtain a reliable estimate of T (and K) for the formation based on the determination of the flow model. A secondary objective was to obtain an estimate of the hydraulic head (h_s) / static formation pressure (P_s) for the tested interval. Details of the interval and test duration are provided in Tab. 4-24.

Tab. 4-24: Hydraulic test BAC1-1-LIA2: Information on the test interval

Test	**Depth**		**Length**	**Packer configuration**	**Hydraulic testing**		
	from [m MD]	to [m MD]	[m]		Start date	End date	Duration [h]
BAC1-1-LIA2	915.70	929.07	13.37	Double	05.11.2021	08.11.2021	79.0

4.5.2.2 Test execution

Fig. 4-22 shows the system installation record as provided by the field test contractor. The equipment components are described in Section 4.2.

The HTT was installed in borehole BAC1-1 on 04.11.2021. The packers were seated in competent rock within the Staffelegg Formation in accordance with information from cores, the fullbore formation microimage log and the caliper log. The entire borehole, including the test interval, was filled with potassium-silicate drilling fluid during the BAC1-1-LIA2 testing period. The test was started by inflating the bottom packer (INF1) and then the top packer (INF2) with a 2:1 mixture of anti-freeze:water. The SIT was opened when the top packer began to isolate the interval volume.

The COM phase lasted 3 hours and 10 minutes which allowed some of the pressure and temperature transients caused by tool installation and packer inflation to dissipate before the SIT was again closed to initiate the PSR phase. The PSR phase lasted 6 hours in order to allow the test interval pressure to establish a recovery trend after being isolated. After this period a pulse withdrawal (PW) was initiated by retracting a 250 ml piston inside the PPG housing. The PW lasted for a period of 35 hours and 55 minutes. Late in the PW phase, the test tubing was swabbed to lower the pressure in the tubing (P4) below the pressure in the test interval (P2) so that a slug withdrawal (SW) test could be initiated by opening the SIT. A slim packer was installed in the test tubing with 4-mm inner diameter slim tubing to reduce the wellbore storage during the SW. Then the SIT was opened to initiate the SW that was terminated after 9 hours and 1 minute by closing the SIT to initiate a slug withdrawal shut-in phase (SWS). The SWS phase lasted 24 hours and 30 minutes. The deflation of the slim tubing packer and the deflation (DEF) of the packers was started while the SIT was closed. After finishing the removal of the slim tubing, the HTT was moved 14 m upward to the next hydraulic test interval of BAC1-1-OPA1.

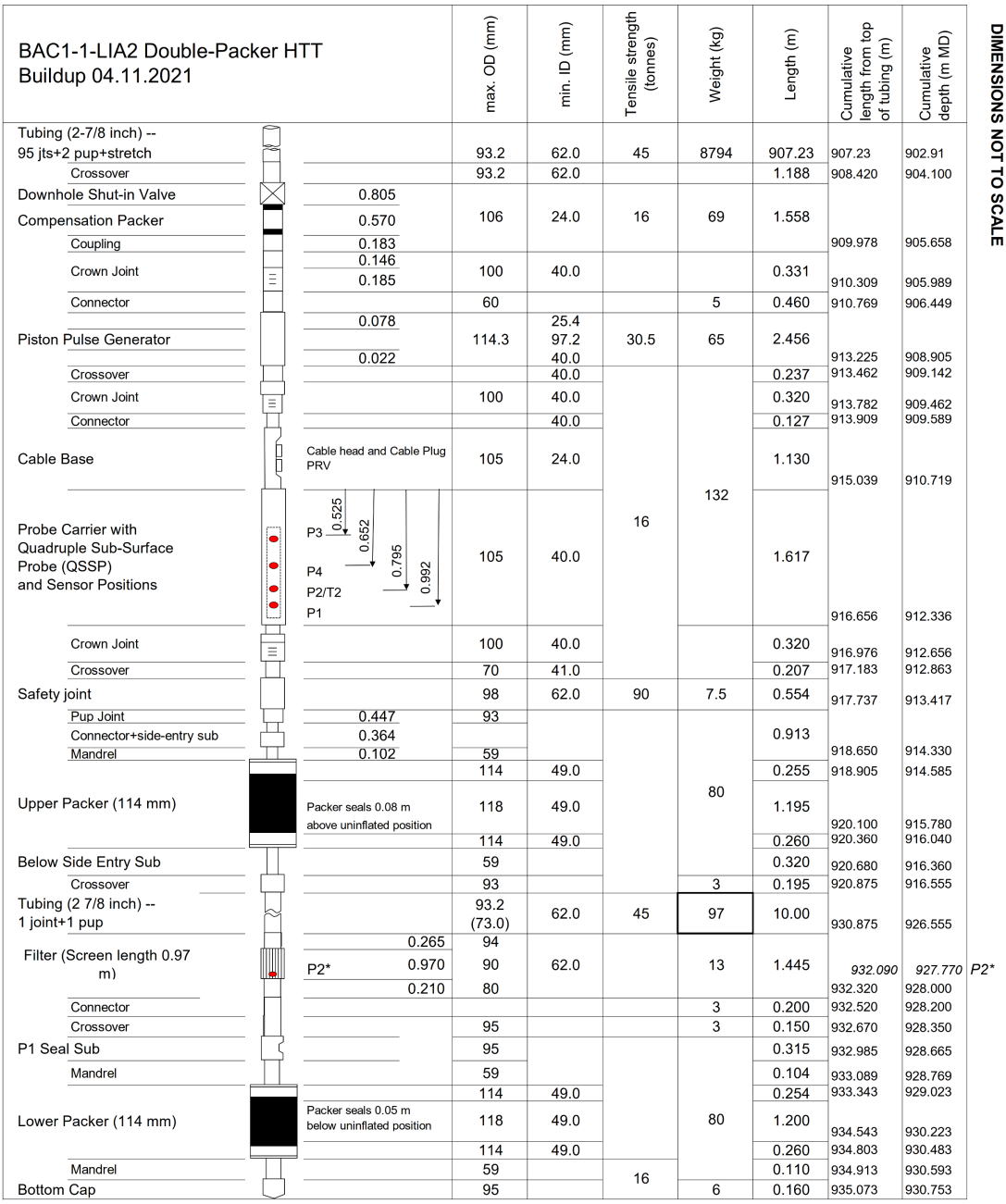

Fig. 4-22: Hydraulic test BAC1-1-LIA2: Downhole equipment installation record with system layout as used in the field test

4.5.2.3 Analysis

Borehole pressure history

The borehole pressure history used for the analysis of test BAC1-1-LIA2 is shown in Fig. B-19 and summarised in Tab. 4-25. The calculation of the mean fluid density based on the measurements of the P2 pressure sensor (prior to packer inflation) gave a density of 1'192 kg m^{-3}. This value corresponds to the documented density of the drilling fluid during drilling (1'200 kg m^{-3}). For periods without a level measurement (e.g. during petrophysical logging), the drilling fluid level was assumed to be at the level of the drain pipe. During periods with no active drilling fluid circulation, the drillers generally kept the borehole full to this level and this corresponds to the situation where the HTT had reached the test depth. Therefore, the pressure measured by the P2 pressure sensor at the time the test depth had been reached was used for those periods (10'678 kPa). During coring, checktrips and circulation, Geodata monitored the drilling fluid circulation pressures with a pressure gauge mounted above the rig floor. These pressures were extrapolated to the depth of the P2 transducer (911.51 m MD) by adding the measured pressure at the P2 gauge when the HTT was first installed, and the borehole filled with drilling fluid (10'678 kPa). During the BAC1-1-LIA1 hydraulic test, the BAC1-1-LIA2 test interval was in the annulus above the HTT and remained nearly unaffected by the negligible 16-kPa pressure change that occurred during this period of testing. Therefore, the pressure history over the duration of BAC1-1-LIA1 was approximated as full borehole conditions using a constant pressure value of 10'678 kPa.

Tab. 4-25: Hydraulic test BAC1-1-LIA2: Borehole pressure history

[1] Pressure at the P2 sensor level (911.51 m MD) was calculated from the history information, i.e. fluid level and density.

[2] Drilling through interval midpoint (922.39 m MD).

[3] Pressure measured when the borehole was filled with drilling fluid (i.e. when the P2 sensor arrived at test depth and before packer inflation).

Description	**Start date and time**	**Duration** [h]	**Pressure** [1] [kPa]	
		Total: 264.08	**Start**	**End**
Drilling [2]	25.10.2021 00:27	45.55	13'807	10'678 [3]
Pull out of hole (POOH) of coring string	26.10.2021 22:00	19.75	10'678 [3]	10'678 [3]
Checktrip	27.10.2021 17:45	14.25	10'678 [3]	10'678 [3]
Petrophysical logging	28.10.2021 08:00	68.00	10'678 [3]	10'678 [3]
BOP test	31.10.2021 04:00	24.18	10'678 [3]	10'678 [3]
BAC1-1-LIA1	01.11.2021 04:11	92.35	10'678 [3]	10'678 [3]
Start testing BAC1-1-LIA2 (inflation of the second packer)	05.11.2021 00:32	-	10'678 [3]	-

Flow model evaluation

The hydraulic test sequence was analysed using a radial homogeneous flow model with a time-varying step-changing skin considering the analyses of the Ramey B diagnostic plots for the PW and SW phases and a log-log diagnostic plot for the SWS phase. Figs. B-20 and B-21 show the diagnostic plots of the PW and the SW phases, respectively, with pressures normalised to an assumed static formation pressure of 10'300 kPa. Fig. B-22 provides the log-log diagnostic plot of the SWS with a simple derivative. The derivative of the PW phase indicates a possible presence of a negative skin of which, however, the diagnostic plot of the SW phase bears no indication. The log-log diagnostic plot of the SWS phase illustrates only a domination of the wellbore storage for the entire period of this phase. Therefore, the existence of a negative skin cannot be generally ruled out and a traditional skin model was applied with a step change in the hydraulic conductivity per test phase in a small near-borehole zone (K_s).

Analysis of the test sequence (PW-SW-SWS)

In the analysis, the temperature changes inside the test interval were considered during all test phases. The measurements of the memory gauge (T2*) provided the temperature in the test interval. The time-dependent skin zone properties of hydraulic conductivity (K_s) and specific storage (S_{ss}) were defined twice. One parameter set was used for the simulation of the PW and the previous pressure history duration. A second parameter set was applied for the SW and SWS phases. Both parameter sets were optimised together with the skin zone thickness (t_s) and the formation parameters static pressure (P_f) and hydraulic conductivity (K). The specific storage of the formation (S_s) was held constant at the theoretical value based on estimated properties for the rock compressibility and the porosity taken from Nagra (2001). After some initial simulations including a parameter optimisation, a perturbation of 1'000 optimisation runs was performed based on a match of the pressure data during the PW-SW-SWS sequence. A fit discriminant of 1.3 was used to eliminate outliers and to serve as the base of the uncertainty range estimation. 673 perturbation optimisations were accepted as providing reasonable fits to the data. Figs. B-23 and B-24 present the distribution of the normalised objective function value over the matched formation parameters. Tab. 4-26 shows the best estimates and the resulting uncertainty ranges.

Tab. 4-26: Hydraulic test BAC1-1-LIA2: Formation parameter estimation based on the perturbation analysis of the sequence PW-SW-SWS using a radial homogeneous flow model with a time-varying step-changing skin considering the borehole pressure history and temperature changes inside the test interval

[1] Fixed, pre-defined value taken from Nagra (2001).

[2] Static formation pressure at the depth of the P2 sensor (911.51 m MD).

PW-SW-SWS results	**K** [m s^{-1}]	**Ss** [1] [m^{-1}]	**P_f** [2] [kPa]
Best estimate	8.5×10^{-14}	1.7×10^{-6}	10'803
Uncertainty range	6.7×10^{-14} – 1.0×10^{-13}	-	10'650 – 11'034

All selected simulations provided lower normalised objective function values as defined by the fit discriminant. In general, the simulation results represent the measured pressure well, except for an early-time mismatch between the SW Ramey B derivative and simulations. Figs. B-25 and B-26 show the Cartesian and Ramey B horsetail plots, respectively, of the PW phase for these 673 simulations. Figs. B-27 and B-28 show the Cartesian and Ramey B horsetail plots, respec-

tively, of the SW phase. Figs. B-29 and B-30 present the Cartesian and log-log horsetail plots, respectively, of the SWS phase for these 673 simulations. Only the simulations of the SW phase have a slightly different curvature than the measured pressure curve.

Formation parameter estimates and associated uncertainty ranges

The best estimates and uncertainty ranges for both the static formation pressure and the hydraulic conductivity were derived from the analysis of the test sequence PW-SW-SWS.

The Jacobian plots (Fig. B-31 presents these for the longest test phase PW) show that the sensitivity to K and P_f was still rising at the end of the test phase, indicating that the maximum sensitivities of these parameters were not reached. By contrast, the sensitivities of the skin zone properties (K_S, S_{SS} and t_S) reached their maximum early in the test phase. The quantile-normal plot of the residuals for the longest test phase PW (Fig. B-32, top left) and the SW phase (Fig. B-32, top right) display reasonably normal distributions apart from the tails, while the quantile-normal plot of the residuals for the SWS phase (Fig. B-32, bottom left) shows that the distribution of residuals is not as normal as desired. Fig. B-33 presents the distribution of the residuals over time. The highest residuals are observed at the start of the PW phase, when pressure was changing most rapidly. However, the structure in the residual plots indicates that processes and/or properties not included in the numerical model have influenced the measured pressure data. Therefore, in addition to the uncertainty in the analysis model used, an additional source of uncertainties in the results must be considered.

One additional source of uncertainty is the temperature change inside the test string between the SIT and the slim packer during the slug phase. Normally, the downhole pressure measurements of a slug phase are independent of temperature changes in the test interval, as the temperature-induced change in the volume is compensated by the temperature-induced change in the density of the water column. When using a slim tubing in the uppermost part of the test string, however, this is no longer the case. The temperature-induced change of the test fluid level (due to the volume change) is amplified by the radius reduction through the slim tubing. To evaluate this influence, a sampling analysis of the tubing radius (characterising the changed conditions in the borehole) was performed. The best estimate of the slim tubing radius resulting from the lowest discrepancy between the simulated and measured pressure curve is 2.94 mm. This value is slightly higher than the calculated theoretically effective slim tubing radius of 2.77 mm used in the analysis of the PW-SW-SWS test sequence. The calculated radius is based on the physical radius of 2 mm and the sum of all components defining the total wellbore storage of the interval (Black et al. 1987). Fig. B-34 shows the distribution of the normalised objective function value over the sampled slim tubing radius. However, the uncertainties of the formation parameters are within the ranges of the perturbation analysis results. Fig. B-35 presents the results for the formation parameters K and P_f as scatter plots versus the sampled slim tubing radius. Tab. 4-27 states the best estimates for formation parameters and uncertainty ranges based on a fit discriminant of 1.7 (155 resulting simulations).

Tab. 4-27: Hydraulic test BAC1-1-LIA2: Formation parameter estimation based on the sampling analysis of the slim tubing radius using a radial homogeneous flow model with a time-varying step-changing skin considering the borehole pressure history and temperature changes inside the test interval

[1] Fixed, pre-defined value taken from Nagra (2001).

[2] Static formation pressure at the depth of the P2 sensor (911.51 m MD).

[3] Best estimate using a slim tubing radius of 2.94 mm.

PW-SW-SWS results	**K** [m s^{-1}]	**Ss** [1] [m^{-1}]	**P_f** [2] [kPa]
Best estimate [3]	9.8×10^{-14}	1.7×10^{-6}	10'674
Uncertainty range	8.2×10^{-14} – 1.0×10^{-13}	-	10'663 – 10'875

The slug test phase, which was performed with a slim tubing while thermal equilibration in the test tubing was still ongoing**,** was affected by thermal expansion of the fluid in the test tubing below the slim packer. However, the measured pressure recovery of 52 kPa during the SW phase was matched adequately by the simulations. Furthermore, the shut-in test phases PW and SWS were simulated in comparable quality with the same estimates of the formation parameters.

Other sources of uncertainty in the formation parameter estimates are the borehole pressure history and the description of the interval conditions during shut-in phases. However, further analyses to assess the effect of the borehole pressure history on the uncertainty of the results were not considered due to prior analysis results from other TBO boreholes. The influence of the borehole pressure history is always included in the analysis as described above (see Tab. 4-25) using pressure records from measurements taken during coring and hydraulic testing. Previous analysis results (in both the BUL1-1 and MAR1-1 boreholes) showed no significant influence of small changes in drilling fluid density. The test zone compressibility was determined from the pressure change measured with the QSSP P2 sensor at the pulse initiation (Fig. B-36) and the associated volume change, whereby the volume change was clearly defined by the piston volume of the PPG. Inaccuracies in the determination of the wellbore storage and the associated volume change are thereby reduced to a minimum.

The best estimate and the bandwidth of the hydraulic conductivity are taken from the combined analysis of the PW-SW-SWS sequence. The best estimate and range of static formation pressure were taken directly from the perturbations result. Tab. 4-28 presents the results of the analysis of the formation parameters for the hydraulic test BAC1-1-LIA2.

Tab. 4-28: Hydraulic test BAC1-1-LIA2: Best estimates for the formation parameters and associated uncertainty ranges

[1] Static formation pressure at midpoint of test interval (922.39 m MD).

Results	**K** [m s^{-1}]	**P_S** [1] [kPa]
Best estimate	9×10^{-14}	10'931
Uncertainty range	$6 \times 10^{-14} – 1 \times 10^{-13}$	10'778 – 11'162

4.6 Summary and discussion of hydraulic tests

4.6.1 Summary tables and plots

The results of the transmissivity and hydraulic conductivity estimates for all tested intervals are summarised in Tab. 4-29, and the estimated freshwater hydraulic heads and static formation pressures are documented in Tab. 4-30. Both tables present the best estimates along with confidence ranges as determined by the field test contractor and documented in the corresponding analysis reports. The results of the fluid logging (*cf.* Section 3) have been included in these tables as no hydraulic packer test was carried out within the logged borehole section.

The permeabilities for all tested intervals are summarised in Tab. 4-31 and were calculated based on the hydraulic conductivities provided in Tab. 4-29. An assumed density of 1'000 kg m^{-3} and a dynamic viscosity of 1×10^{-3} Pa s were used for the calculation of the hydraulic permeabilities.

The hydraulic parameters T, K, P_S and h_S (in terms of m TVD and m asl) are illustrated with respect to both the borehole depth (in m MD) and the geological profile in Figs. 4-23 to 4-27. The best estimates for these parameters are indicated by vertical lines in the corresponding interval position. The associated confidence ranges are shown as dashed rectangles, delimited vertically by the corresponding interval extent and laterally by the minimum and maximum values.

Tab. 4-29: Summary of the hydraulic testing in borehole BAC1-1: Transmissivity and hydraulic conductivity

[1] Based on the results presented by the field test contractor. Values are rounded.

[2] T and K for the entire logged interval; hydraulic parameters of inflow zones identified from the fluid logging are given in Section 3.2.

[3] Time-varying skin properties.

[4] Tests BAC1-1-BDO3 and BAC1-1-OPA3 were performed in test intervals which contained a drilling-induced fracture. Both hydraulic test analyses did not provide conclusive hydraulic parameters. The measured pressure responses are influenced by processes that cannot be represented by the models used.

[5] Test BAC1-1B-BDO4 was performed in sidetrack BAC1-1B. The test showed short time pressure response correlations between the test interval (QSSP P2) and the bottom zone interval (QSSP P1). The test data does therefore not allow to estimate reliable hydraulic parameters.

Test interval details and hydraulic model							**Transmissivity and hydraulic conductivity**					
Test name	**Interval depth**				**Interval length**	**Hydraulic model**	**Best estimate** [1]		**Lowest estimate** [1]		**Highest estimate** [1]	
	From [m MD]	**To** [m MD]	**From** [m asl]	**To** [m asl]	[m]		**T** [$m^2 s^{-1}$]	**K** [$m s^{-1}$]	T_{min} [$m^2 s^{-1}$]	K_{min} [$m s^{-1}$]	T_{max} [$m^2 s^{-1}$]	K_{max} [$m s^{-1}$]
BAC1-1-FL1-MAL [2]	513.00	700.00	-62.65	-249.65	187.00	homogeneous with skin	4×10^{-11}	2×10^{-13}	3×10^{-11}	2×10^{-13}	2×10^{-10}	7×10^{-13}
BAC1-1-MAL1	712.56	735.00	-262.21	-284.65	22.44	homogeneous with skin [3]	2×10^{-12}	1×10^{-13}	1×10^{-12}	4×10^{-14}	3×10^{-12}	2×10^{-13}
BAC1-1-BDO2	736.00	758.44	-285.65	-308.09	22.44	homogeneous with skin [3]	2×10^{-12}	8×10^{-14}	1×10^{-12}	5×10^{-14}	3×10^{-12}	2×10^{-13}
BAC1-1-BDO3 [4]	769.00	816.17	-318.65	-365.82	47.17	-	-	-	-	-	-	-
BAC1-1-BDO1	776.40	798.84	-326.05	-348.49	22.44	homogeneous with skin [3]	4×10^{-12}	2×10^{-13}	1×10^{-12}	4×10^{-14}	2×10^{-11}	6×10^{-13}
BAC1-1B-BDO4 [5]	797.00	812.72	-346.65	-362.37	15.72	-	-	-	-	-	-	-
BAC1-1-OPA3 [4]	800.00	822.44	-349.65	-372.09	22.44	-	-	-	-	-	-	-
BAC1-1-OPA2	880.80	894.17	-430.45	-443.82	13.37	homogeneous with skin	3×10^{-13}	2×10^{-14}	2×10^{-13}	1×10^{-14}	5×10^{-13}	4×10^{-14}
BAC1-1-OPA1	901.70	915.07	-451.35	-464.72	13.37	radial-composite model	2×10^{-12}	1×10^{-13}	1×10^{-12}	8×10^{-14}	3×10^{-12}	2×10^{-13}
BAC1-1-LIA2	915.70	929.07	-465.35	-478.72	13.37	homogeneous with skin [3]	1×10^{-12}	9×10^{-14}	8×10^{-13}	6×10^{-14}	2×10^{-12}	1×10^{-13}
BAC1-1-LIA1	930.20	952.00	-479.85	-501.65	21.80	homogeneous with skin [3]	2×10^{-10}	1×10^{-11}	1×10^{-10}	5×10^{-12}	2×10^{-9}	7×10^{-11}

Tab. 4-29: continued

Test interval details and hydraulic model							**Transmissivity and hydraulic conductivity**					
Test name	**Interval depth**				**Interval length** [m]	**Hydraulic model**	**Best estimate** [1]		**Lowest estimate** [1]		**Highest estimate** [1]	
	From [m MD]	**To** [m MD]	**From** [m asl]	**To** [m asl]			**T** [$m^2 s^{-1}$]	**K** [$m s^{-1}$]	**T_{min}** [$m^2 s^{-1}$]	**K_{min}** [$m s^{-1}$]	**T_{max}** [$m^2 s^{-1}$]	**K_{max}** [$m s^{-1}$]
BAC1-1-KEU1	957.20	979.00	-506.85	-528.65	21.80	radial-composite with skin [3]	2×10^{-7}	8×10^{-9}	5×10^{-8}	2×10^{-9}	6×10^{-7}	3×10^{-8}
BAC1-1-KEU2	957.20	968.21	-506.85	-517.86	11.01	homogeneous with skin [3]	3×10^{-11}	3×10^{-12}	7×10^{-12}	6×10^{-13}	5×10^{-11}	4×10^{-12}
BAC1-1-MUK1	1'080.90	1'129.00	-630.55	-678.65	48.10	radial-composite with skin [3]	2×10^{-5}	4×10^{-7}	1×10^{-5}	2×10^{-7}	3×10^{-5}	5×10^{-7}

Tab. 4-30: Summary of the hydraulic testing in borehole BAC1-1: Hydraulic head estimates

[1] Based on the results presented by the field test contractor.

[2] Time-varying skin properties

[3] Tests BAC1-1-BDO3 and BAC1-1-OPA3 were performed in test intervals which contained a drilling-induced fracture. Both hydraulic test analyses did not provide conclusive hydraulic parameters. The measured pressure responses are influenced by processes that cannot be represented by the models used.

[4] Test BAC1-1B-BDO4 was performed in sidetrack BAC1-1B. The test showed short time pressure response correlations between the test interval (QSSP P2) and the bottom zone interval (QSSP P1). The test data does therefore not allow to estimate reliable hydraulic parameters.

Test interval details and associated hydraulic model							**Hydraulic head** [m TVD]			**Hydraulic head** [m asl]			**Formation pressure**		
Test name	**Interval depth**				**Interval length**	**Hydraulic model**	**Best** [1] **h**	**Lowest** [1] **h_{min}**	**Highest** [1] **h_{max}**	**Best** [1] **h**	**Lowest** [1] **h_{min}**	**Highest** [1] **h_{max}**	**Best** [1] **P_S**	**Lowest** [1] **$P_{S\,min}$**	**Highest** [1] **$P_{S\,max}$**
	From [m MD]	**To** [m MD]	**From** [m asl]	**To** [m asl]	[m]		[m TVD]	[m TVD]	[m TVD]	[m asl]	[m asl]	[m asl]	[kPa]	[kPa]	[kPa]
BAC1-1-FL1-MAL	513.00	700.00	-62.65	-249.65	187.00	homogeneous with skin	-22	34	-27	473	416	477	6'167	5'615	6'215
BAC1-1-MAL1	712.56	735.00	-262.21	-284.65	22.44	homogeneous with skin [2]	-95	-62	-120	545	512	570	8'027	7'709	8'277
BAC1-1-BDO2	736.00	758.44	-285.65	-308.09	22.44	homogeneous with skin [2]	-131	-96	-171	581	546	622	8'615	8'271	9'011
BAC1-1-BDO3 [3]	769.00	816.17	-318.65	-365.82	47.17	-	-	-	-	-	-	-	-	-	-
BAC1-1-BDO1	776.40	798.84	-326.05	-348.49	22.44	homogeneous with skin [2]	-171	-135	-438	621	586	888	9'405	9'054	12'024
BAC1-1B-BDO4 [4]	797.00	812.72	-346.65	-362.37	15.72	-	-	-	-	-	-	-	-	-	-
BAC1-1-OPA3 [3]	800.00	822.44	-349.65	-372.09	22.44	-	-	-	-	-	-	-	-	-	-

Tab. 4-30: continued

Test interval details and associated hydraulic model							**Hydraulic head** [m TVD]			**Hydraulic head** [m asl]			**Formation pressure**		
Test name	**Interval depth**				**Interval length**	**Hydraulic model**	**Best** [1] **h**	**Lowest** [1] **h_{min}**	**Highest** [1] **h_{max}**	**Best** [1] **h**	**Lowest** [1] **h_{min}**	**Highest** [1] **h_{max}**	**Best** [1] **P_S**	**Lowest** [1] **$P_{S\,min}$**	**Highest** [1] **$P_{S\,max}$**
	From [m MD]	**To** [m MD]	**From** [m asl]	**To** [m asl]	[m]		[m TVD]	[m TVD]	[m TVD]	[m asl]	[m asl]	[m asl]	[kPa]	[kPa]	[kPa]
BAC1-1-OPA2	880.80	894.17	-430.45	-443.82	13.37	homogeneous with skin	-472	-393	-544	923	844	994	13'339	12'566	14'040
BAC1-1-OPA1	901.70	915.07	-451.35	-464.72	13.37	radial-composite model	-221	-205	-275	671	656	726	11'079	10'927	11'612
BAC1-1-LIA2	915.70	929.07	-465.35	-478.72	13.37	homogeneous with skin [2]	-192	-176	-215	642	627	666	10'931	10'778	11'162
BAC1-1-LIA1	930.20	952.00	-479.85	-501.65	21.80	homogeneous with skin [2]	-108	-105	-112	559	556	563	10'296	10'267	10'334
BAC1-1-KEU1	957.20	979.00	-506.85	-528.65	21.80	radial-composite with skin [2]	100	101	100	350	349	351	8'512	8'506	8'518
BAC1-1-KEU2	957.20	968.21	-506.85	-517.86	11.01	homogeneous with skin [2]	78	88	72	372	362	379	8'676	8'577	8'742
BAC1-1-MUK1	1'080.90	1'129.00	-630.55	-678.65	48.10	radial-composite with skin [2]	97	98	96	353	352	354	9'886	9'875	9'898

Tab. 4-31: Summary of the hydraulic testing in borehole BAC1-1: Permeability

[1] The calculation is based on the hydraulic conductivity provided by the field test contractor in the corresponding DR and standard conditions (density: 1'000 kg m^{-3}, dynamic viscosity: 1×10^{-3} Pa s). Values are rounded.

[2] Permeability for the entire logged interval; hydraulic parameters of inflow zones identified from the fluid logging are given in Section 3.2.

[3] Tests BAC1-1-BDO3 and BAC1-1-OPA3 were performed in test intervals which contained a drilling-induced fracture. Both hydraulic test analyses did not provide conclusive hydraulic parameters. The measured pressure responses are influenced by processes that cannot be represented by the models used.

[4] Test BAC1-1B-BDO4 was performed in sidetrack BAC1-1B. The test showed short time pressure response correlations between the test interval (QSSP P2) and the bottom zone interval (QSSP P1). The test data does therefore not allow to estimate reliable hydraulic parameters.

Test interval details						**Permeability estimates** [1]		
Test name	**Interval depth**				**Interval length**	**Best k**	**Lowest k_{min}**	**Highest k_{max}**
	From [m MD]	**To** [m MD]	**From** [m asl]	**To** [m asl]	[m]	[m^2]	[m^2]	[m^2]
BAC1-1-FL1-MAL [2]	513.00	700.00	-62.65	-249.65	187.00	4×10^{-14}	2×10^{-20}	7×10^{-20}
BAC1-1-MAL1	712.56	735.00	-262.21	-284.65	22.44	1×10^{-20}	4×10^{-21}	1×10^{-20}
BAC1-1-BDO2	736.00	758.44	-285.65	-308.09	22.44	8×10^{-21}	5×10^{-21}	1×10^{-20}
BAC1-1-BDO3 [3]	769.00	816.17	-318.65	-365.82	47.17	-	-	-
BAC1-1-BDO1	776.40	798.84	-326.05	-348.49	22.44	2×10^{-20}	4×10^{-21}	5×10^{-20}
BAC1-1B-BDO4 [4]	797.00	812.72	-346.65	-362.37	15.72	-	-	-
BAC1-1-OPA3 [3]	800.00	822.44	-349.65	-372.09	22.44	-	-	-
BAC1-1-OPA2	880.80	894.17	-430.45	-443.82	13.37	2×10^{-21}	1×10^{-21}	3×10^{-21}
BAC1-1-OPA1	901.70	915.07	-451.35	-464.72	13.37	1×10^{-20}	9×10^{-21}	1×10^{-20}
BAC1-1-LIA2	915.70	929.07	-465.35	-478.72	13.37	9×10^{-21}	6×10^{-21}	1×10^{-20}
BAC1-1-LIA1	930.20	952.00	-479.85	-501.65	21.80	1×10^{-18}	5×10^{-19}	6×10^{-18}
BAC1-1-KEU1	957.20	979.00	-506.85	-528.65	21.80	8×10^{-16}	2×10^{-16}	2×10^{-15}
BAC1-1-KEU2	957.20	968.21	-506.85	-517.86	11.01	3×10^{-19}	6×10^{-20}	3×10^{-19}
BAC1-1-MUK1	1'080.90	1'129.00	-630.55	-678.65	48.10	4×10^{-14}	2×10^{-14}	4×10^{-14}

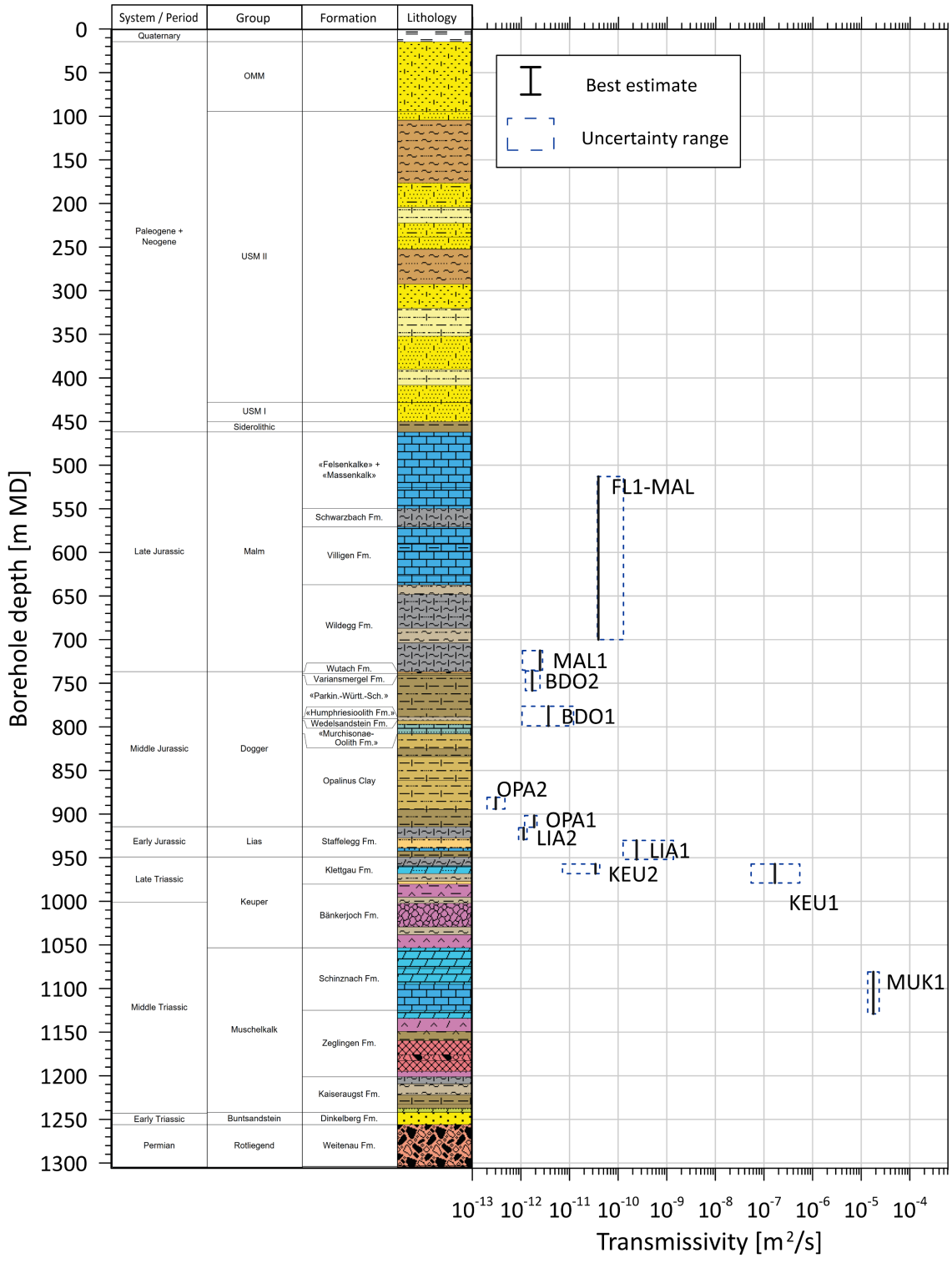

Fig. 4-23: Summary of the hydraulic testing in borehole BAC1-1: Formation transmissivity profile

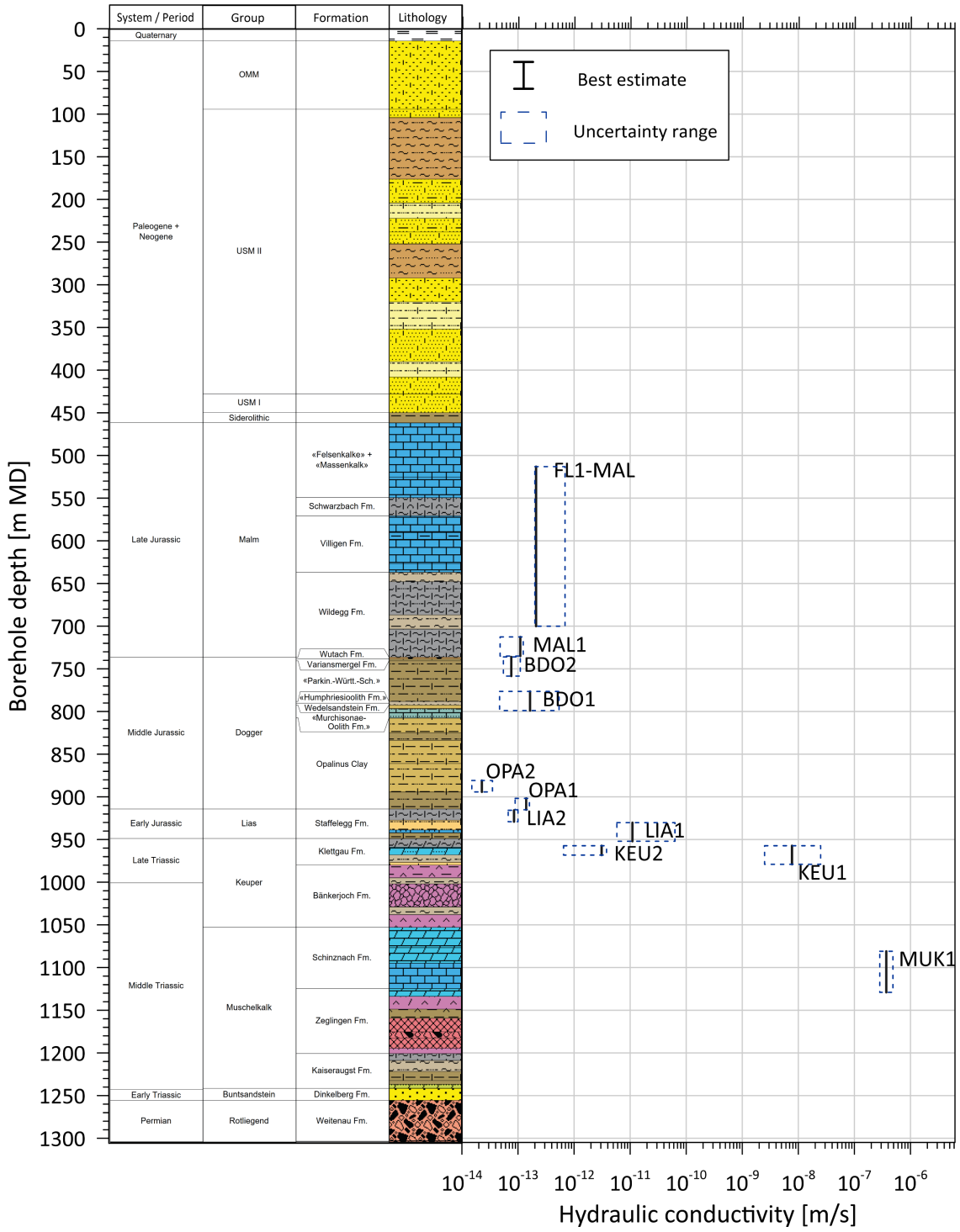

Fig. 4-24: Summary of the hydraulic testing in borehole BAC1-1: Formation hydraulic conductivity profile

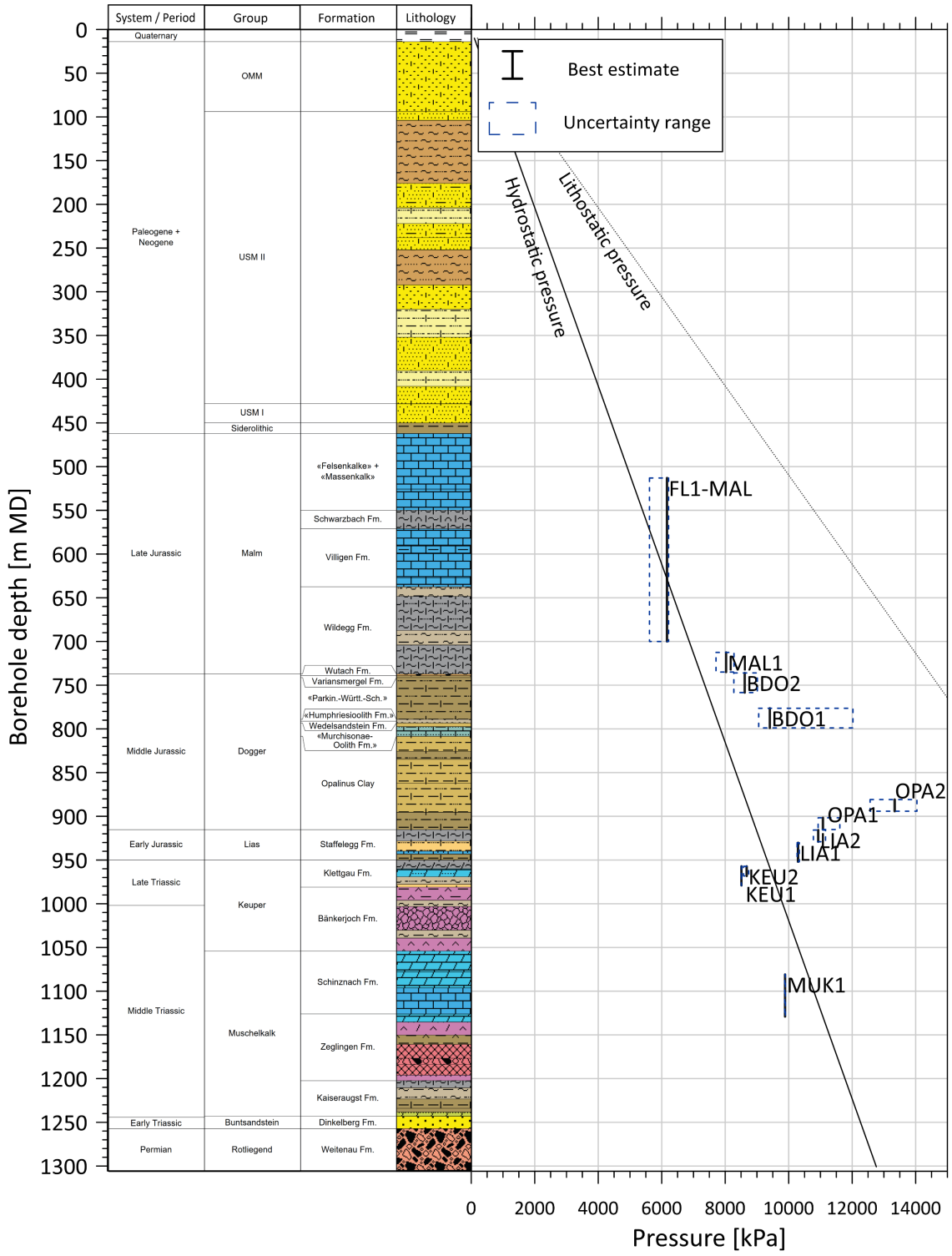

Fig. 4-25: Summary of the hydraulic testing in borehole BAC1-1: Static formation pressure profile

The lithostatic pressure is based on the assumption of a mean density of 2'000 kg m^{-3}.

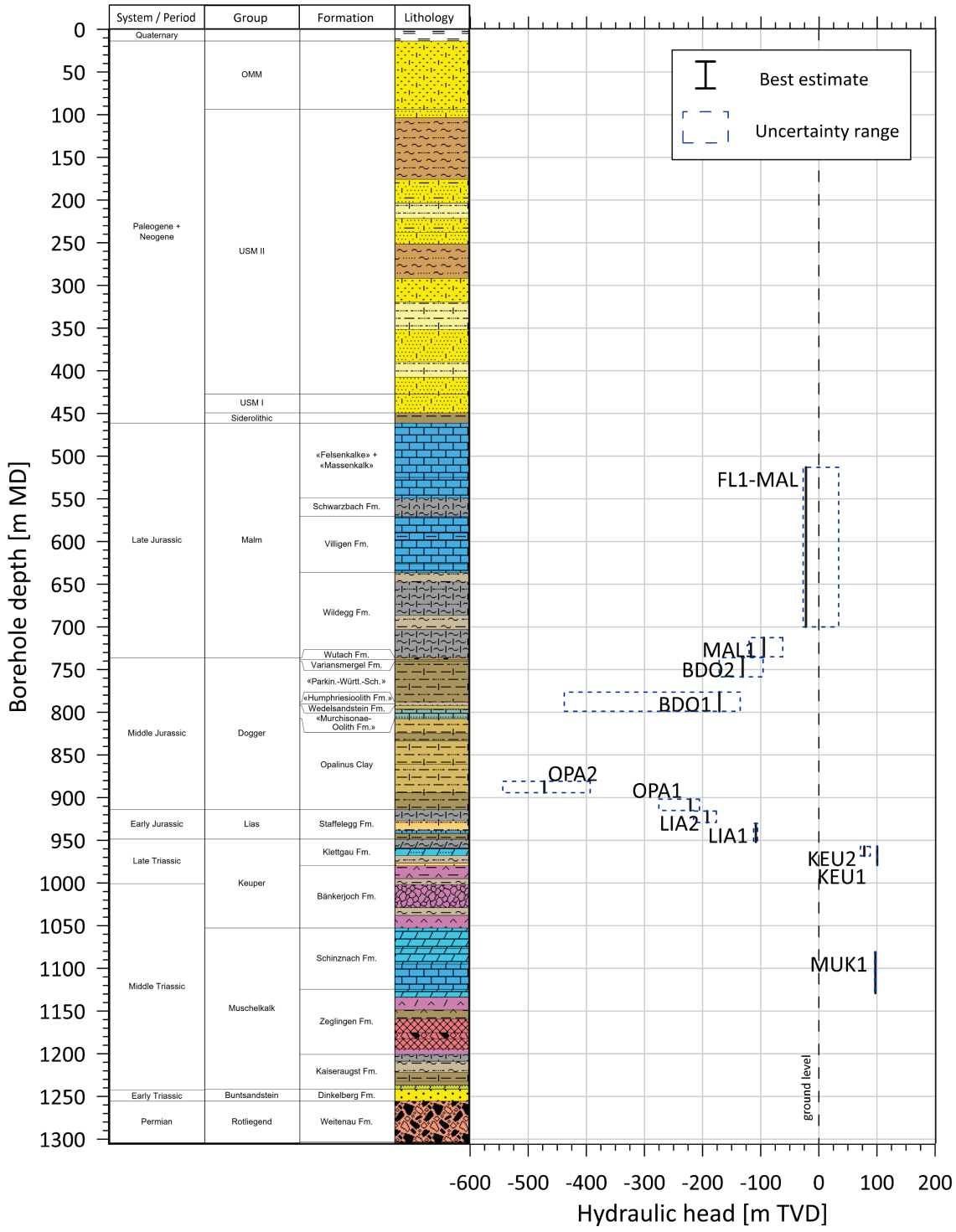

Fig. 4-26: Summary of the hydraulic testing in borehole BAC1-1: Formation hydraulic head profile (m TVD)

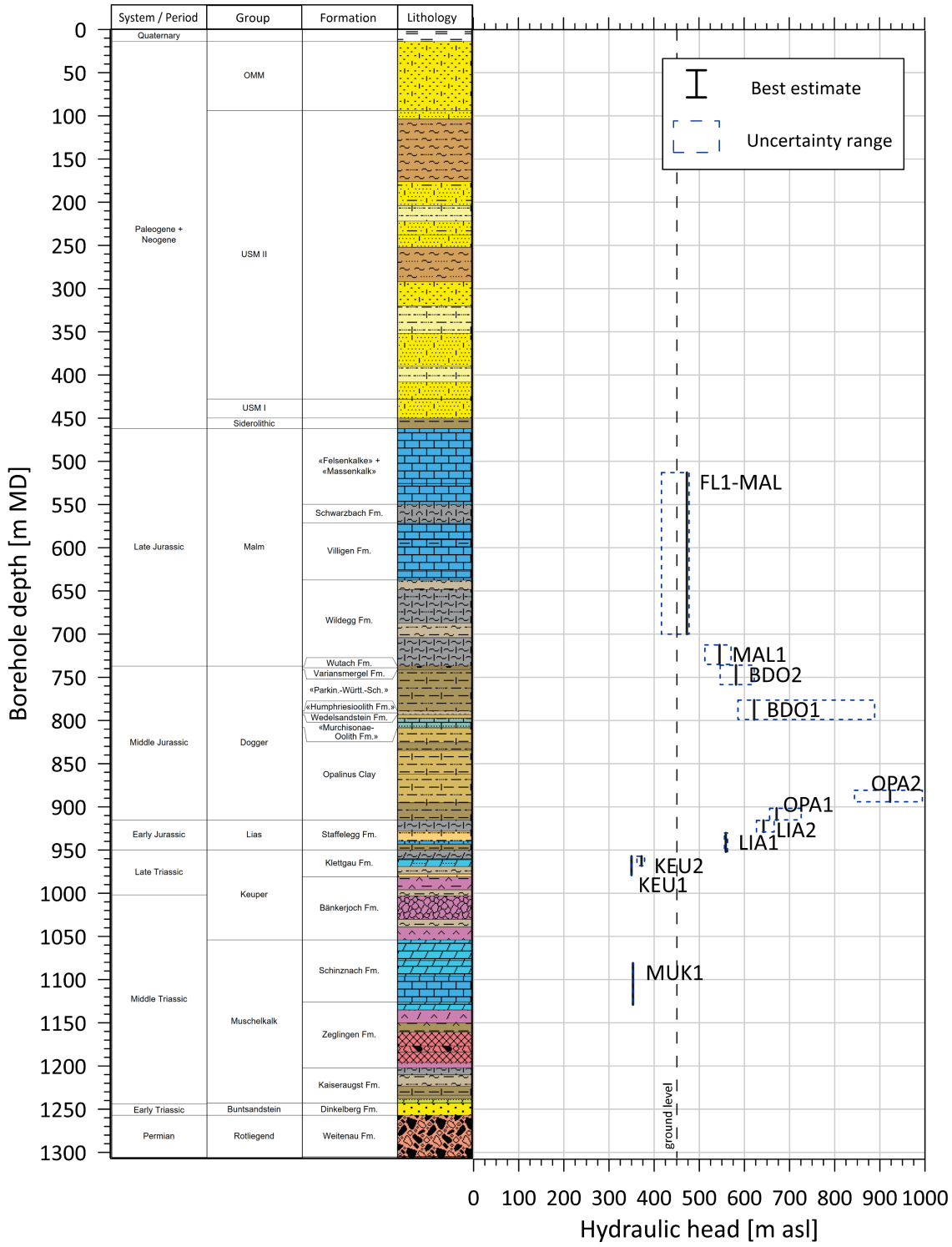

Fig. 4-27: Summary of the hydraulic testing in borehole BAC1-1: Formation hydraulic head profile (m asl)

4.6.2 Discussion of data and test results

The test interval highest up in borehole BAC1-1 is that of the hydraulic test BAC1-1-MAL1 at 712.56 – 735.00 m MD. Nevertheless, the hydraulic test was performed late in the main test series, the reason being that the fluid logging campaign BAC1-1-FL1-MAL had not indicated any significant inflow in the logged depth of 513.00 – 700.00 m MD (*cf.* Section 3). Once petrophysical logging and core analysis had identified a structure of interest between 726 and 728 m MD, the test interval for hydraulic test BAC1-1-MAL1 was positioned to investigate this lowermost part of the Effingen Member of the Wildegg Formation of the Malm Group. The best estimate of the hydraulic transmissivity of 2×10^{-12} m^2 s^{-1} (hydraulic conductivity of 1×10^{-13} m s^{-1}) was achieved using a homogeneous flow model with a discrete skin zone with time-varying properties. The estimate of the hydraulic transmissivity bears only a small uncertainty. The skin properties and the static formation pressure, however, could not be estimated reliably given the low transmissivity and various factors contributing to uncertainties such as the relatively short test duration, the long pressure history and processes that were not included in the numerical model, e.g. poroelastic effects in the near surroundings of the interval. For test BAC1-1-MAL1, the estimated freshwater hydraulic head is considered an 'apparent' hydraulic head.

The Dogger Group was investigated with seven hydraulic tests. The test intervals of tests BAC1-1-BDO2 and BAC1-1-BDO1 were positioned in the upper part («Brauner Dogger»). The test intervals of tests BAC1-1-BDO3, BAC1-1B-BDO4 and BAC1-1-OPA3 (in the order of increasing depth of the top of the test interval) included the topmost part of the Opalinus Clay, while the test intervals of tests BAC1-1-OPA2 and BAC1-1-OPA1 were entirely within the Opalinus Clay at the bottom of the Dogger Group. The common objective for tests BAC1-1-OPA3, BAC1-1-BDO1, and BAC1-1-BDO3 was to characterise the contributors to the mud losses of 15 m^3 that occurred while coring through the bottom of the «Murchisonae-Oolith Formation» / the topmost part of the Opalinus Clay. The test intervals of tests BAC1-1-OPA3 and BAC1-1-BDO3 included a drilling-induced fracture visible in core photographs and the fullbore formation microimage log (*cf.* Dossier V). Test BAC1-1B-BDO4 was the only test performed in the sidetrack BAC1-1B (in approximately 20 m horizontal distance from borehole BAC1-1) at about the same depth where the drilling-induced fracture was observed in the main borehole.

The test BAC1-1-BDO2 was performed in the shallowest interval (736.00 – 758.44 m MD) of the tests in the Dogger Group as an overview test in a borehole section of expected low hydraulic transmissivity. The test interval encompasses the Wutach Formation, Variansmergel Formation and the upper part of the «Parkinsoni-Württembergica-Schichten». The analysis is presented in detail in Section 4.5.1. The best estimate for the hydraulic transmissivity is 2×10^{-12} m^2 s^{-1} (hydraulic conductivity of 8×10^{-14} m s^{-1}) with a range between 1×10^{-12} m^2 s^{-1} and 3×10^{-12} m^2 s^{-1} (hydraulic conductivity 5×10^{-14} m s^{-1} – 2×10^{-13} m s^{-1}). The resulting estimate of the freshwater hydraulic head is considered an 'apparent' hydraulic head.

The test BAC1-1-BDO1 (776.40 – 798.84 m MD) covers the «Parkinsoni-Württembergica-Schichten», the «Humphriesioolith Formation», the Wedelsandstein Formation and the Upper part of the «Murchisonae-Oolith Formation». The analysis was based on the test sequence of two pulse withdrawal phases (PW1-PW2), using a homogeneous flow model with a skin zone of time-varying properties. The discrete skin conditions were defined for PW1 and PW2 as indicated by the analysis and one skin behaviour for the history sequence, when the borehole conditions were different. A low hydraulic transmissivity of 4×10^{-12} m^2 s^{-1} (hydraulic conductivity 2×10^{-13} m s^{-1}) with small uncertainty was attained. However, the determination of the static formation pressure was subject to a significantly higher degree of uncertainty. The resulting estimate of the freshwater hydraulic head is considered an 'apparent' hydraulic head.

The particularly long test interval of test BAC1-1-BDO3 (769.00 – 816.17 m MD) covers the «Parkinsoni-Württembergica-Schichten», the «Humphriesioolith Formation», the Wedelsandstein Formation, the «Murchisonae-Oolith Formation» and the topmost part of the Opalinus Clay. It covers the upper part of the test interval of test BAC1-1-OPA3 (800.00 – 822.44 m MD), which included the «Murchisonae-Oolith Formation» and the upper 14.10 m of Opalinus Clay. Both test intervals extend over the depth of a drilling-induced fracture where mud losses occurred in the main borehole BAC1-1.

Test BAC1-1-OPA3 consisted of a sequence of pulse withdrawal, slug and slug recovery tests. The hydraulic test BAC1-1-BDO3 consisted of a sequence of slug and slug recovery test followed by rate injection tests with the objective to determine the reopening pressure of the drilling-induced fracture possibly responsible for the observed mud losses. Unfortunately, the analyses of tests BAC1-1-BDO3 and BAC1-1-OPA3 do not allow to estimate representative hydraulic parameters for the undisturbed formation or a separation between the formation and the fracture transmissivity. It was therefore not possible to estimate hydraulic parameters of either the formation or the fracture. Even the use of complex hydraulic models did not allow to obtain conclusive hydraulic parameters. The measured pressure responses are influenced by processes that cannot adequately be represented by the models used.

Test BAC1-1B-BDO4 (797.00 and 812.72 m MD) was the only test performed in the sidetrack BAC1-1B. The intention of this test was to hydraulically characterise the «Murchisonae-Oolith Formation» and the topmost part of the Opalinus Clay where mud losses are suspected to have occurred in the main borehole BAC1-1. The test was not analysed in detail due to problems during test execution. Several times, unexpected pressure signals of QSSP sensors P1 and P2 indicated irregular short hydraulic communication between the interval below the bottom packer and the test interval, which prevented a reliable analysis of the hydraulic test.

Tests BAC1-1-OPA2 and BAC1-1-OPA1 were performed to study the clay rich lower section of the Opalinus Clay in the intervals 880.80 – 894.17 m MD and 901.70 – 915.07 m MD, respectively. They were conducted sequentially in test intervals of about 13.40 m length. Both tests were performed using a pulse withdrawal phase (PW) prior to a slug withdrawal phase with following shut-in phase (SW, SWS). During tests BAC1-1-OPA1 and BAC1-1-OPA2, the main test phase was the pulse phase PW. The duration of the pressure history was long (379 and 485 hours) as compared to the test duration (52 and 72 hours).

The analysis of test BAC1-1-OPA1 was based on a 2-zone radial composite flow model that considered the observed near borehole conditions (skin) as a separate zone. For the analysis of test BAC1-1-OPA2, a homogeneous flow model with a discrete skin zone of time-varying (step changing per test phase) properties was used. The hydraulic conductivity of the deeper-seated interval of test BAC1-1-OPA1 with a subvertical fault at 911.2 – 911.80 m MD is one order of magnitude higher than that of test BAC1-1-OPA2. For test BAC1-1-OPA1, the hydraulic conductivity ranges between 8×10^{-14} m s^{-1} and 2×10^{-13} m s^{-1}, with a best estimate of 1×10^{-13} m s^{-1}. For test BAC1-1-OPA2, the hydraulic conductivity ranges from 1×10^{-14} m s^{-1} to 4×10^{-14} m s^{-1}, with the best estimate being 2×10^{-14} m s^{-1}. The uncertainty in the estimates of the hydraulic head was generally high for the tests performed in the Opalinus Clay. Like for other boreholes in the TBO campaign, the estimates of the hydraulic head from the tests in the Opalinus Clay yielded 'apparent' hydraulic heads which are not considered realistic due to physical processes that cannot be captured by the hydraulic modelling software used, e.g. poroelastic effects.

The Staffelegg Formation of the Lias Group was screened with two hydraulic tests. The test interval of BAC1-1-LIA2 at the top (915.70 – 929.07 m MD) includes the Gross Wolf, Rietheim and Grünschholz, Breitenmatt and Rickenbach Members. The test interval of BAC1-1-LIA1 extended from 930.20 to 952.00 m MD and represents the Frick, Beggingen and Schambelen Members of the Staffelegg Formation as well as the top of the Klettgau Formation of the Keuper Group. Test BAC1-1-LIA1 includes a fracture zone in the Beggingen Member and at the top of the Schambelen Member. Like most hydraulic tests in borehole BAC1-1, test BAC1-1-LIA2 was performed with a double packer configuration; it is discussed in detail in Section 4.5.2. Test BAC1-1-LIA1 was performed with a single packer configuration. Both tests were analysed with a homogeneous flow model with a discrete skin zone of time-varying (step changing per test phase) properties. The best estimates derived for the hydraulic conductivity differ by two orders of magnitude: 9×10^{-14} m s^{-1} for BAC1-1-LIA2 and 1×10^{-11} m s^{-1} for BAC1-1-LIA1. The estimate for the upper Staffelegg Formation is close in value to that for Opalinus Clay in test BAC1-1-OPA1. Like for other tested formations of very low permeability, the high estimated hydraulic pressure is considered not realistic due to physical processes that cannot be captured by the hydraulic modelling software used.

Two hydraulic tests were dedicated to the Klettgau Formation of the Keuper Group. For test BAC1-1-KEU1, the HTT system was used in a single packer configuration. No mud losses were observed during coring of the Klettgau Formation in borehole BAC1-1. Nevertheless, the test was performed to characterise all potentially permeable members of the Klettgau Formation, i.e. the Seebi, Gansingen and Ergolz Members. The analysis was based on a radial 2-zone composite flow model with an additional time-varying skin zone for the observed skin, which was also evident in the flow model diagnosis (a total of three radially symmetric shells). The test consisted of a slug withdrawal and a slug recovery phase followed by a multi-rate withdrawal phase of nearly 61 hours and a pressure recovery phase observed for 21.6 hours. It was possible to collect a water sample at the end of the rate withdrawal phase. The hydraulic conductivity was best estimated to be 8×10^{-9} m s^{-1} and the best estimate for the freshwater hydraulic head was 350 m asl (100 m TVD). Both estimates have small ranges of uncertainty.

The interval of test BAC1-1-KEU2 has the same top depth as that of test BAC1-1-KEU1 but excludes the bottom of the Gansingen and the Ergolz Member. The objective was to characterise the lower permeability members of the Klettgau Formation. The hydraulic conductivity was best estimated to be 3×10^{-12} m s^{-1} and the best estimate for the freshwater hydraulic head was 372 m asl (78 m TVD). Again, both estimates have small ranges of uncertainty. They were obtained from the analysis of the slug withdrawal and slug recovery phases using a homogeneous flow model.

A single hydraulic test was performed in the Schinznach Formation of the Muschelkalk Group (including about 3 m of the Zeglingen Formation below). Test BAC1-1-MUK1 was performed with a single packer configuration after mud losses (approximately 5 m^3 water-based polymers) had occurred during coring and test preparation. The test consisted of a slug withdrawal and a slug recovery phase, a multi-rate withdrawal phase, followed by a pressure recovery phase. For the test analyses of the multi-rate and pressure recovery phases, a radial 2-zone composite flow model was used with an additional time-varying skin zone for the observed skin, which was also evident in the flow model diagnosis (a total of three radially symmetric shells). For the analysis of the slug and slug recovery phases one shell less was adequate to reproduce the flow behaviour. The hydraulic conductivity was best estimated to be 4×10^{-7} m s^{-1} (with an uncertainty range between 2×10^{-7} m s^{-1} and 5×10^{-7} m s^{-1}) and the best estimate for the hydraulic head was 353 m asl (97 m TVD). The hydraulic head estimate had a small associated range of uncertainty of ± 1 m. A water sample was collected successfully.

5 Summary

Borehole Bachs-1-1 (BAC1-1) is the fourth exploratory borehole drilled in the TBO project in the siting region Nördlich Lägern.

Between October 2021 and April 2022, a total of twelve intervals were investigated with hydraulic packer tests and one interval with fluid logging in the cored section of borehole BAC1-1. Another hydraulic test was conducted in the sidetrack BAC1-1B. All hydraulic tests were performed using an HTT system in single or double packer configuration (*cf.* Tab. 4-19). The test activities were performed in the following geological formations (*cf.* Dossier III):

- Malm Group with a focus on the lowermost part of the Effingen Member of the Wildegg Formation (BAC1-1-MAL1) and a fluid logging campaign focusing on the lower part of the «Felsenkalke» + «Massenkalk», the Villigen Formation, the Schwarzbach Formation the upper part of the Wildegg Formation (BAC1-1-FL1-MAL)
- Dogger Group («Brauner Dogger») focusing on the Wutach Formation, Variansmergel Formation and «Parkinsoni-Württembergica-Schichten» (BAC1-1-BDO2) and on the «Parkinsoni-Württembergica-Schichten», «Humphriesioolith Formation», Wedelsandstein Formation and part of the «Murchisonae-Oolith Formation» (BAC1-1-BDO1). Two additional tests aimed at characterising a section containing a drilling-induced fracture at the bottom of «Murchisonae-Oolith Formation» / top of the Opalinus Clay (BAC1-1-BDO3 and BAC1-1B-BDO4)
- Dogger Group with a focus on sub-units of the Opalinus Clay (BAC1-1-OPA1, BAC1-1-OPA2) and including the bottom of the «Murchisonae-Oolith Formation» containing a drilling-induced fracture (BAC1-1-OPA3)
- Staffelegg Formation of the Lias Group with the Gross Wolf, Rietheim, Grünschholz, Breitenmatt, Rickenbach and Frick Members (BAC1-1-LIA2) and an interval comprising the Frick, Beggingen and Schambelen Members of the Staffelegg Formation as well as Gruhalde Member of the Klettgau Formation of the Keuper Group (BAC1-1-LIA1)
- Klettgau Formation of the Keuper Group with the Gruhalde, Seebi, Gansingen and Ergolz Members (BAC1-1-KEU1) and excluding the Ergolz Member (BAC1-1-KEU2)
- Muschelkalk Group with mostly the Schinznach Formation including the Stamberg, Liederswil, Leutschenberg and Kienberg Members, and the top of the Zeglingen Formation (BAC1-1-MUK1)

All hydraulic tests were supported by an on-site field analysis to optimise the test procedure. The pressures and rates measured during the tests are illustrated in Figs. 4-7 to 4-20. The main results and best estimates of the hydraulic formation parameters are presented in Tabs. 4-29 to 4-31 and Figs. 4-23 to 4-27. The fluid logging analysis (BAC1-1-FL1-MAL; *cf.* Section 3.2) and two hydraulic test analyses (BAC1-1-BDO2 and BAC1-1-LIA2; *cf.* Sections 4.5.1 and 4.5.2) were selected for a detailed description in this report.

The best estimates and the uncertainty of the hydraulic conductivities and transmissivities lie in a reasonable range and are within the expected spectrum of values for the investigated formations (e.g. Nagra 2008, Nagra 2014a and b). The hydraulic conductivities in the Dogger Group with «Brauner Dogger» and Opalinus Clay are very low with narrow uncertainty ranges.

For the bottom of the «Murchisonae-Oolith Formation» / uppermost part of the Opalinus Clay, where several investigation methods indicate the potential presence of a drilling-induced fracture, conclusive hydraulic parameters could not be derived. In the light of the good quality test data available from both undisturbed and faulted rock sections, no further attempts were undertaken to deepen the analysis of the flawed test data. However, the magnitude of the minimum horizontal stress could successfully be estimated in the side track (BAC1-1B-BDO4) at the stratigraphic level of the drilling-induced fracture; see Dossier VI for results.

The extrapolated hydraulic heads are within an expected range (Luo et al. 2014) for test BAC1-1-KEU2 and a few tens of metres lower for tests BAC1-1-KEU1 and BAC1-1-MUK1. For the hydraulic tests performed in the Dogger Group including the Opalinus Clay, the Lias Group and the tested section of the lower Malm the extrapolated hydraulic heads overestimate the expected ranges (Luo et al. 2014). Due to inevitable, short-term borehole test conditions, the hydraulic heads estimated for BAC1-1-MAL1, BAC1-1-BDO1, BAC1-1-BDO2, BAC1-1-OPA1, BAC1-1-OPA2, BAC1-1-LIA1 and BAC1-1-LIA2 are considered as 'apparent' hydraulic heads.

General investigations concerning the physical explanation for the overestimation of the hydraulic head are continuing. The presented analysis considers the temperature effects in the test interval and the pressure induced effects resulting from the high-density drilling fluid during the entire time since drilling through the interval midpoint. Nagra installed long-term pressure monitoring systems in borehole STA3-1 and other selected boreholes to study these and further findings in detail.

6 References

Barker, J.A. (1988): A generalized radial flow model for hydraulic tests in fractured rock. Water Resour. Res. 24/10, 1796-1804.

Black, J., Holmes, D., Brightman, M. (1987): Crosshole investigations – Hydrogeological results and interpretations. Nagra Technical Report NTB 87-37.

Bourdet, D., Ayoub, J.A. & Pirard, Y.M. (1989): Use of pressure derivative in well-test interpretation. Society of Petroleum Engineers, SPE Formation Evaluation, 293-302.

Detournay, E. & Cheng, A.H.-D. (1988): Poroelastic response of a borehole in a non-hydrostatic stress field. International Journal of Rock Mechanics and Mining Sciences & Geomechanics Abstracts 25/3, 171-182.

Doughty C. & C.F. Tsang (2005): Signatures in flowing fluid electric conductivity logs. Journal of Hydrology 310, 157-180.

Geofirma Engineering Ltd. & INTERA Inc. (2011): nSIGHTS Version 2.50 User Manual. INTERA Inc., Austin, TX, USA.

Grauls, D. (1999): Overpressures: Causal mechanisms, conventional and hydromechanical approaches. Oil & Gas Science and Technology – Rev. IFP 54, 667-678.

Horne, R.N. (1995): Modern well test analysis: A computer-aided approach. 2nd Edition. Petroway Inc., Palo Alto, CA, USA.

Horner, D.R. (1951): Pressure buildup in wells. Proceedings Third World Petroleum Congress 2, 503-523, The Hague, Netherlands. Reprinted 1967. Pressure Analysis Methods, AIME Reprint Series 9, 45-50. SPE.

Isler, A., Pasquier, F. & Huber, M. (1984): Geologische Karte der zentralen Nordschweiz 1:100'000. Herausgegeben von der Nagra und der Schweiz. Geol. Komm.

Jäggi, K. & Vogt, T. (2020): OPA: Sondierbohrung Benken: Langzeitbeobachtung 2019, Dokumentation der Messdaten. Nagra Arbeitsbericht NAB 20-05.

Lisjak, A., Garitte, B., Grasselli, G., Müller, H.R. & Vietor, T. (2015): The excavation of a circular tunnel in a bedded argillaceous rock (Opalinus Clay): Short-term rock mass response and FDEM numerical analysis. Tunnelling and Underground Space Technology 45, 227-248.

Lorenz, G.D. & Stopelli, E. *(in prep.)*: Borehole BAC1-1 (Bachs-1-1): Fluid sampling and analytical hydrochemical data report. Nagra Arbeitsbericht NAB 23-32.

Luo, J., Monningkoff, B. & Becker, J.K. (2014): Hydrogeological model Nördlich Lägern. Nagra Arbeitsbericht NAB 13-25.

Marschall, P., Croisé, J., Schlickenrieder, L., Boisson, J.Y., Vogel, P. & Yamamoto, S. (2003): Synthesis of hydrogeological investigations at the Mont Terri site (Phases 1 – 5). Mont Terri Technical Report TR 01-02. Mont Terri Project, Switzerland.

Nagra (1997): Hydrological investigations at Wellenberg: Hydraulic packer testing in boreholes SB4a/v and SB4a/s. Methods and field results. Nagra Technischer Bericht NTB 95-02.

Nagra (2001): Sondierbohrung Benken – Untersuchungsbericht. Nagra Technischer Bericht NTB 00-01.

Nagra (2008): Vorschlag geologischer Standortgebiet für das SMA- und das HAA-Lager – Geologische Grundlagen. Nagra Technischer Bericht. NTB 08-04.

Nagra (2014a): SGT Etappe 2: Vorschlag weiter zu untersuchender geologischer Standortgebiete mit zugehörigen Standortarealen für die Oberflächenanlage. Geologische Grundlagen. Dossier II: Sedimentologische und tektonische Verhältnisse. Nagra Technischer Bericht NTB 14-02 Dossier II.

Nagra (2014b): SGT Etappe 2: Vorschlag weiter zu untersuchender geologischer Standortgebiete mit zugehörigen Standortarealen für die Oberflächenanlage. Geologische Grundlagen. Dossier VI: Barriereneigenschaften der Wirt- und Rahmengesteine. Nagra Technischer Bericht NTB 14-02 Dossier VI.

Pietsch, J. & Jordan, P. (2014): Digitales Höhenmodell Basis Quartär der Nordschweiz – Version 2013 (SGT E2) und ausgewählte Auswertungen. Nagra Arbeitsbericht NAB 14-02.

Ramey, H.J., Jr., Agarwal, R.G. & Martin, I. (1975): Analysis of 'Slug Test' or DST Flow Period Data. Journal of Canadian Petroleum Technology 14/3, 37-47.

Richards, D.J. (1981): Technical manual on radiometrics – Geophysical field manual for technicians No. 2. South African Geophysical Association.

Tsang, C.F. & Hufschmied, P.A. (1988): Borehole fluid conductivity logging method for the determination of fracture inflow parameters. Nagra Technischer Bericht NTB 88-13.

Appendix A: Abbreviations, nomenclature and definitions

Tab. A-1: Lithostratigraphy abbreviations for test names in BAC1-1

Lithostratigraphy	**Abbreviation**
Malm Group	MAL
Brauner Dogger (Dogger)	BDO
Opalinus Clay (Dogger)	OPA
Lias Group	LIA
Keuper Group	KEU
Muschelkalk Group	MUK

Tab. A-2: Test name definitions for hydraulic packer testing

[1] Based on the preliminary information.

Abbreviation	**Example**
Borehole abbreviation – lithostratigraphy abbreviation[1] + number of test	BAC1-1-MUK1: First test interval in Muschelkalk aquifer in borehole BAC1-1

Tab. A-3: Test event abbreviations for hydraulic packer testing

Test phase	**Abbreviation**
Compliance phase	COM
Packer deflation phase	DEF
Packer inflation phase	INF
Pulse injection test	PI
Initial pressure recovery 'static pressure recovery' (SIT closed)	PSR
Pulse withdrawal test	PW
Injection test with constant flow rate	RI
Pressure recovery after injection test with constant flow rate (shut-in)	RIS
Pumping test with constant flow rate ('rate withdrawal test')	RW
Pressure recovery after pumping test with constant flow rate (shut-in)	RWS
Slug injection test	SI
Slug withdrawal test (flow phase)	SW
Slug withdrawal test – pressure recovery with closed SIT (shut-in)	SWS
Wellbore storage test	WBS

Tab. A-4: Parameter definitions

Abbreviation / symbol	**Description**	**Unit**
c_{tz}	Test zone compressibility	1/Pa
C_i	Concentration (salinity) of one inflow i	g l^{-1}
EC_i	Electrical conductivity of one inflow i	µS cm^{-1}
g	Acceleration due to gravity (9.81)	m s^{-2}
h_s	Static hydraulic head (freshwater head) $h_s = z_{ref} - z_{int} + \left[\frac{P_f + \rho_{int}\, g\, (z_{int} - z_2) - P_{atm} - P_{offset}}{\rho_w\, g}\right]$	m asl
k	Intrinsic permeability	m^2
K	Hydraulic conductivity	m s^{-1}
K_{in}	Inner-zone hydraulic conductivity	m s^{-1}
K_{out}	Outer-zone hydraulic conductivity	m s^{-1}
K_s	Hydraulic conductivity of skin zone	m s^{-1}
n	Fractional flow dimension, e.g. Barker (1988)	-
P	Pressure (at QSSP-P2 level, if not otherwise specified)	Pa, kPa
P1	Pressure below bottom packer / interval P1 (downhole probe)	Pa, kPa
P2	Pressure in test interval (downhole probe)	Pa, kPa
P2*	(Absolute) pressure in test interval (memory gauge)	Pa, kPa, kPaa
P3	Pressure in annulus (above top packer, downhole probe)	Pa, kPa
P4	Pressure in test tubing above SIT (downhole probe)	Pa, kPa
P_{atm}	Atmospheric pressure	Pa, kPa
P_f	Static formation pressure (fitting parameter, at QSSP-P2 level, respectively P2* level)	Pa, kPa
P_{int}	Pressure at midpoint of test interval	Pa, kPa
P_{offset}	Offset of a pressure probe at atmospheric pressure	Pa, kPa
P_S	Static formation pressure (at midpoint of test interval if not specified otherwise)	Pa, kPa
ΔP_{packer}	Interval packer pressure changes	bar
q	Flow rate	m^3 s^{-1}
q_i	Flow rate of one inflow i	m^3 s^{-1}
Q, Q_{tot}	Cumulative flow volume	m^3
r_d	Radius of discontinuity	m
r_s	Radius of the skin zone extension	m
$r_{w\,int}$	Borehole radius of the test interval	mm
ρ_{int}	Density of interval fluid	kg m^{-3}

Tab. A-4: continued

Abbreviation / symbol	**Description**	**Unit**
ρ_w	Density of formation water (fluid)	kg m^{-3}
S	Storage coefficient	-
s	Skin factor	-
S_s	Specific storage	m^{-1}
$S_{s\ in}$	Inner-zone specific storage	m^{-1}
$S_{s\ out}$	Outer-zone specific storage	m^{-1}
S_{ss}	Specific storage of skin zone	m^{-1}
t_s	Thickness of the skin zone extension	m
T	Transmissivity	$m^2\ s^{-1}$
T_i	Transmissivity of one inflow i	$m^2\ s^{-1}$
t, dt	Time, elapsed time	s
T_{int}, T1, T2, T3, T4, T2*	Temperature in test interval, temperaturedownhole probe (sensors 1, 2, 3 or 4 associated with specific transducer; sensor T2* associated with memory gauge)	°C
ΔV_{int}	Interval volume changes	mL
z_2	Depth of pressure sensor of test interval P2	m MD
z_{int}	Depth of interval midpoint	m MD
z_{ref}	Reference point elevation	m asl

Tab. A-5: Non-parameter abbreviations

Abbreviation	**Description**	**Unit**
ΔP	Change in pressure	Pa, kPa
ΔV	Change in volume	m^3
1D	One dimensional	
2D	Two dimensional	
3D	Three dimensional	
AG	Aktiengesellschaft (company limited by shares "Ltd.")	
API	American Petroleum Institute	
BHPH	Borehole pressure history	
BOP	Blow out preventer	
BAC1-1	Bachs-1 drill site, borehole 1	
cps	Counts per second	
CU	Copper	

Tab. A-5: continued

Abbreviation	**Description**	**Unit**
DA	Detailed analysis	
DAS	Data acquisition system	
DR	Detailed report	
EU	External upset coupling	
EUE	External upset end	
FM	Flow model	
FS	Full scale	
GmbH	Gesellschaft mit beschränkter Haftung (company with limited liability)	
GTPT	Gas threshold pressure test	
HLW	High level waste	
HTT	Hydraulic test tool	
IARF	Infinite acting radial flow region	
ID	Inner diameter	
IPI	Inflatable Packers International, Perth, Australia	
IT	Information technology	
L/ILW	Low and intermediate level waste	
ln	Litre normal	ln
MAR1-1	Marthalen-1 drill site, borehole 1	
MD	Measured depth	m
MHF	Micro-hydraulic fracturing	
NBR	Nitrile butadiene rubber	
NDSA	Naphthalene disulfonate acid	
NL	Siting region Nördlich Lägern	
OD	Outer diameter	
PA1	Bottom packer of the hydraulic line of the HTT	
PA2	Top packer of the hydraulic line of the HTT	
PCP	Progressive cavity pump	
POOH	Pull out of hole	
PPG	Piston pulse generator	
PRV	Pressure release valve	
QC	Quality control	
QLA	Quick look analysis	
QLR	Quick look report	

Tab. A-5: continued

Abbreviation	**Description**	**Unit**
QSSP	Quadruple sub-surface probe	
Rd	Reading	
RIH	Run in hole	
SIT	Shut-in tool	
SSE	Sum of squared errors	
TBO	Tiefbohrung(en) (German for deep borehole(s))	
TVD	True vertical depth	m
WS	Water sample	
WT	Water table	
WTW	Wissenschaftlich-technische Werkstätten GmbH	
ZH	Zürich	

Appendix B: Analysis plots of the hydraulic packer tests BAC1-1-BDO2 and BAC1-1-LIA2

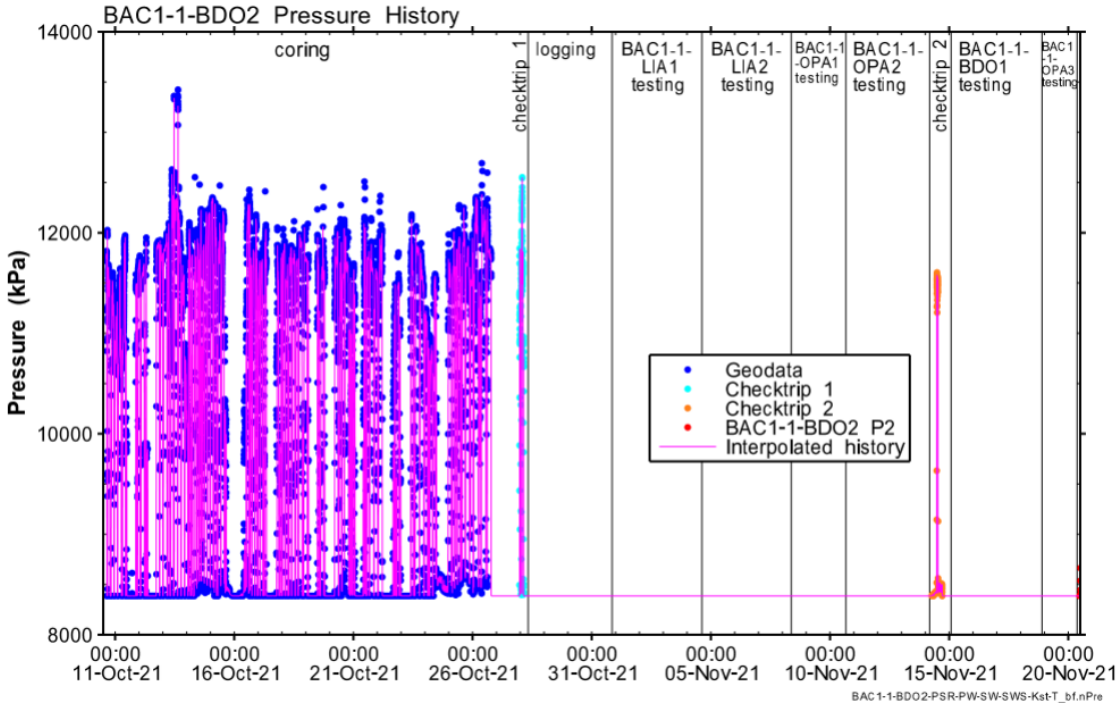

Fig. B-1: Hydraulic test BAC1-1-BDO2: Entire record of the borehole pressure history used in the analysis

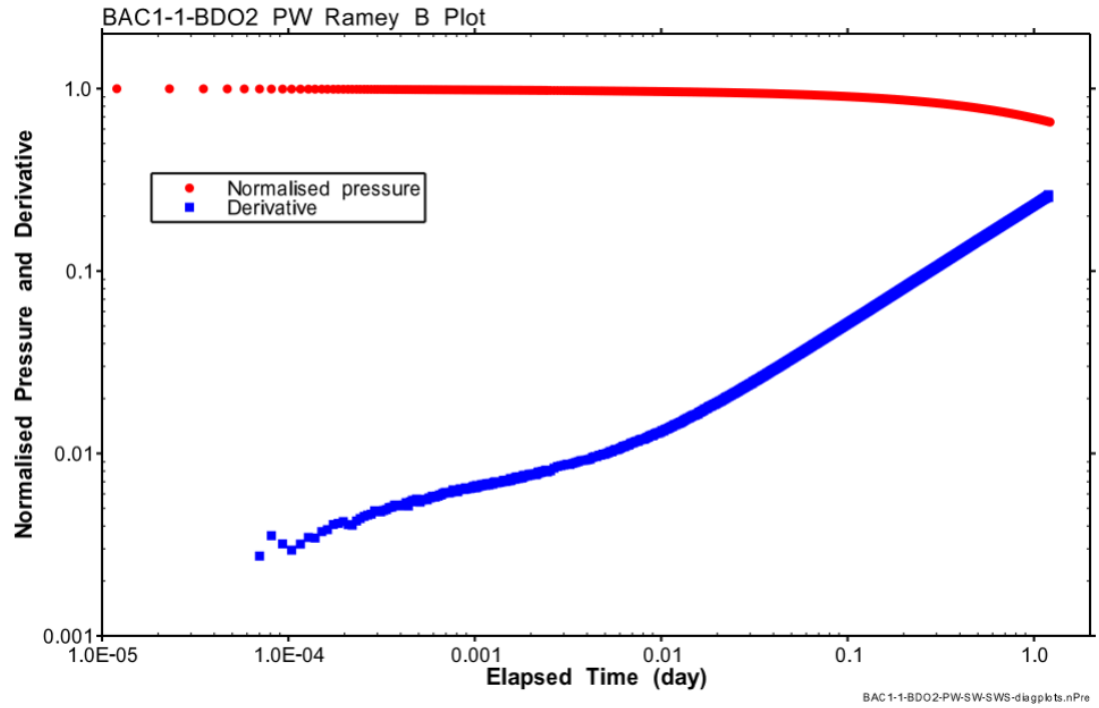

Fig. B-2: Hydraulic test BAC1-1-BDO2: Ramey B diagnostic plot of the PW phase

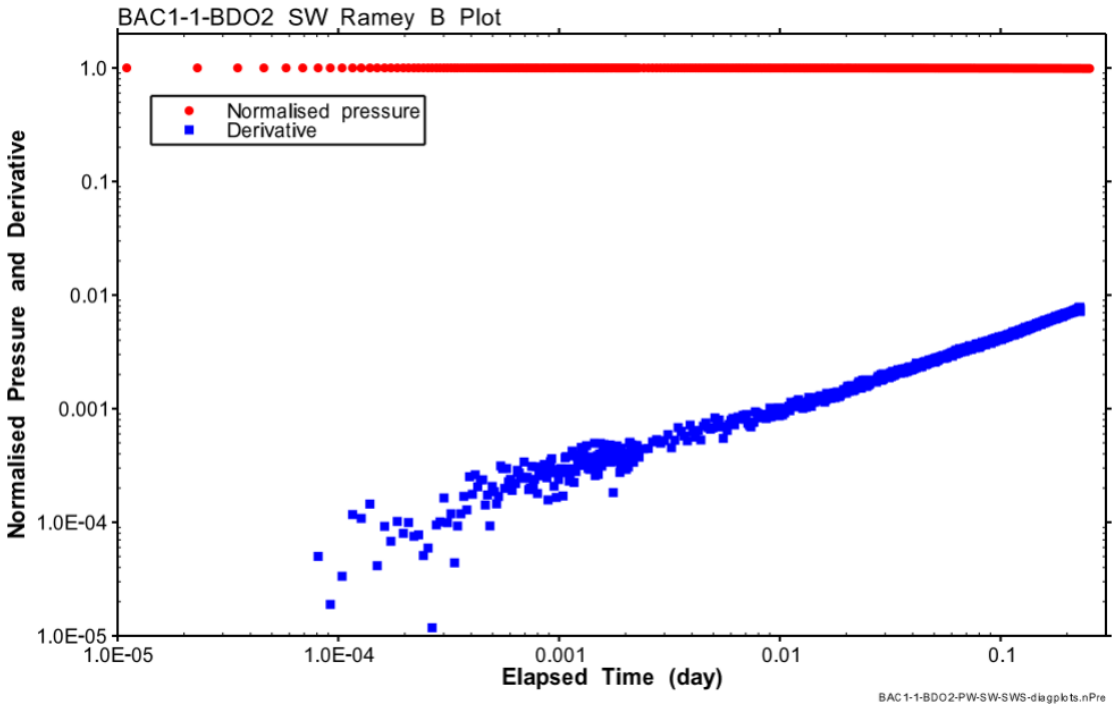

Fig. B-3: Hydraulic test BAC1-1-BDO2: Ramey B diagnostic plot of the SW phase

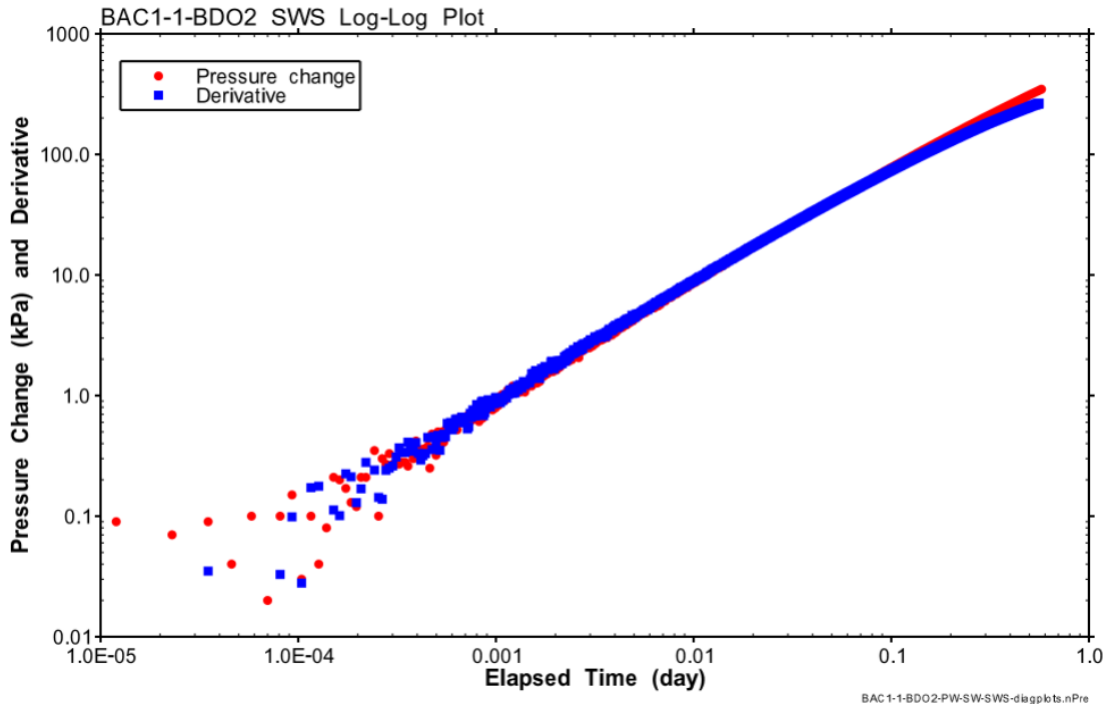

Fig. B-4: Hydraulic test BAC1-1-BDO2: Log-log diagnostic plot of the SWS phase

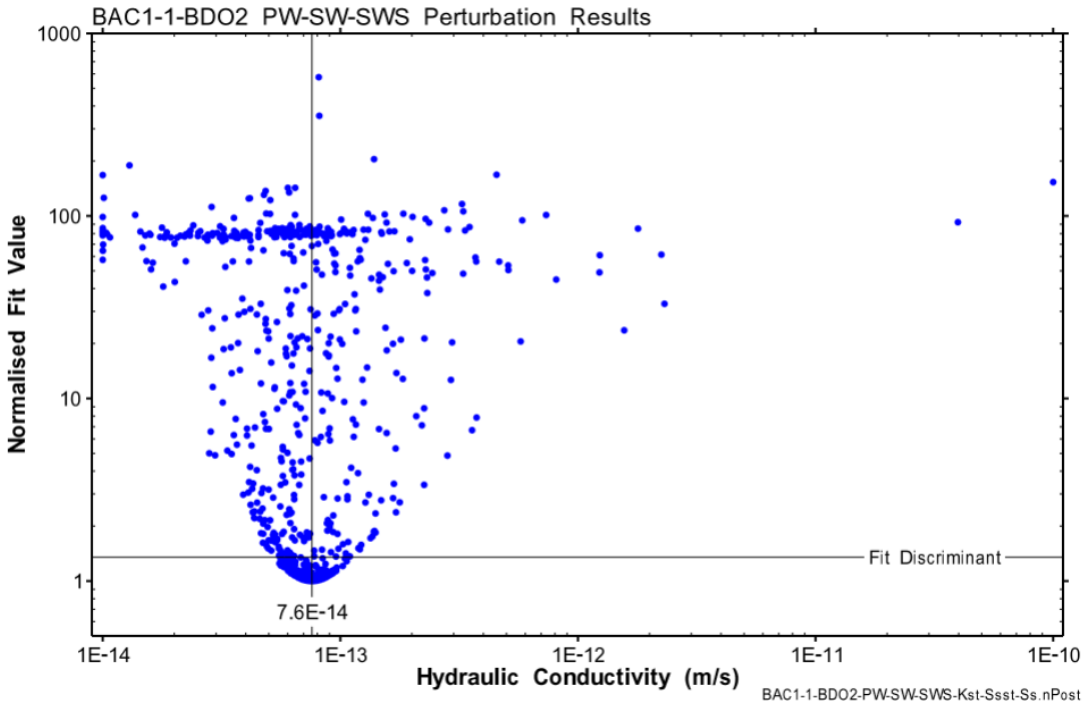

Fig. B-5: Hydraulic test BAC1-1-BDO2: Distribution of the normalised objective function value over K for the perturbation result of the PW-SW-SWS test sequence

994 / 1'000 results with a normalised objective function value less than 1'000.

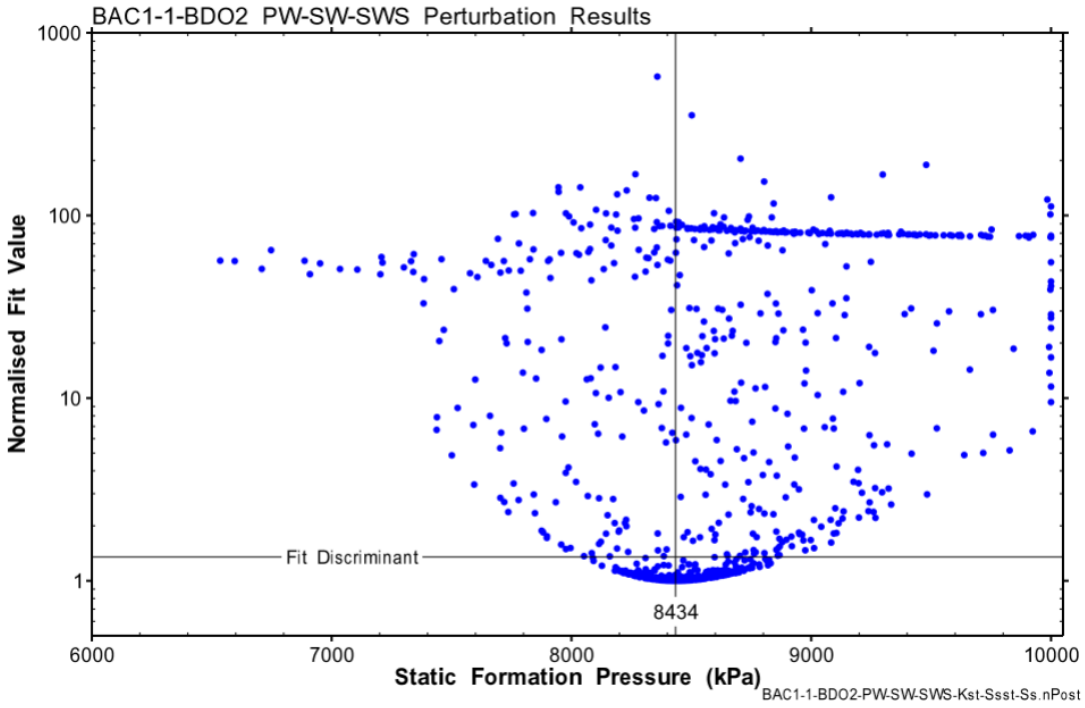

Fig. B-6: Hydraulic test BAC1-1-BDO2: Distribution of the normalised objective function value over P_f for the perturbation result of the PW-SW-SWS test sequence

994 / 1'000 results with a normalised objective function value less than 1'000.

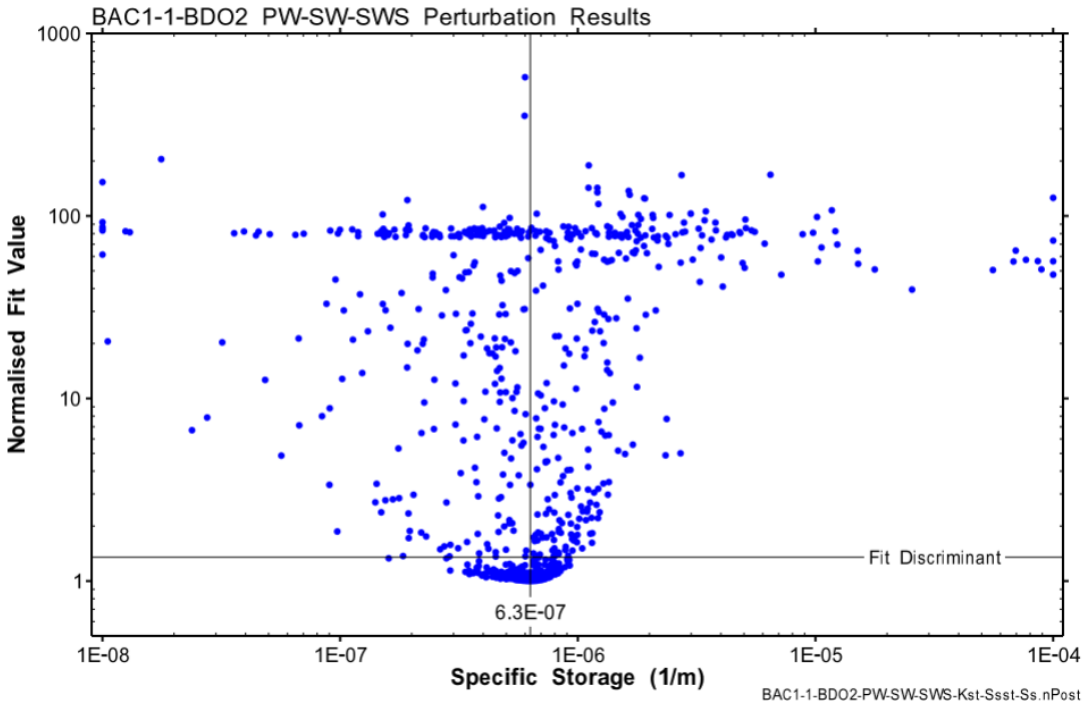

Fig. B-7: Hydraulic test BAC1-1-BDO2: Distribution of the normalised objective function value over S_S for the perturbation result of the PW-SW-SWS test sequence

994 / 1'000 results with a normalised objective function value less than 1'000.

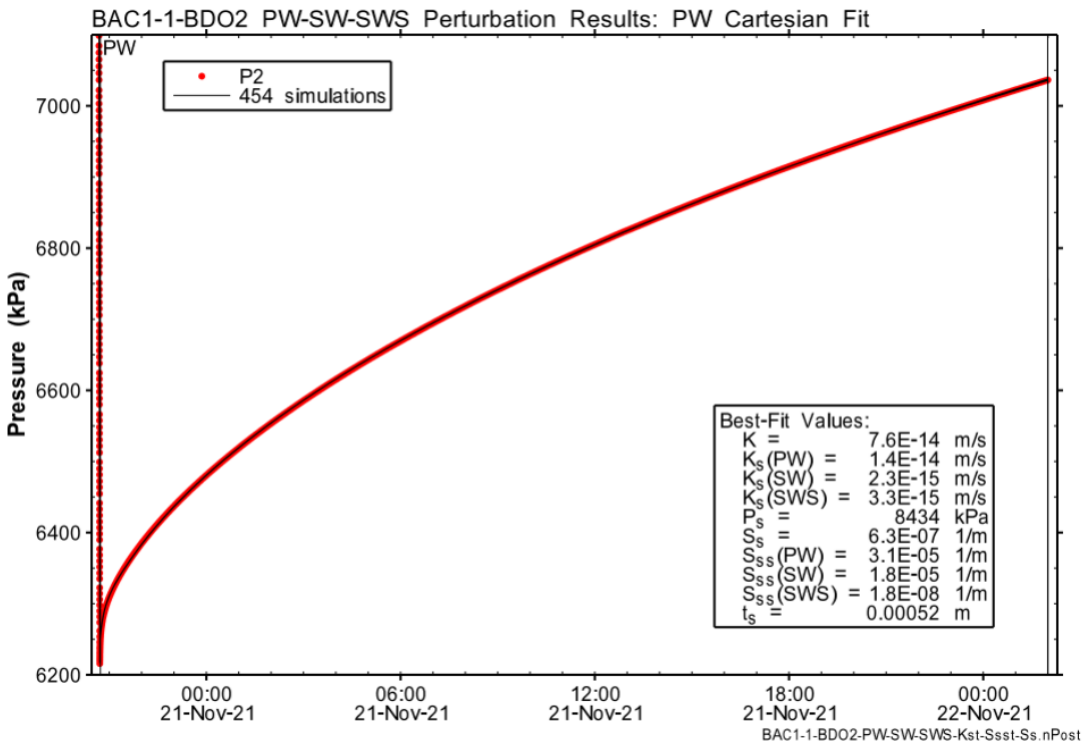

Fig. B-8: Hydraulic test BAC1-1-BDO2: Cartesian horsetail plot of the perturbation simulations on the PW phase, accepting the fit discriminant

454 / 1'000 results with a normalised objective function value less than 1.35.

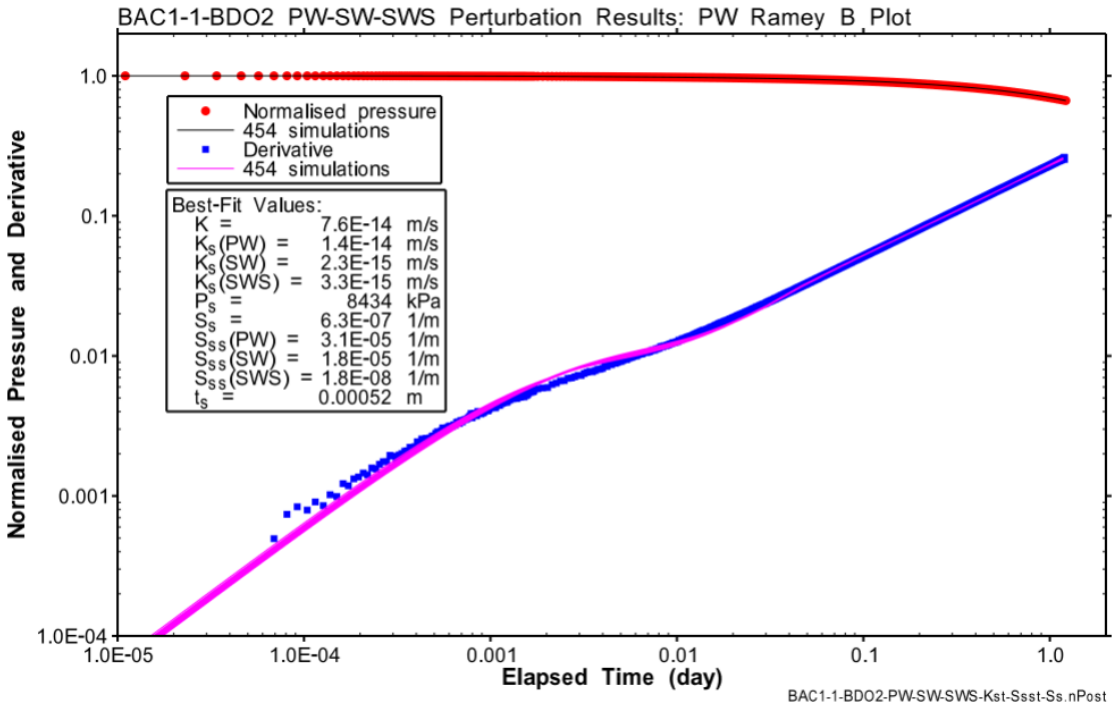

Fig. B-9: Hydraulic test BAC1-1-BDO2: Ramey B horsetail plot of the perturbation simulations on the PW phase, accepting the fit discriminant

454 / 1'000 results with a normalised objective function value less than 1.35.

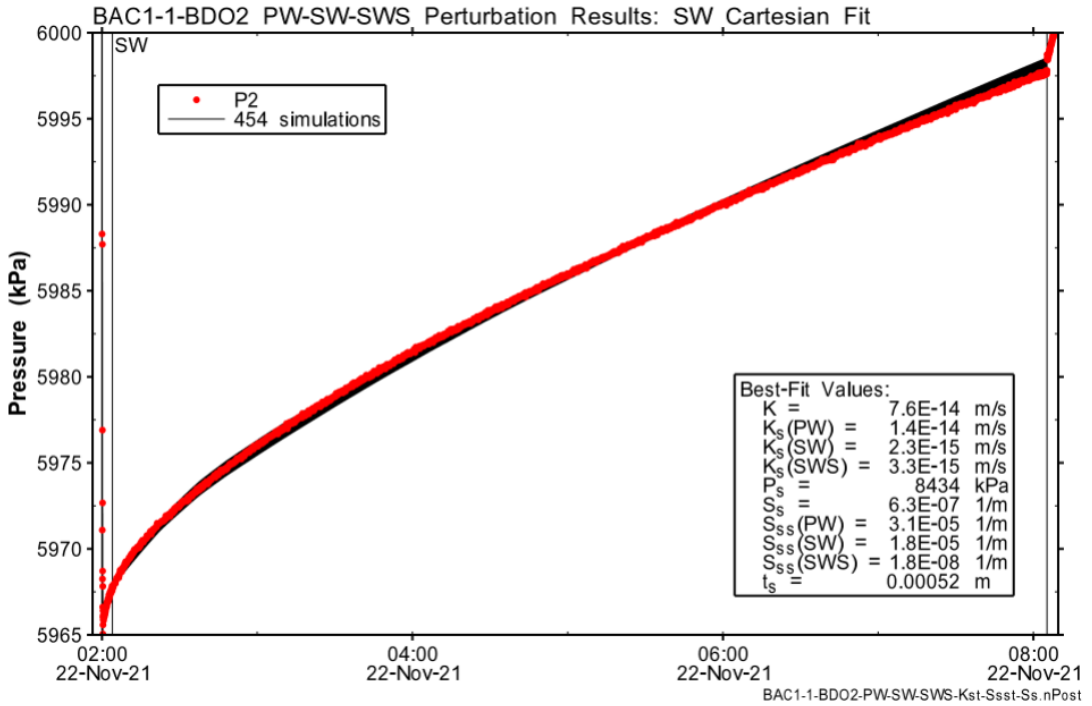

Fig. B-10: Hydraulic test BAC1-1-BDO2: Cartesian horsetail plot of the perturbation simulations on the SW phase, accepting the fit discriminant

454 / 1'000 results with a normalised objective function value less than 1.35.

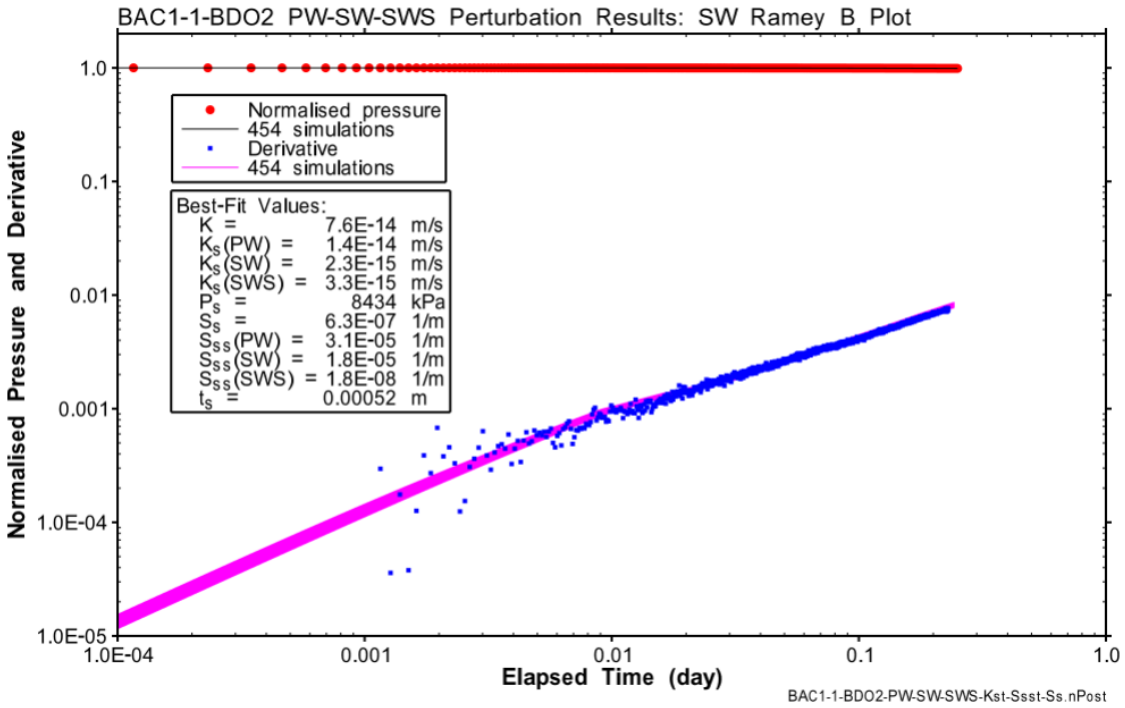

Fig. B-11: Hydraulic test BAC1-1-BDO2: Ramey B horsetail plot of the perturbation simulations on the SW phase, accepting the fit discriminant

454 / 1'000 results with a normalised objective function value less than 1.35.

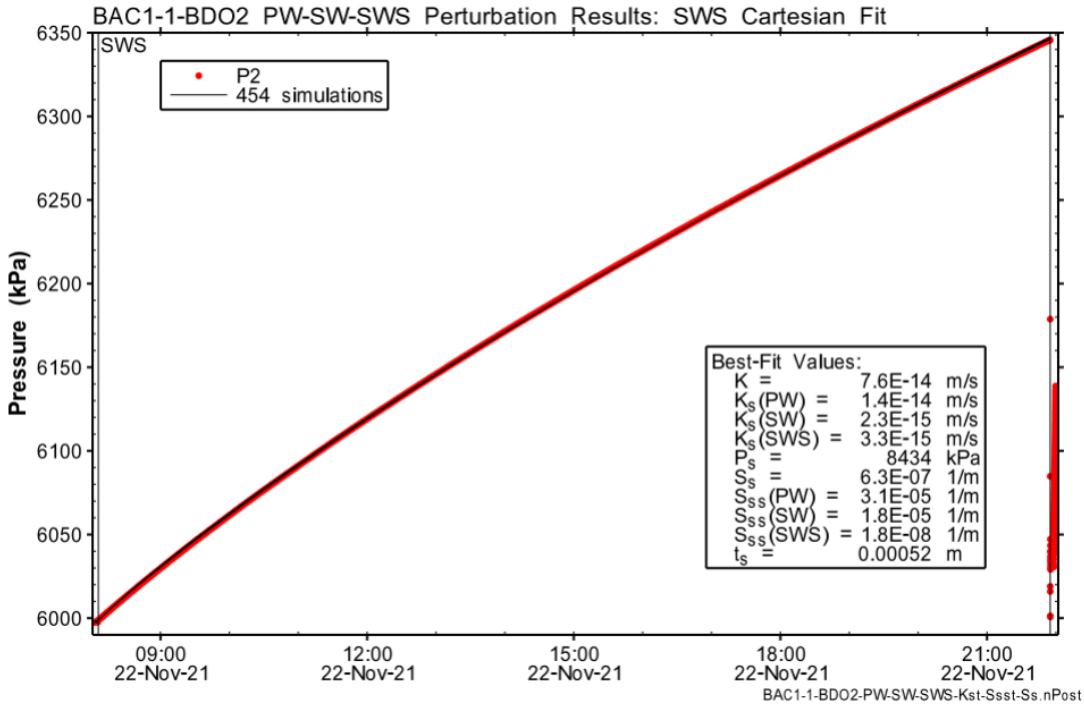

Fig. B-12: Hydraulic test BAC1-1-BDO2: Cartesian horsetail plot of the perturbation simulations on the SWS phase, accepting the fit discriminant

454 / 1'000 results with a normalised objective function value less than 1.35.

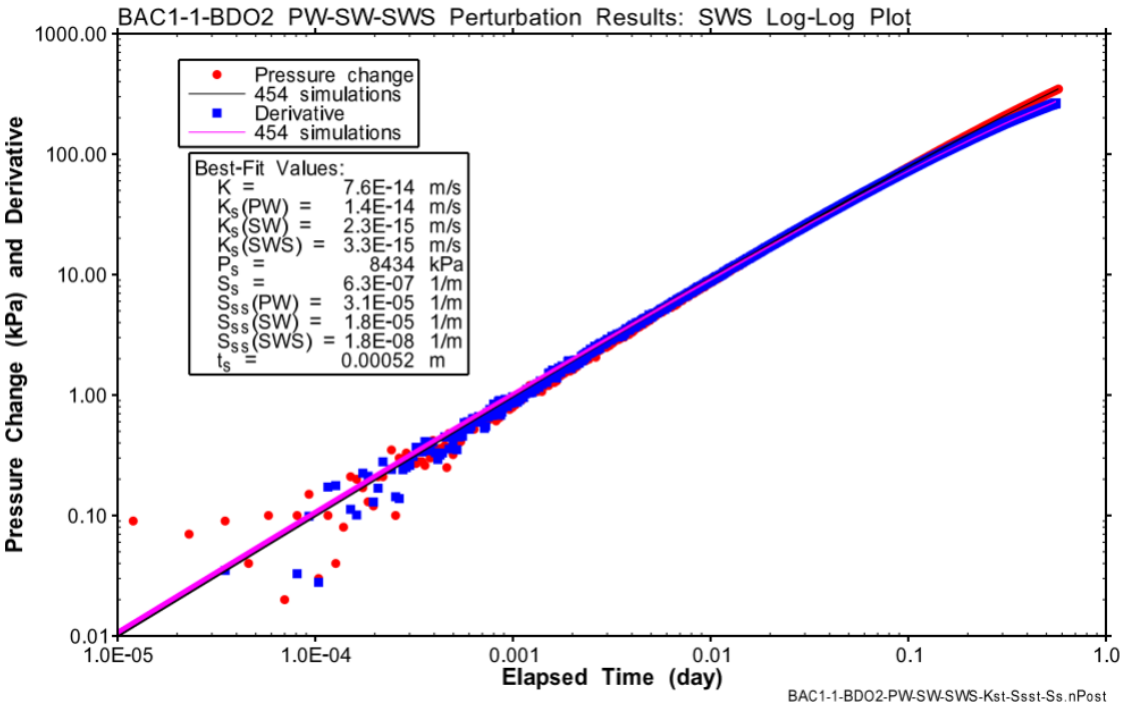

Fig. B-13: Hydraulic test BAC1-1-BDO2: Log-log horsetail plot of the perturbation simulations on the SWS phase, accepting the fit discriminant

454 / 1'000 results with a normalised objective function value less than 1.35.

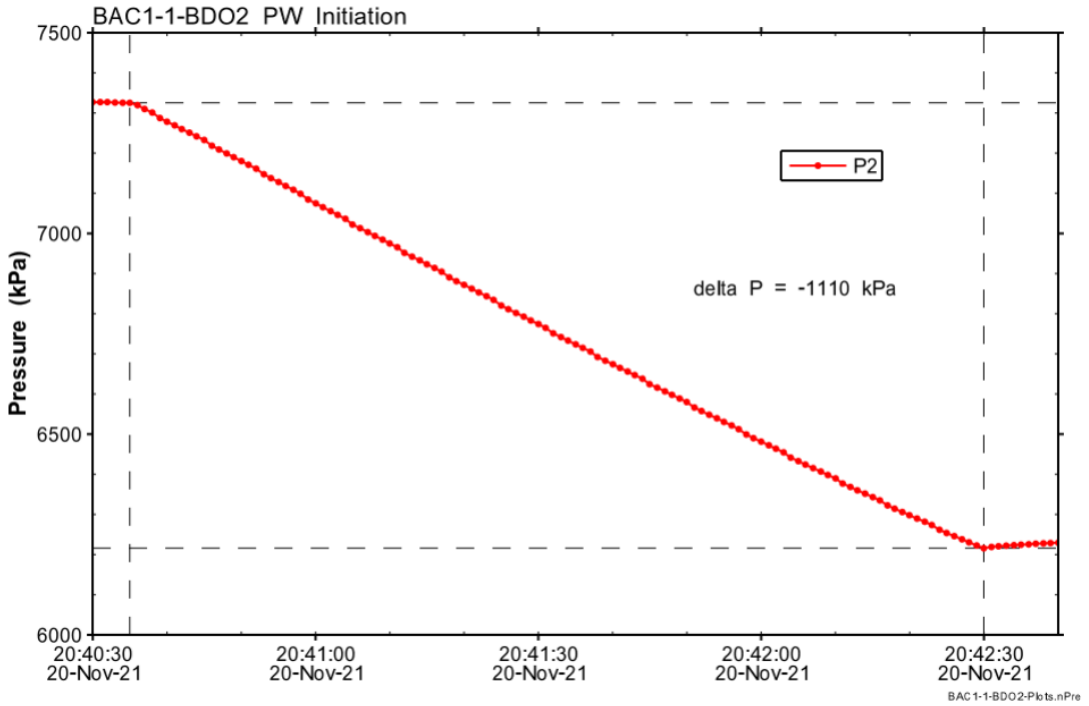

Fig. B-14: Hydraulic test BAC1-1-BDO2: Interval pressure change during the initiation of the PW phase

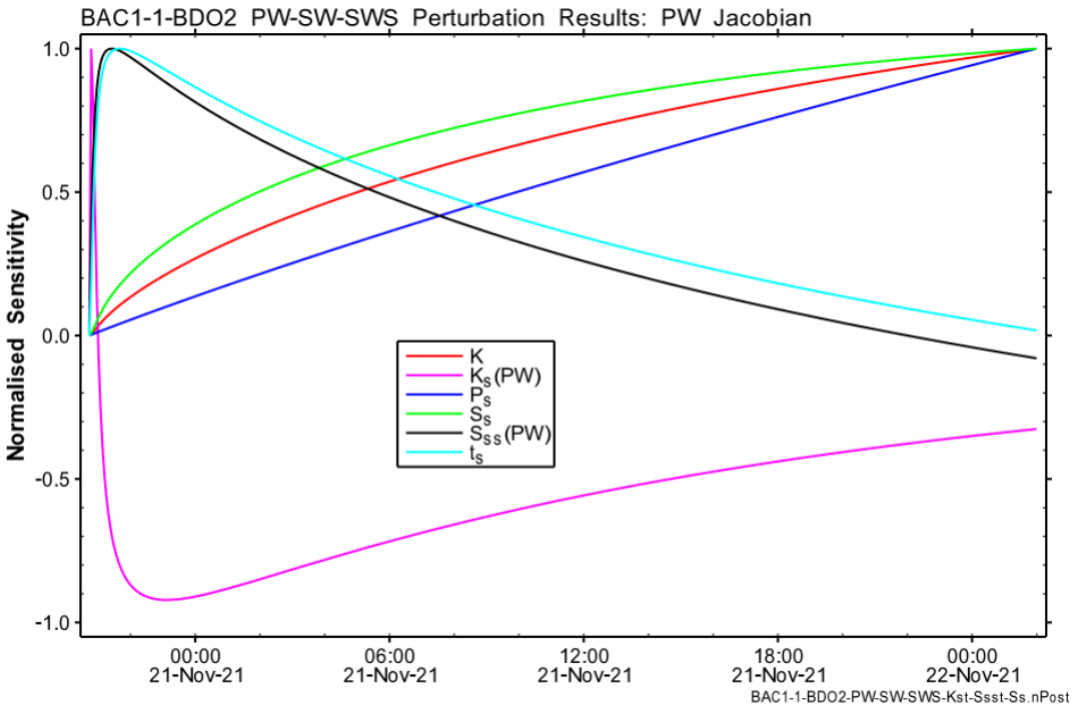

Fig. B-15: Hydraulic test BAC1-1-BDO2: Jacobian plots of parameter sensitivities during the PW phase

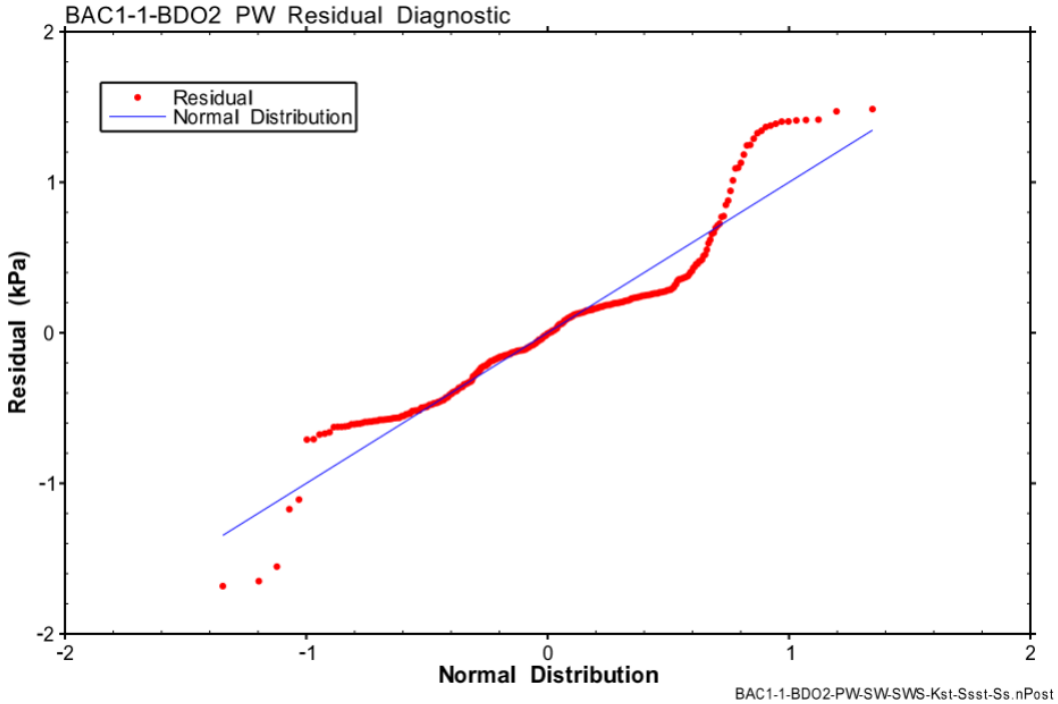

Fig. B-16: Hydraulic test BAC1-1-BDO2: Quantile-normal plot of residuals from the best Cartesian fit to PW phase data

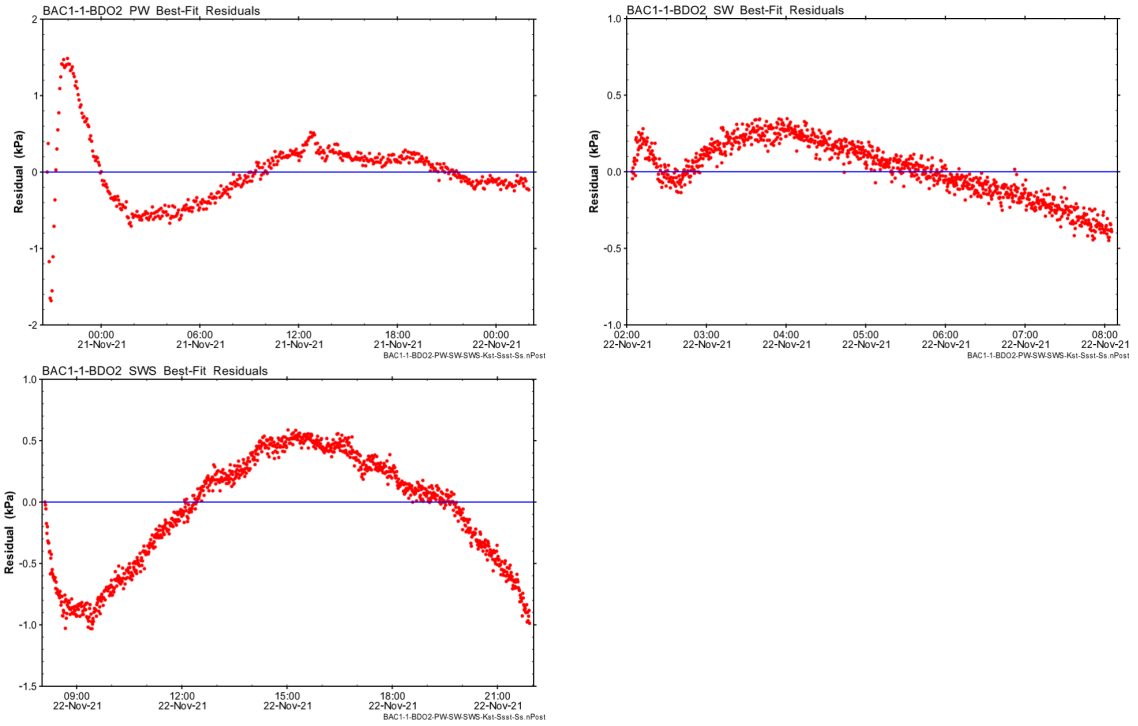

Fig. B-17: Hydraulic test BAC1-1-BDO2: Residuals from the best Cartesian fit to PW phase (top left), SW phase (top right) and SWS phase data (bottom left)

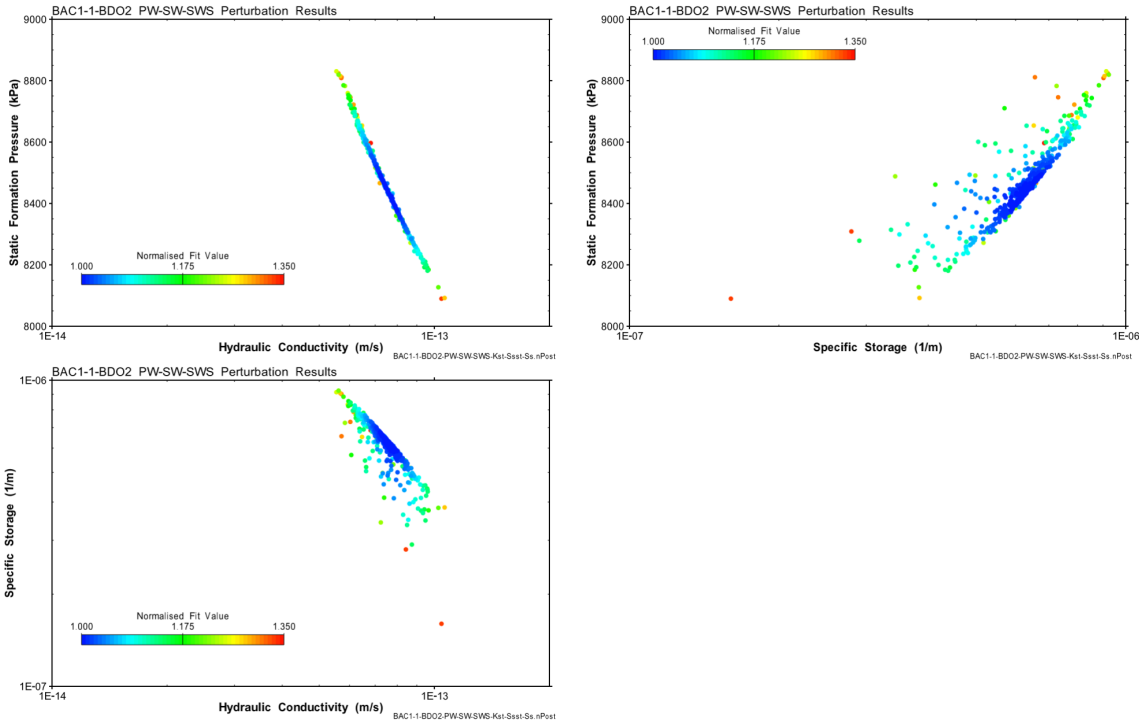

Fig. B-18: Hydraulic test BAC1-1-BDO2: Parameter correlations as a result of the perturbation analysis for P_f vs. K (top left), P_f vs. S_S (top right) and S_S vs. K (bottom left)

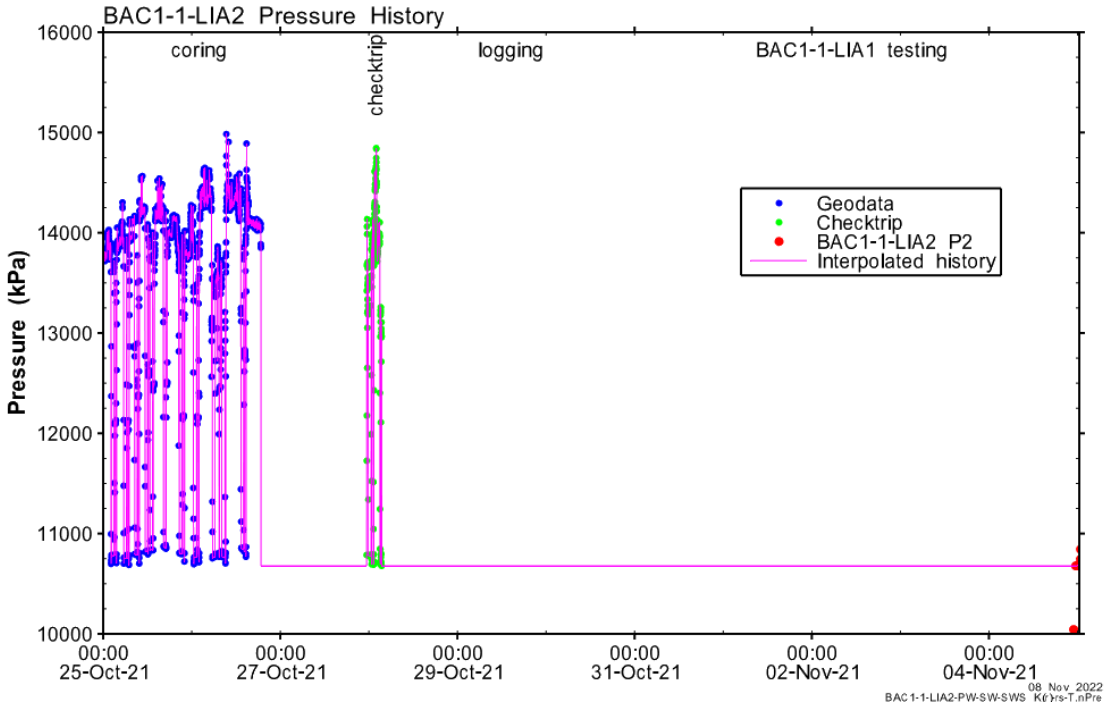

Fig. B-19: Hydraulic test BAC1-1-LIA2: Entire record of the borehole pressure history used in the analysis

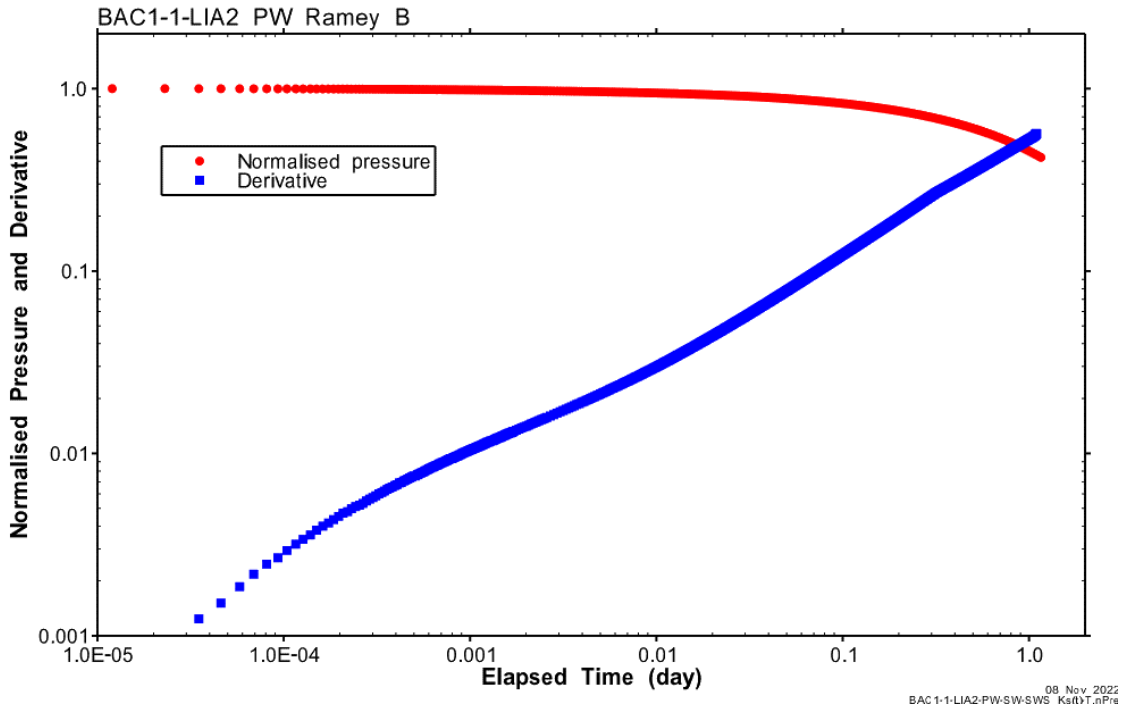

Fig. B-20: Hydraulic test BAC1-1-LIA2: Ramey B diagnostic plot of the PW phase
Truncated at the time at which the response was affected by swabbing at late time.

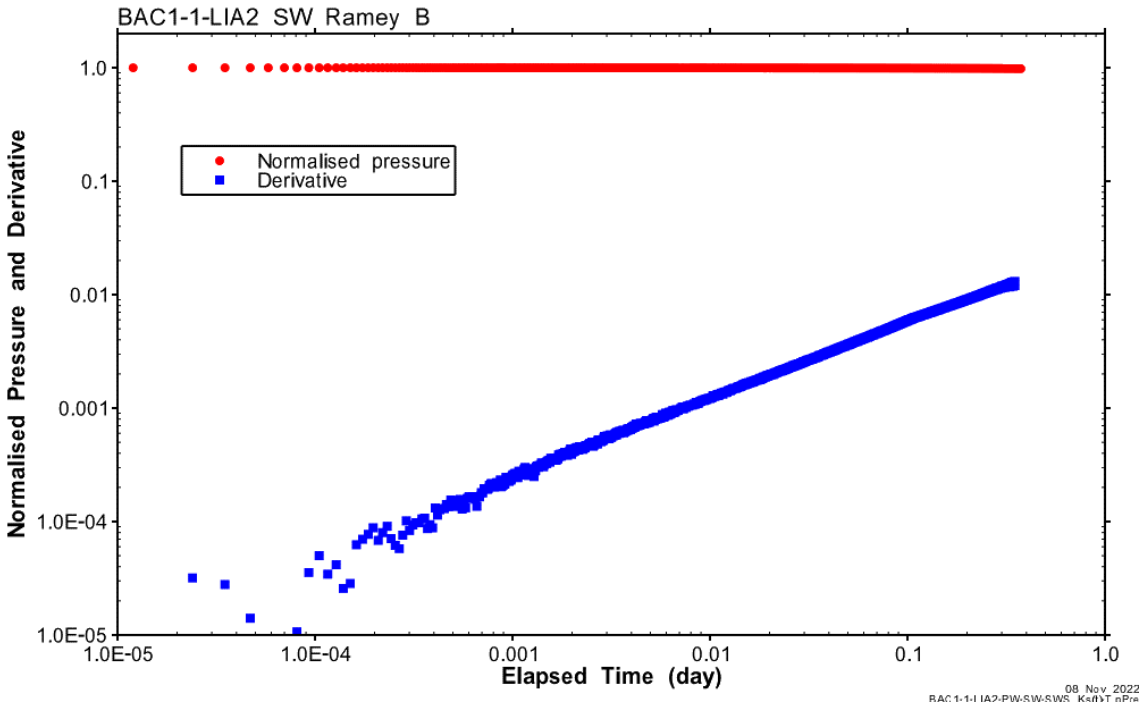

Fig. B-21: Hydraulic test BAC1-1-LIA2: Ramey B diagnostic plot of the SW phase

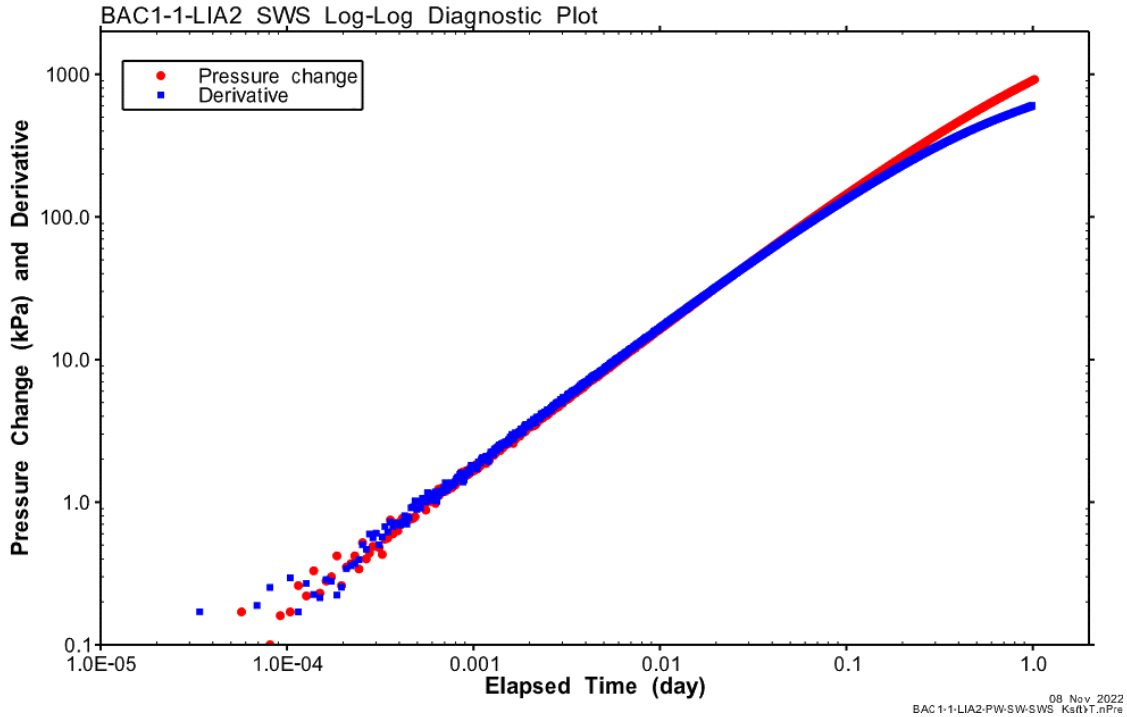

Fig. B-22: Hydraulic test BAC1-1-LIA2: Log-log diagnostic plot of the SWS phase

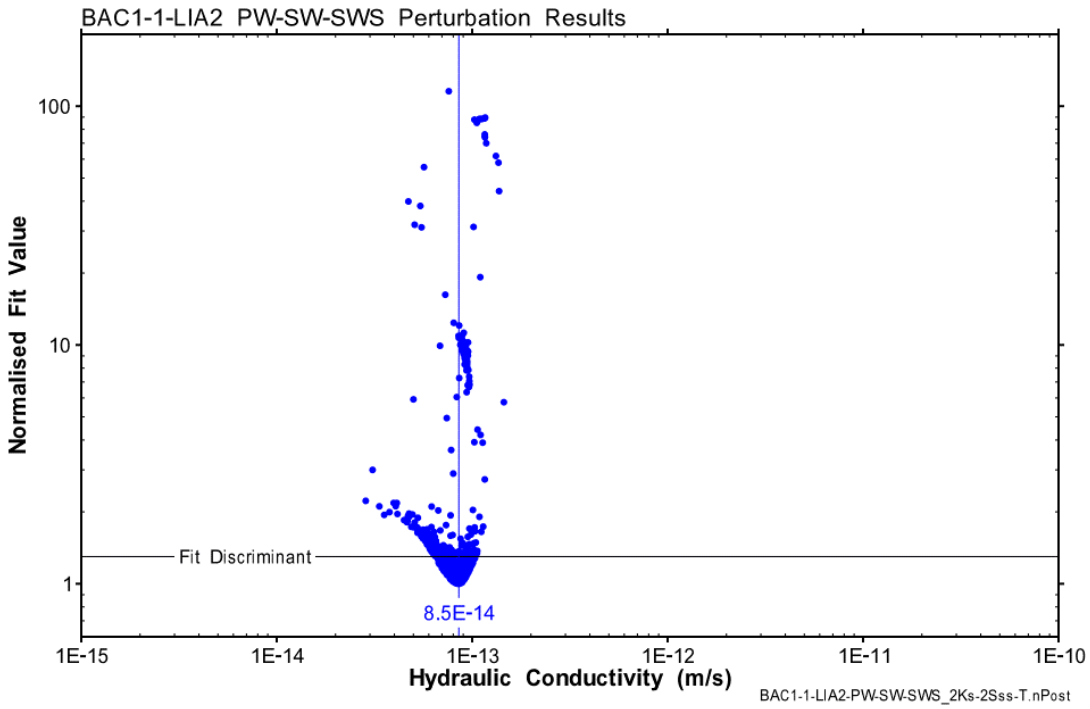

Fig. B-23: Hydraulic test BAC1-1-LIA2: Distribution of the normalised objective function value over K for the perturbation result of the PW-SW-SWS test sequence

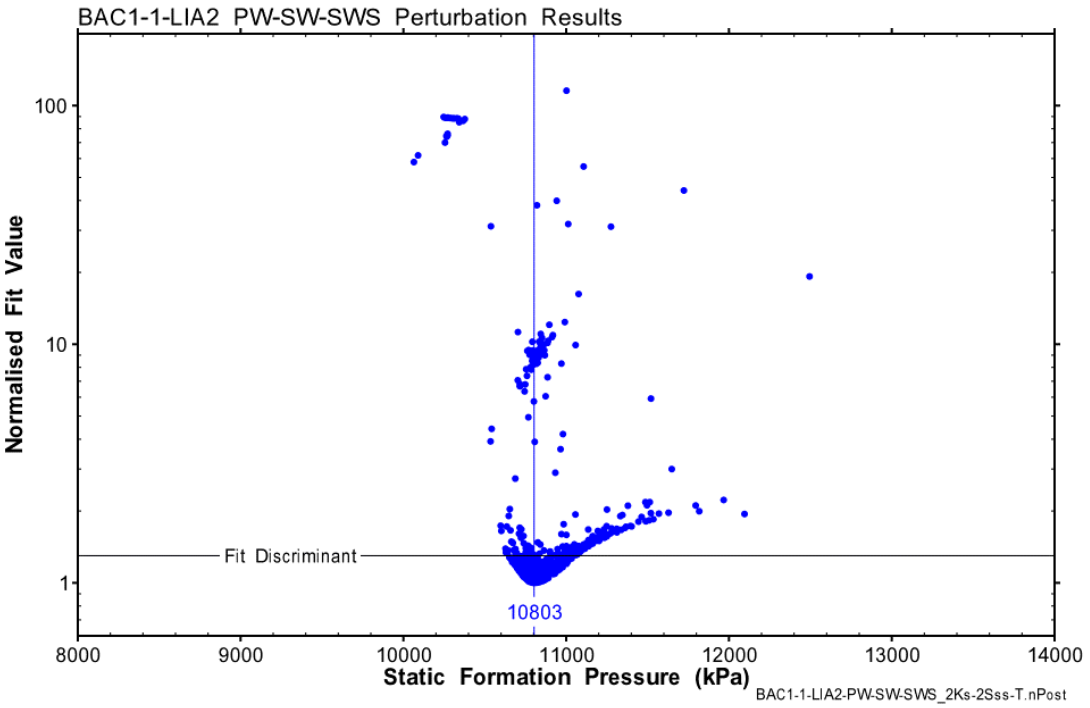

Fig. B-24: Hydraulic test BAC1-1-LIA2: Distribution of the normalised objective function value over P_f for the perturbation result of the PW-SW-SWS test sequence

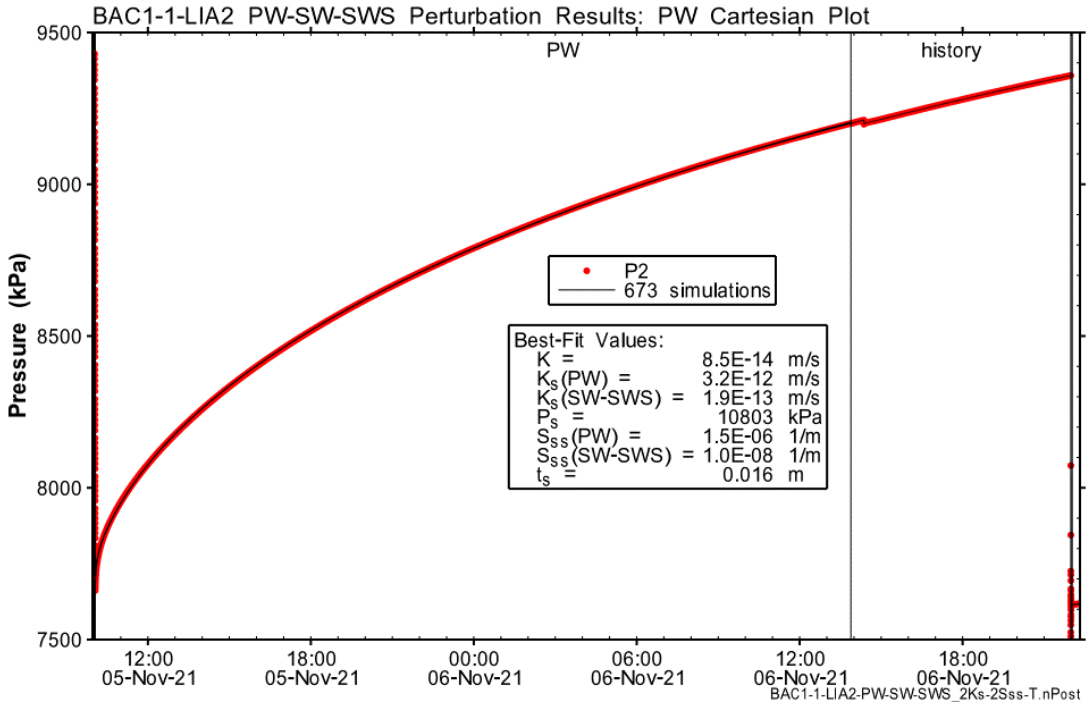

Fig. B-25: Hydraulic test BAC1-1-LIA2: Cartesian horsetail plot of the perturbation simulations on the PW phase, accepting the fit discriminant

673 / 1'000 results with a normalised objective function value less than 1.30.

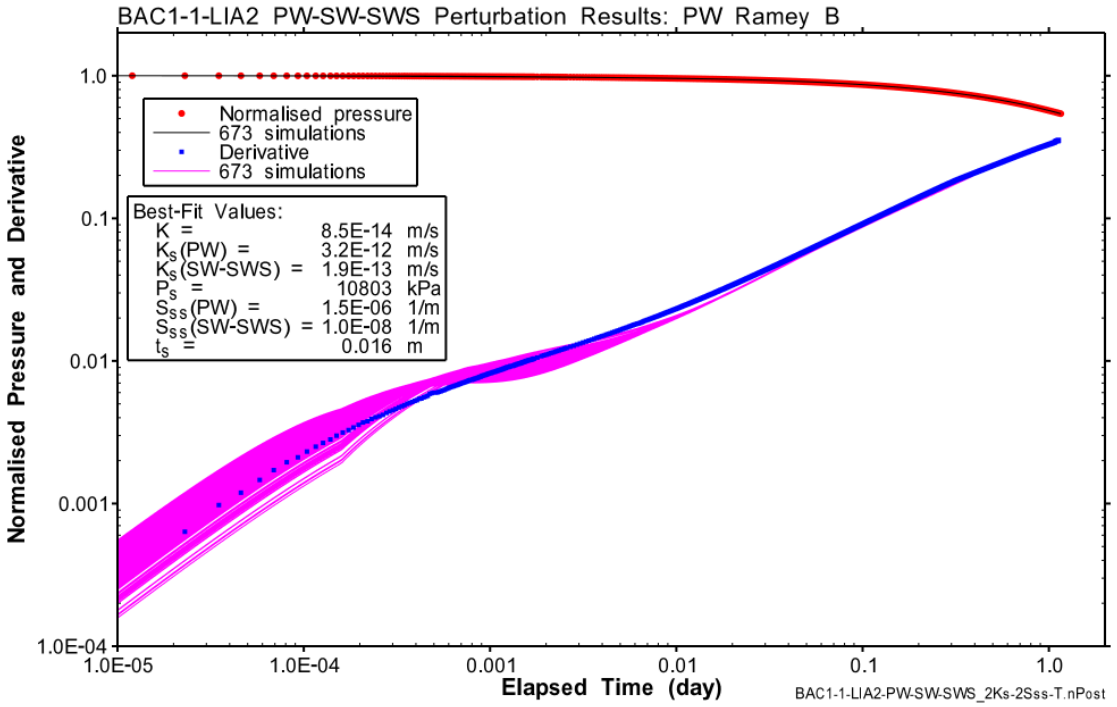

Fig. B-26: Hydraulic test BAC1-1-LIA2: Ramey B horsetail plot of the perturbation simulations on the PW phase, accepting the fit discriminant

673 / 1'000 results with a normalised objective function value less than 1.30.

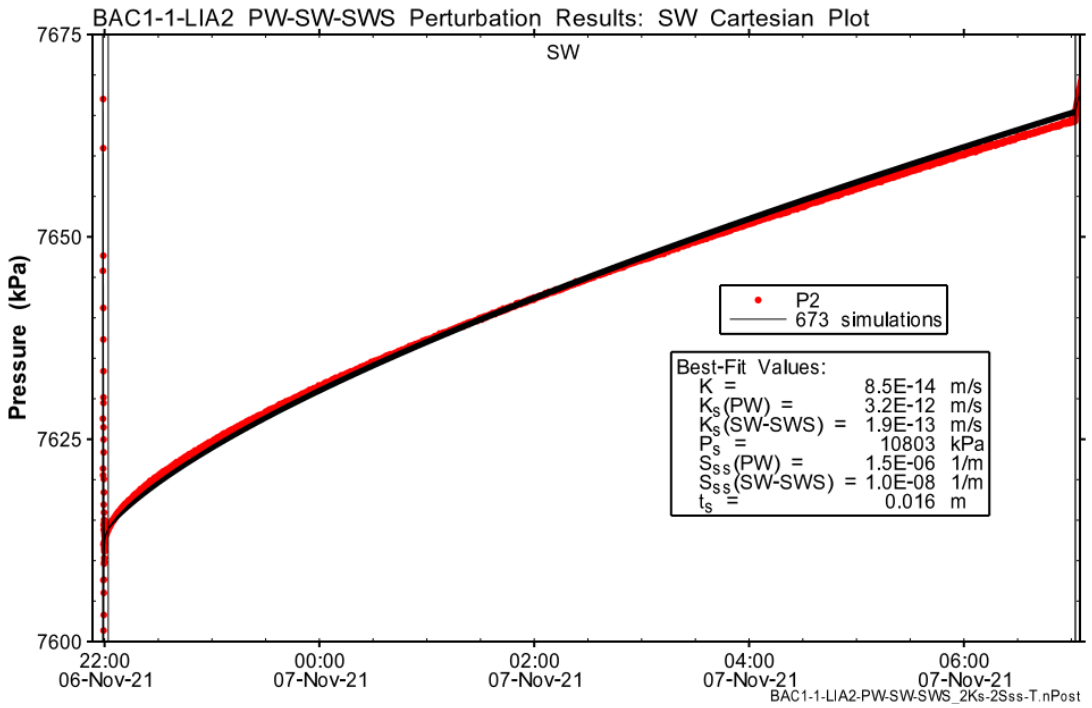

Fig. B-27: Hydraulic test BAC1-1-LIA2: Cartesian horsetail plot of the perturbation simulations on the SW phase, accepting the fit discriminant

673 / 1'000 results with a normalised objective function value less than 1.30.

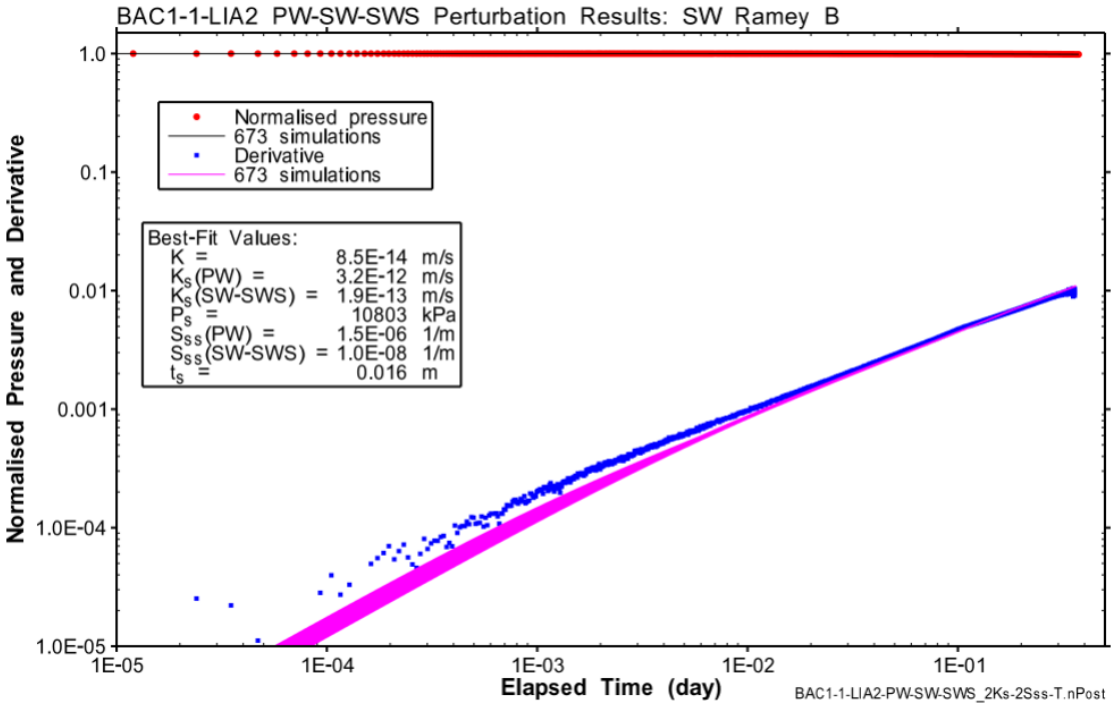

Fig. B-28: Hydraulic test BAC1-1-LIA2: Ramey B horsetail plot of the perturbation simulations on the SW phase, accepting the fit discriminant

673 / 1'000 results with a normalised objective function value less than 1.30.

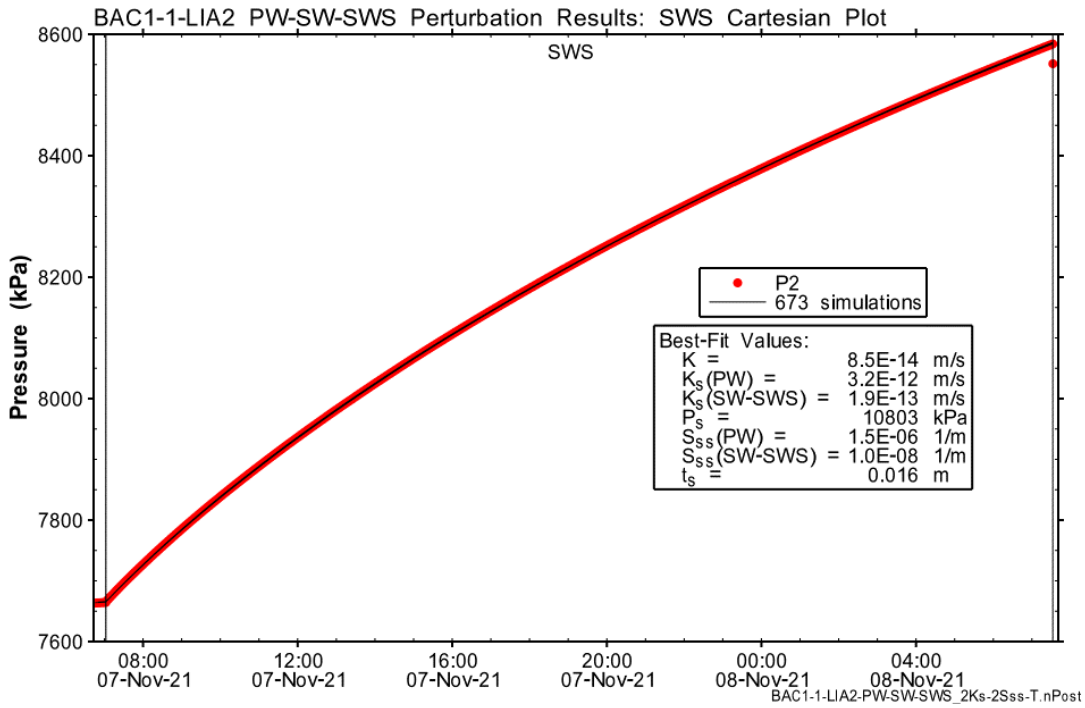

Fig. B-29: Hydraulic test BAC1-1-LIA2: Cartesian horsetail plot of the perturbation simulations on the SWS phase, accepting the fit discriminant

673 / 1'000 results with a normalised objective function value less than 1.30.

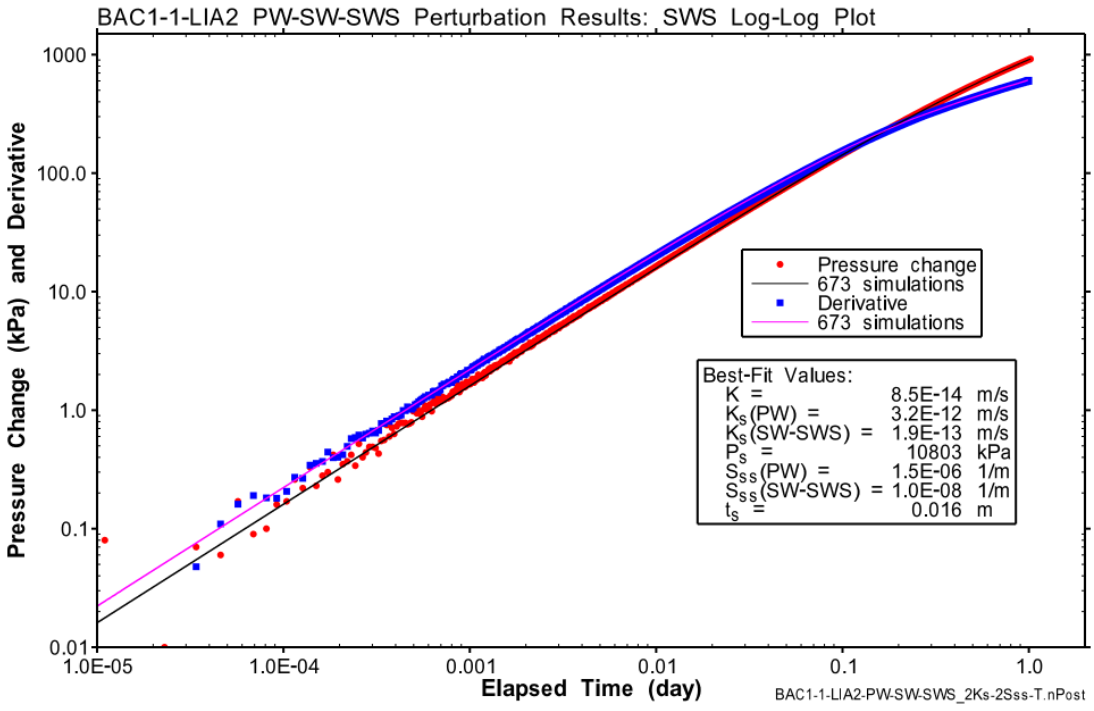

Fig. B-30: Hydraulic test BAC1-1-LIA2: Log-log horsetail plot of the perturbation simulations on the SWS phase, accepting the fit discriminant

673 / 1'000 results with a normalised objective function value less than 1.30.

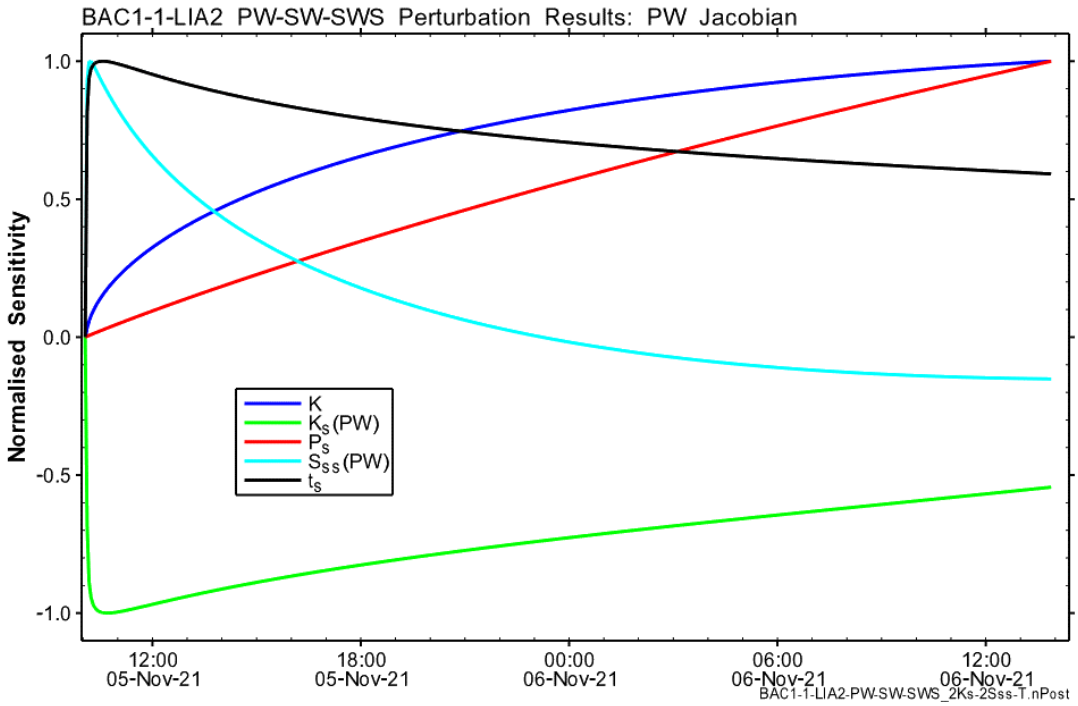

Fig. B-31: Hydraulic test BAC1-1-LIA2: Jacobian plot of parameter sensitivities during the PW phase

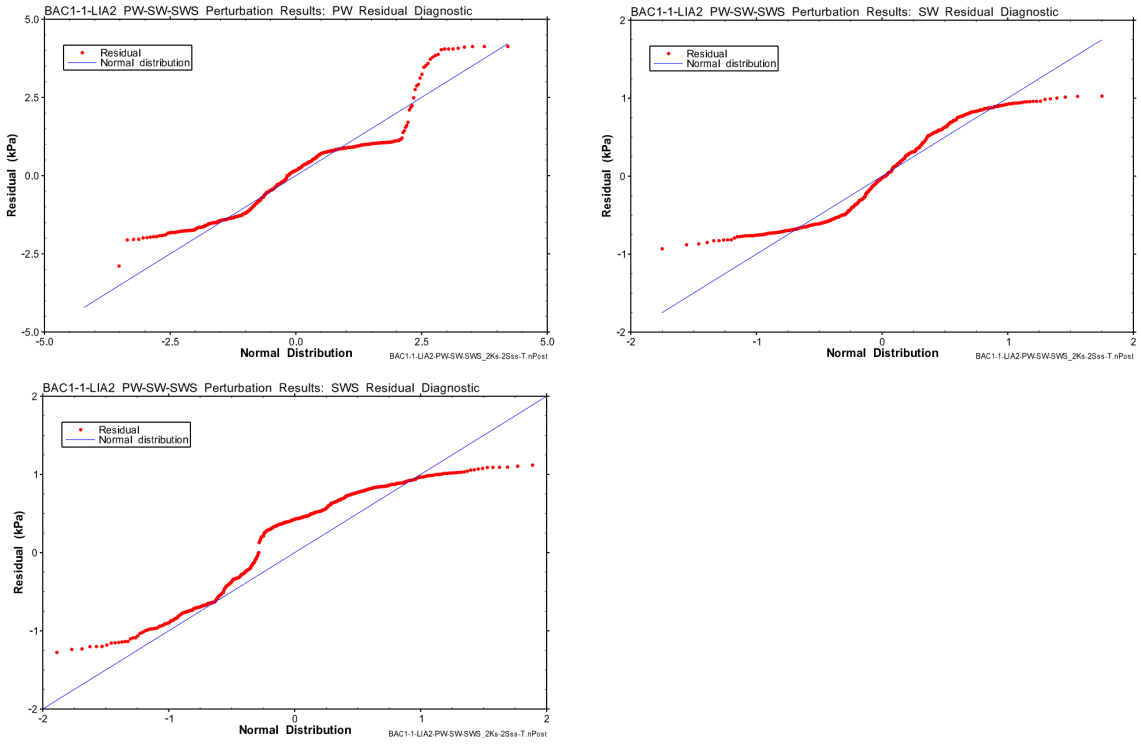

Fig. B-32: Hydraulic test BAC1-1-LIA2: Quantile-normal plot of residuals from the best Cartesian fit to PW phase (top left), SW phase (top right) and SWS phase data (bottom left)

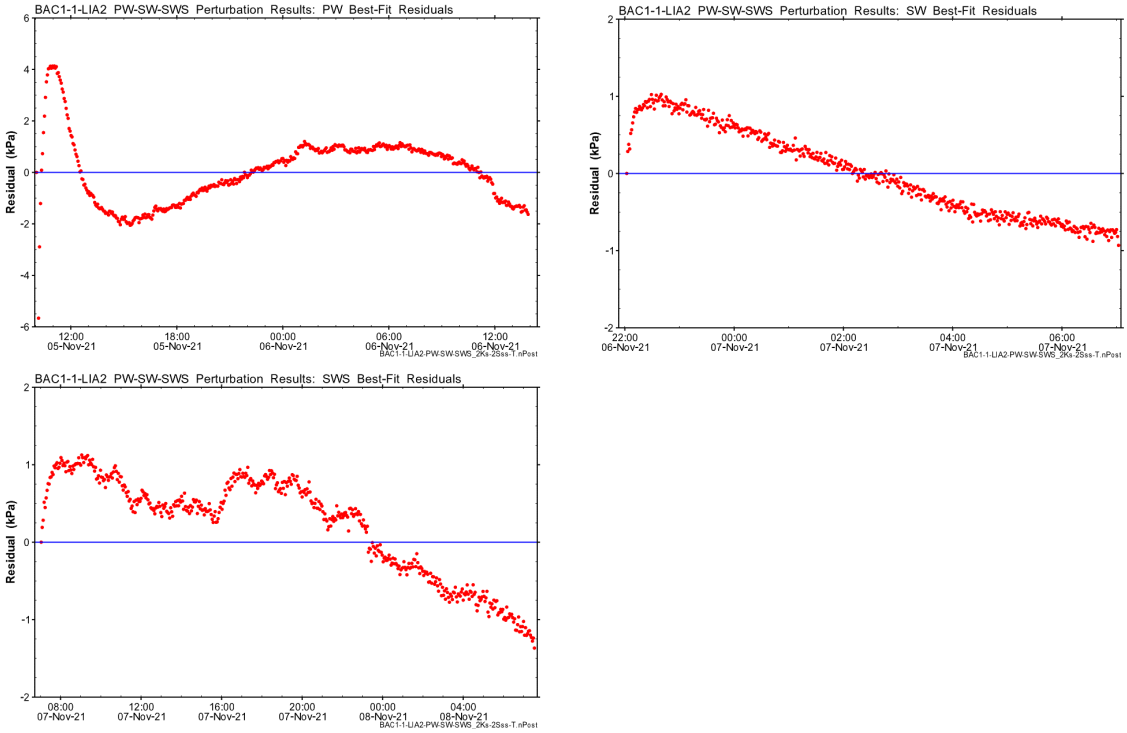

Fig. B-33: Hydraulic test BAC1-1-LIA2: Residuals from the best Cartesian fit to PW phase (top left), SW phase (top right) and SWS phase data (bottom left)

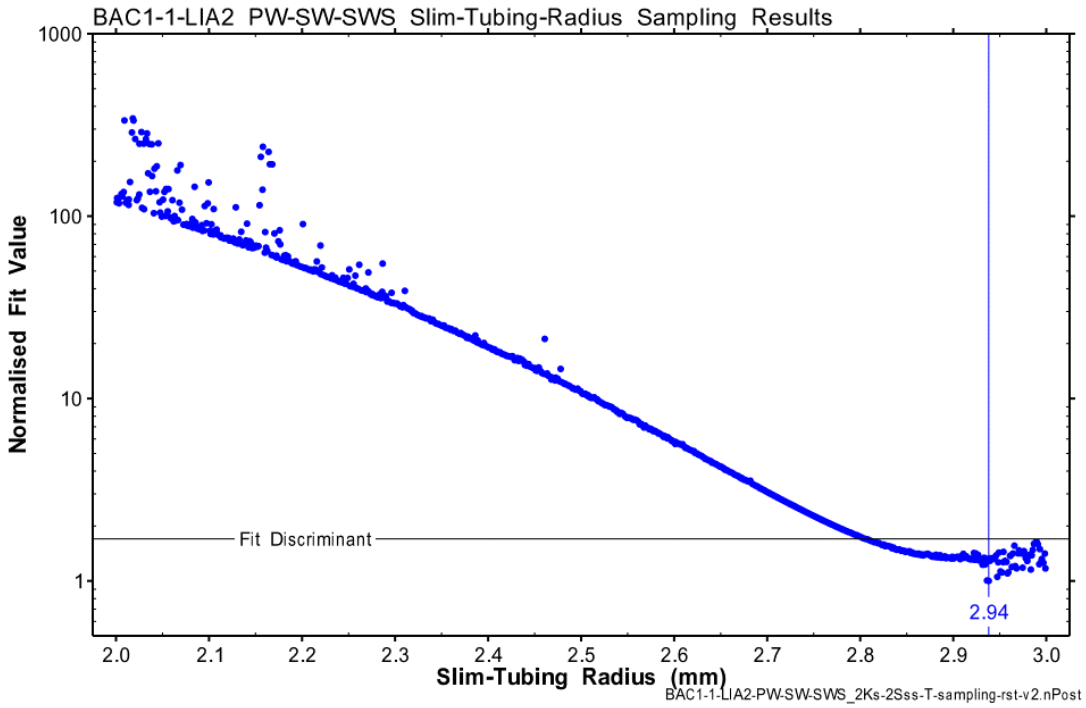

Fig. B-34: Hydraulic test BAC1-1-LIA2: Distribution of the normalised objective function value over the slim tubing radius for the sampling analysis result of the PW-SW-SWS test sequence

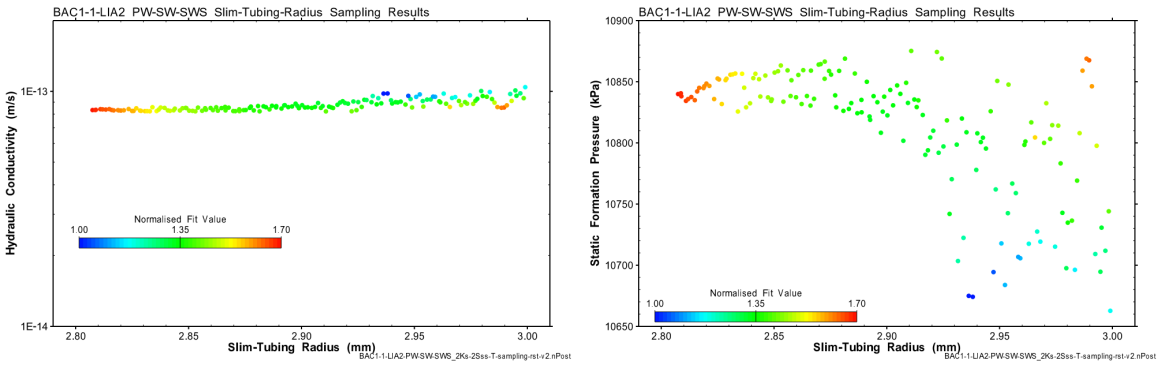

Fig. B-35: Hydraulic test BAC1-1-LIA2: Parameter correlations as a result of the sampling analysis for the formation parameters K (left) and P_f (right) vs. the slim tubing radius

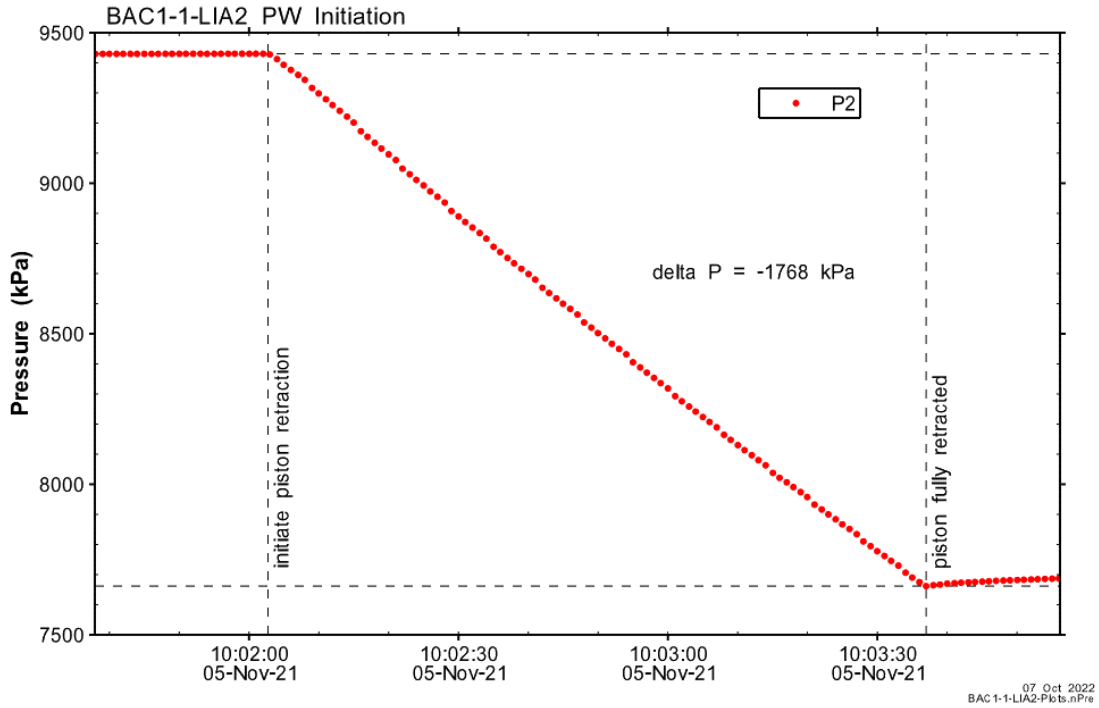

Fig. B-36: Hydraulic test BAC1-1-LIA2: Interval pressure change during the initiation of the PW phase